S-F-N hybrid structures and Josephson junctions for superconducting electronics

S.V. Bakurskiy, A.A. Neilo, V.I. Ruzhickiy, A.E. Schegolev,
N.V. Klenov, I.I. Soloviev, M.Yu. Kupriyanov

Laboratory of nanostructure physics, SINP, Lomonosov Moscow State University

Head of Laboratory – Prof. Kupriyanov M. Yu.

Hybrid structures theory and models – Dr. Bakurskiy S.V.

Circuits design and calculations– Dr. Ruzhickiy V.I.

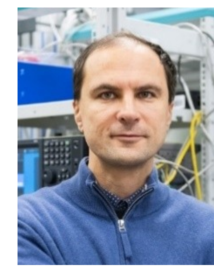

Digital electronics and devices design– Prof. Soloviev I.I.

Neuromorphic technologies – Dr. Schegolev A.E.

Quantum technologies – Prof. Klenov N.V.

In the Lab there are 3 Ph. D. and 7 students

Cooperation with: MIPT (Centre for Advanced Mesoscience and Nanotechnology)
Special thanks to Prof. Stolyarov V.S. and Prof. Golubov A.A.

Also in cooperation with: VNIAA, MISIS, ISSP, MIREA, NNSU, KPFU and others

Digital superconducting circuits

- ❖ ~1980 SFQ circuits development
- ❖ 2000 Digital and mixed signal devices of several 1K JJ/cm² complexity
- ❖ 2013 Cryogenic Computing Complexity (C3)
- ➢ 2020 Functional complexity ~ <u>1 Mb/cm²</u>

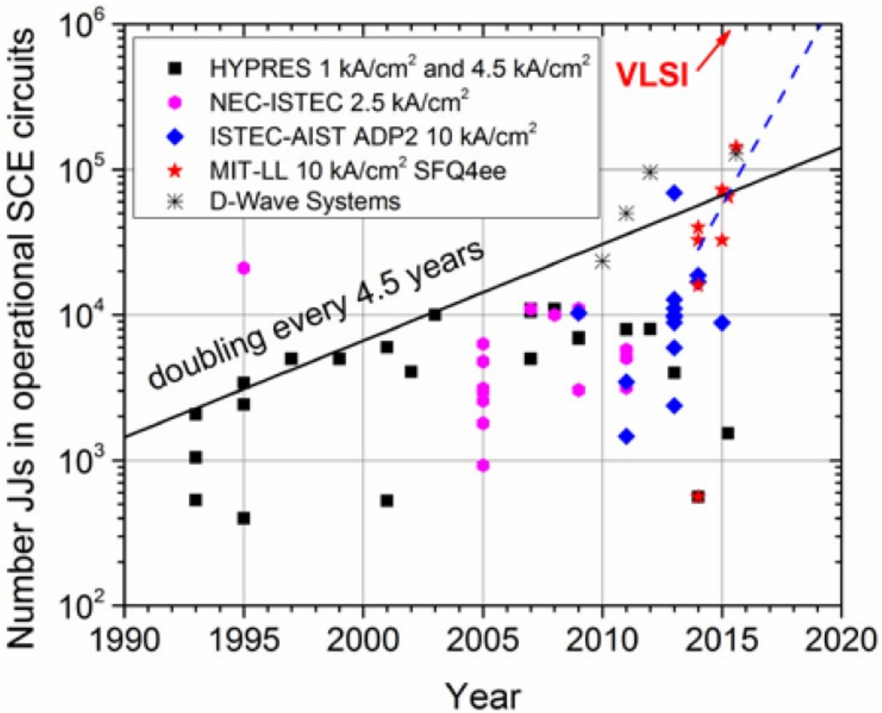

One of the ways is to develop new basic structures!!!

- S.K. Tolpygo et al., Low Temp. Phys. 42, 361 (2016)

Contents

1. Motivation

2. Basic physics – Proximity effect

3. Hybrid S-F-N structures

- spin-valves
- flux traps
- bi-stable phase junctions
- Josephson bridges

4. Implementation in applied schemes

- Bio-inspired neuron
- All-JJ Logic

Superconductor-Ferromagnet proximity effect

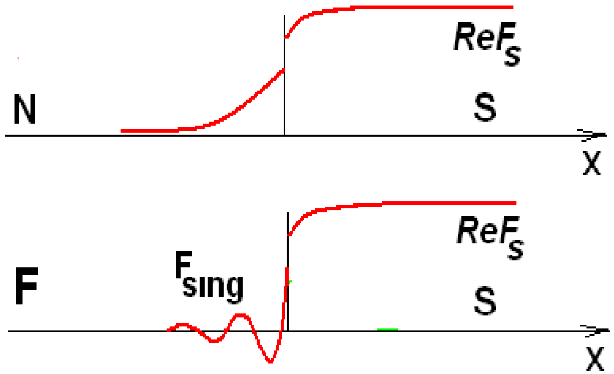

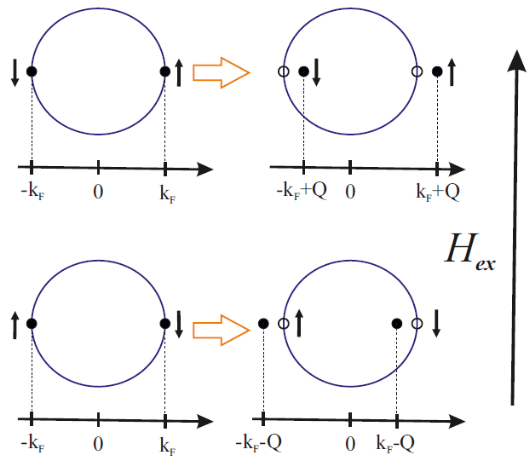

SFS junctions

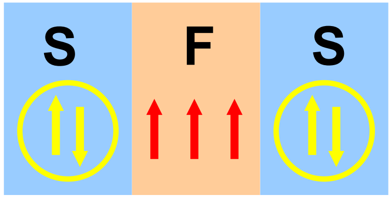

π-transition at $d_F \cong \pi\xi_{F2}$

$$I_S(\varphi) = I_C \sin(\varphi + \pi) = -I_C \sin(\varphi)$$

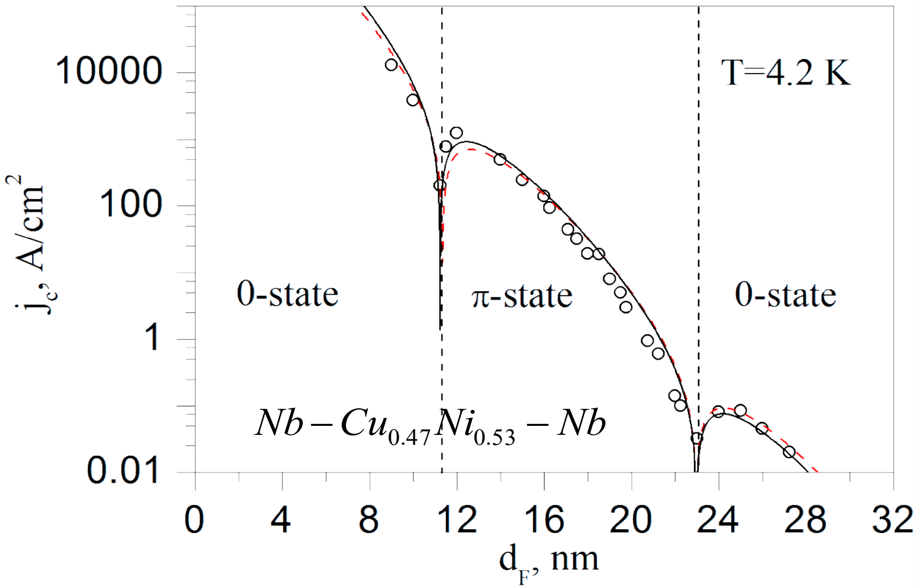

V. V. Ryazanov, V. A. Oboznov, A. Yu. Rusanov, A. V. Veretennikov, A. A. Golubov, and J. Aarts, Phys. Rev. Lett. **86**, 2427 (2001).

S. M. Frolov, D. J. Van Harlingen, V. A. Oboznov, V. V. Bolginov, and V. V. Ryazanov, Phys. Rev. B **70**, 144505, (2004).

Coherence length

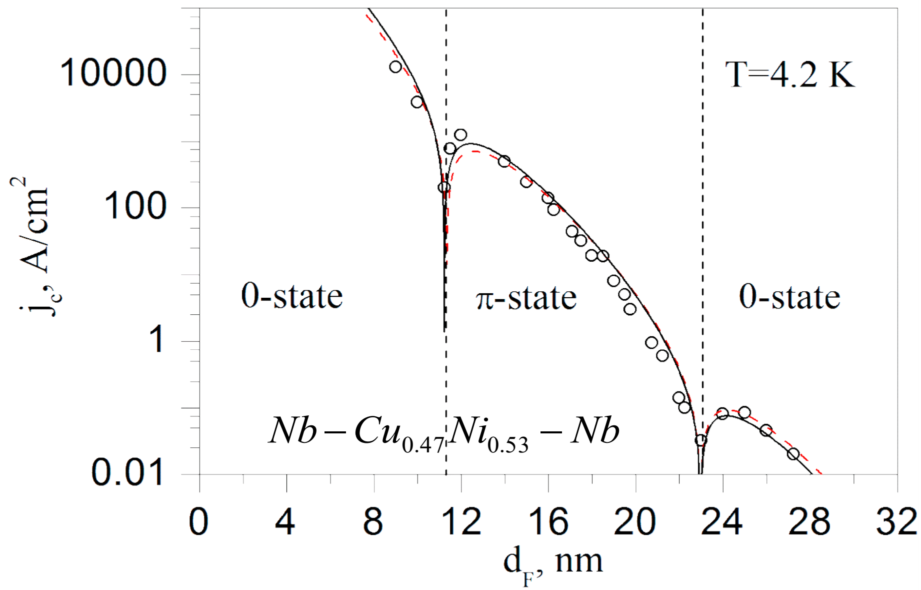

In calculations and normalization, it is convenient to use the characteristic length of material determined by diffusion coefficient

$$\xi_{N,F}^2 = D_{N,F}/2\pi T_C$$

The effective damping and oscillations length depend on temperature, exchange field, and geometrical parameters. In a ferromagnet, it has the form:

$$\xi_{1,2}^* = \sqrt{\frac{\hbar D}{\sqrt{\pi^2 T^2 + H^2} \pm \pi T}}$$

$$I_C(d_F) = A \exp(-d_F/\xi_1)\cos(d_F/\xi_2 + \varphi),$$

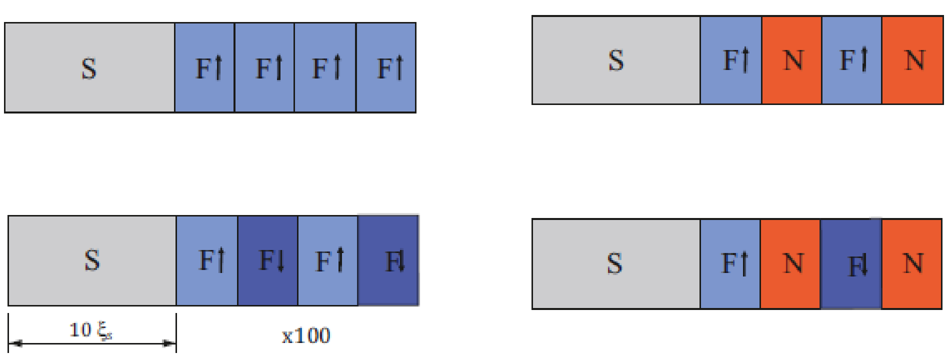

It is often suitable for describing experimental data, but it is not always possible to introduce it.

Proximity effect in SF…F structure in antiferromagnetic configuration for different F layers thickness d_i

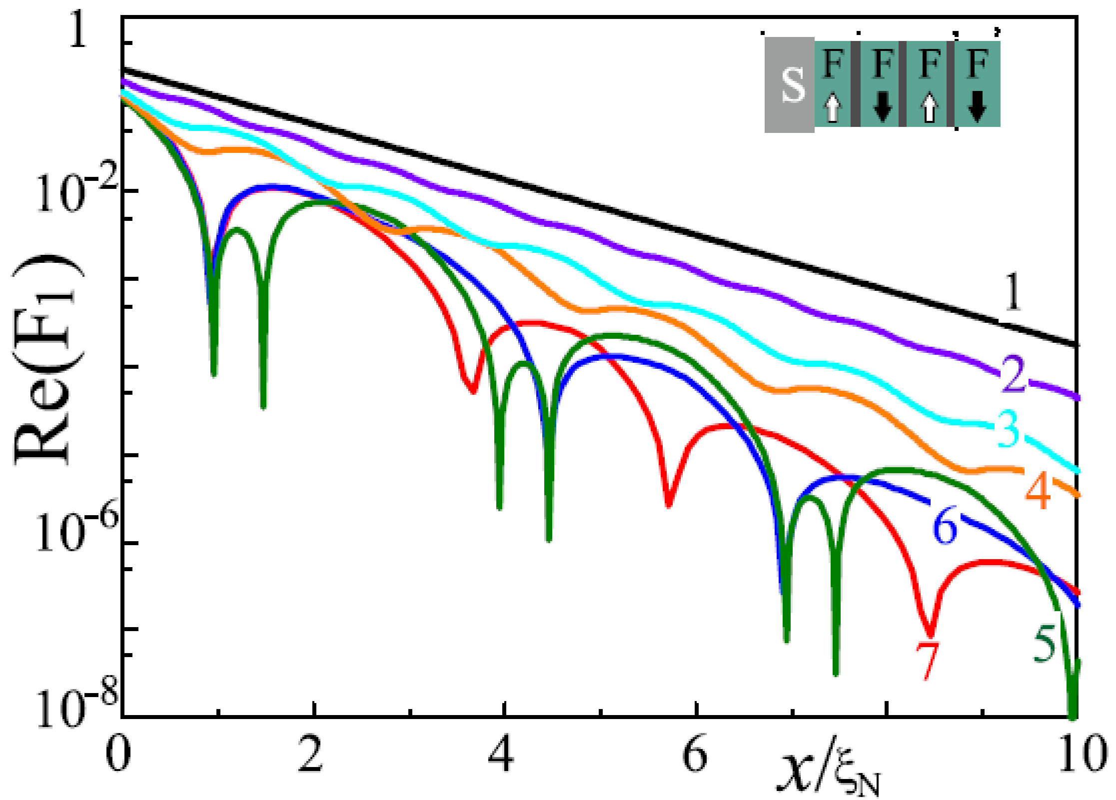

$$d_i = 0.2\xi, 0.51\xi, 0.8\xi, \xi, 1.5\xi, 3\xi, 5\xi$$

$$\Psi(x) = \exp\left(-\frac{x}{\xi_1}\right)\left(A + B\ \cos\left(\frac{x}{\xi_2} + \varphi\right)\right).$$

Bakurskiy, S. V., Kupriyanov, M. Y., Baranov, A. A., Golubov, A. A., Klenov, N. V., & Soloviev, I. I. (2015). Proximity effect in multilayer structures with alternating ferromagnetic and normal layers. *JETP letters*, *102*, 586-593.

Proximity effect in SF structures: domain effect

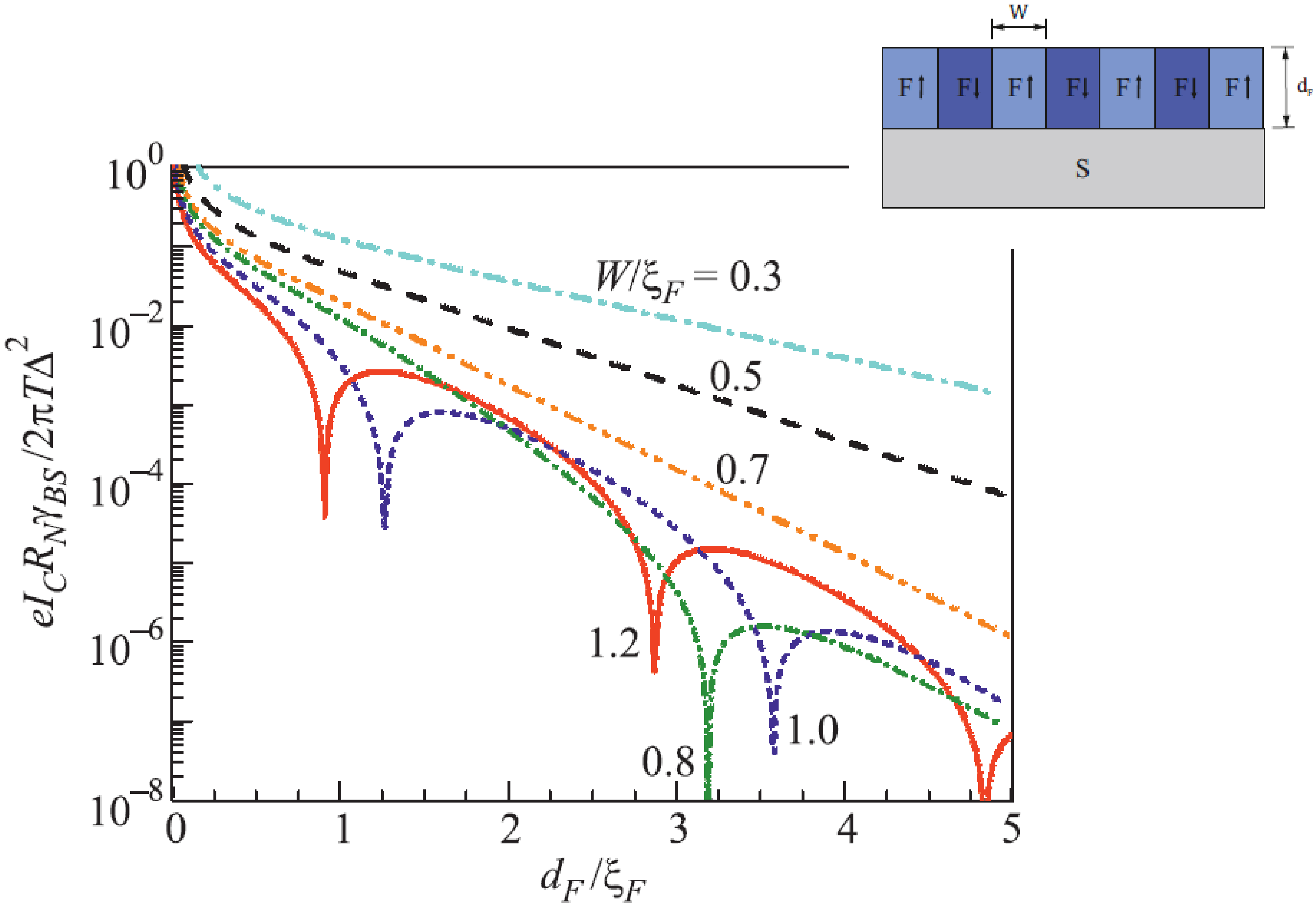

Proximity effect in SF structures: domain effect

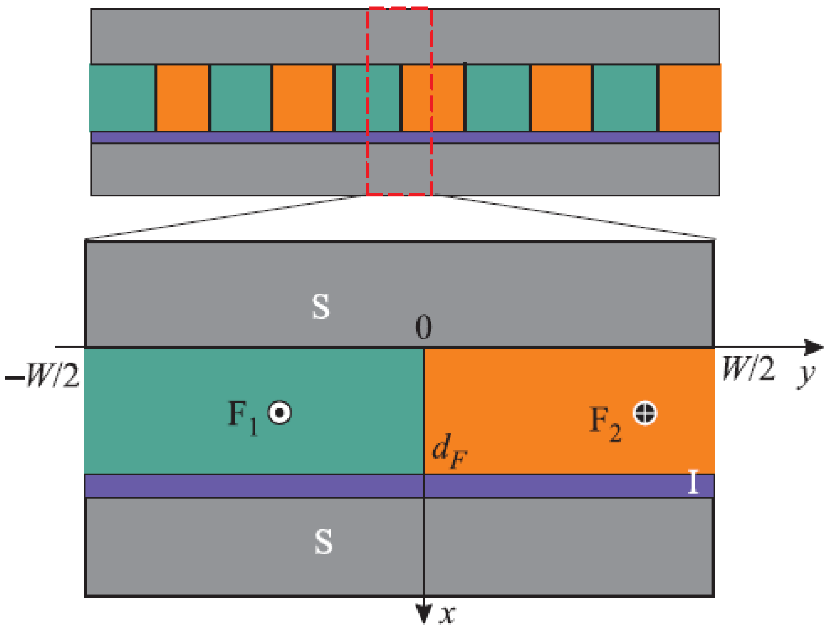

$$\frac{eI_C R_N}{2\pi T_C} = \frac{T}{2WT_C} \sum_{\omega>0} \frac{ZG_0\Delta}{\omega} S(\omega), \qquad (18)$$

$$S(\omega) = \sum_{n=-\infty}^{\infty} (-1)^n \left[\frac{W}{q_+^2} + \frac{W}{q_-^2} - \frac{2S_-S_+(q_-^2 - q_+^2)^2}{\delta q_+^3 q_-^3} \right].$$

$$I_C(d_F) = A\exp(-d_F/\xi_1)\cos(d_F/\xi_2 + \varphi),$$

Bakurskiy, S. V., Golubov, A. A., Klenov, N. V., Kupriyanov, M. Y., & Soloviev, I. I. (2015). Josephson effect in SIFS tunnel junctions with domain walls in the weak link region: In memory of VF Gantmakher. *JETP letters*, *101*, 765-771.

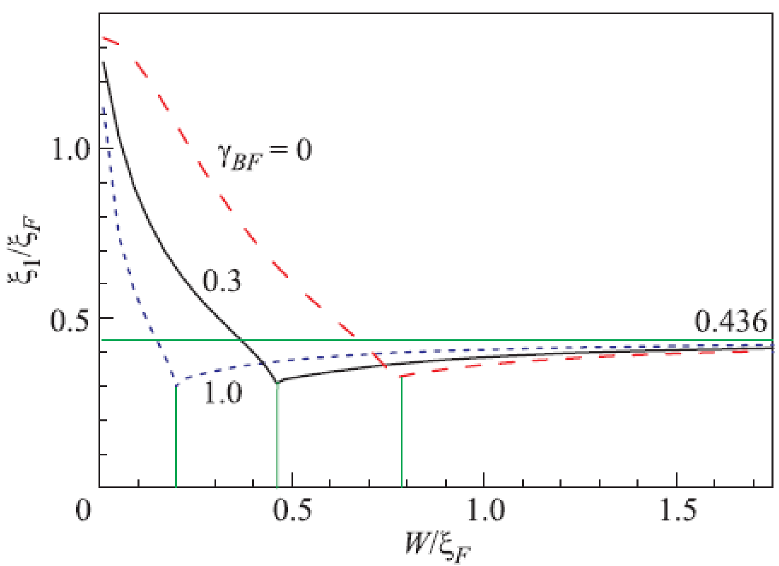

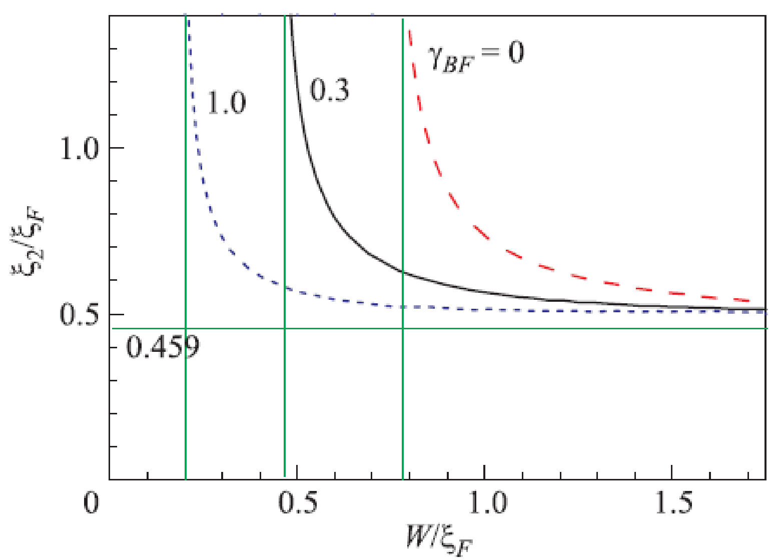

Contents

1. Motivation

2. Basic physics of S-F-N hybrids

3. Hybrid S-F-N structures

   - spin-valves
   - flux traps
   - bi-stable phase junctions
   - Josephson bridges

4. Implementation in applied schemes

   - Bio-inspired neuron
   - All-JJ Logic

Spin valve

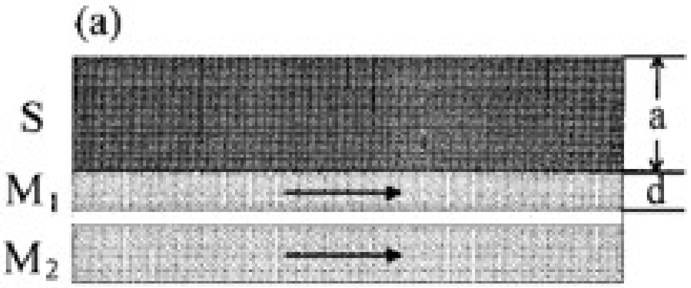

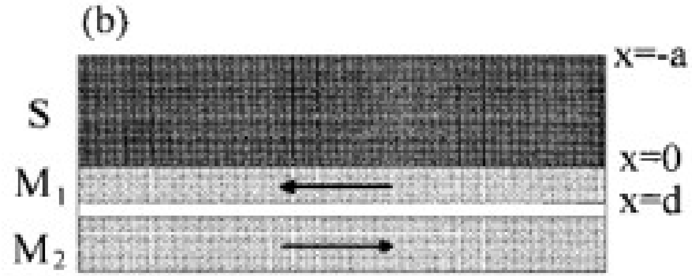

Sangjun Oh, D. Youm, and M. R. Beasley
Appl. Phys. Lett. 71, 2376 (1997);

Three types of spin-valve

1) Control of the critical temperature

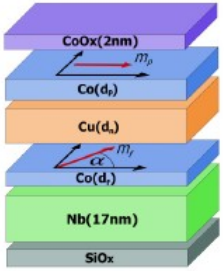

2) Control of the critical current

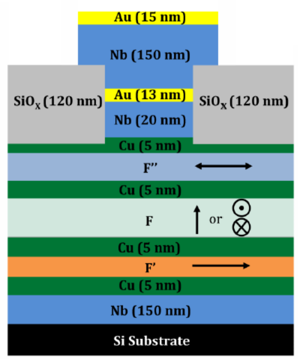

3) Control of the pair amplitude in the part of the structure

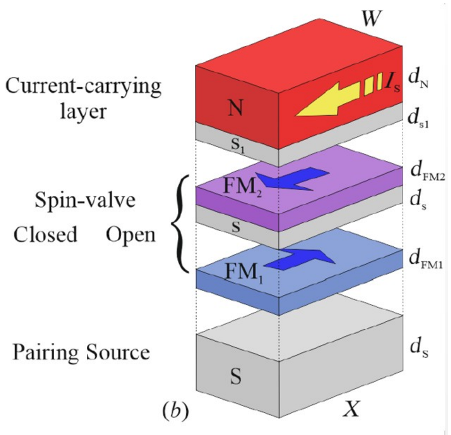

SFF spin valves for control of the critical temperature of S film

V. I. Zdravkov et al,
Phys. Rev. B
87, 144507 (2013)
ΔT_C – 10 mK

P.V. Leksin et al,
Phys. Rev. Let.
109, 057005 (2012)
ΔT_C – 50 mK

A.A. Jara et al.,
Phys. Rev. B
89, 184502 (2014)
ΔT_C – 20 mK

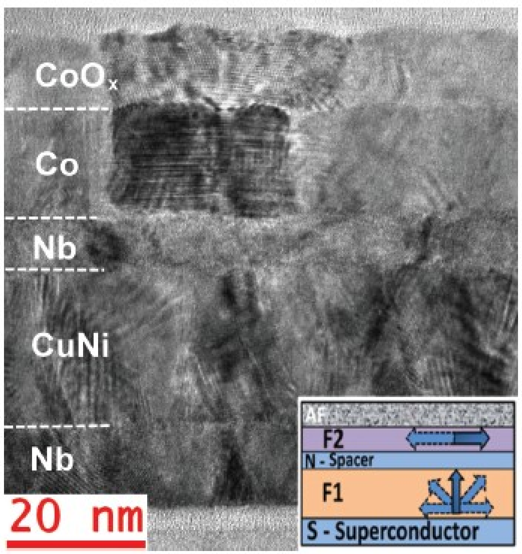

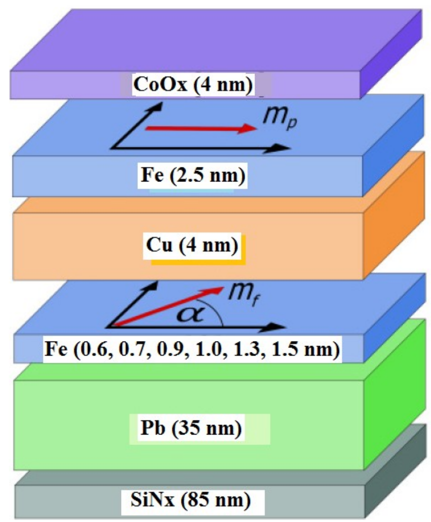

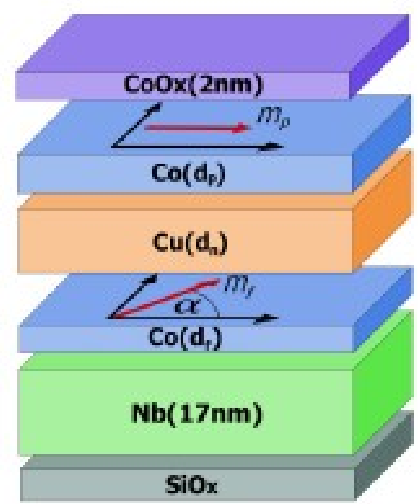

. L. Wang et al.,
hys. Rev. B
9, 184508 (2014)
ΔT_C – 120 mK

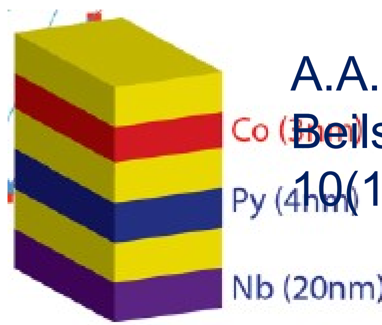

A.A. Kamashev et al.,
Beilstein J. of Nanotech.,
10(1), 1458-1463 (2019)
ΔT_C – 510 mK

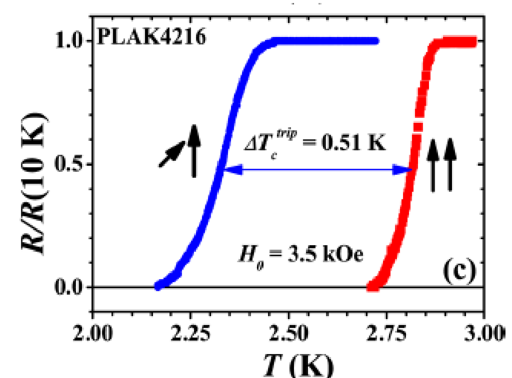

SFF spin valves for control of the critical temperature of S film

Y. V. Fominov, et al., JETP Lett. 91, 308 (2010).

R.G. Deminov et al., JMMM (2014).

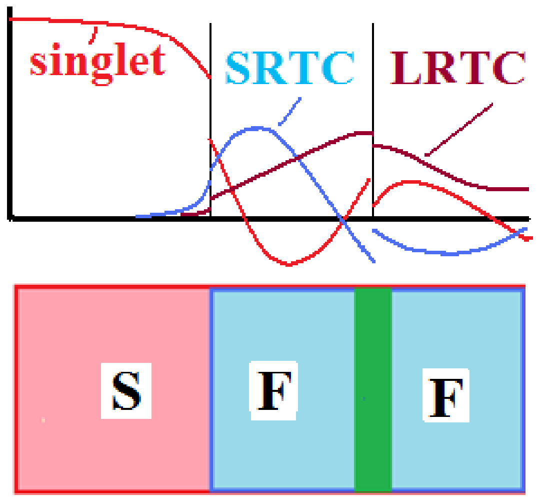

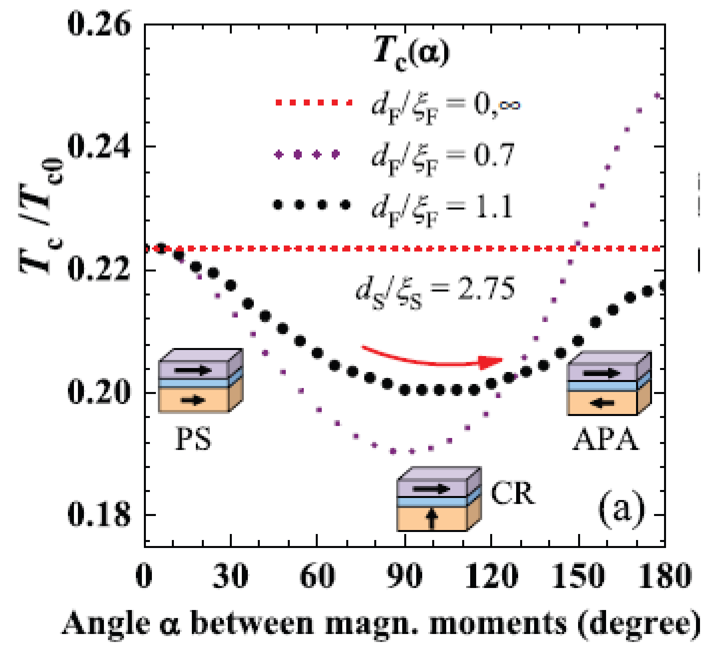

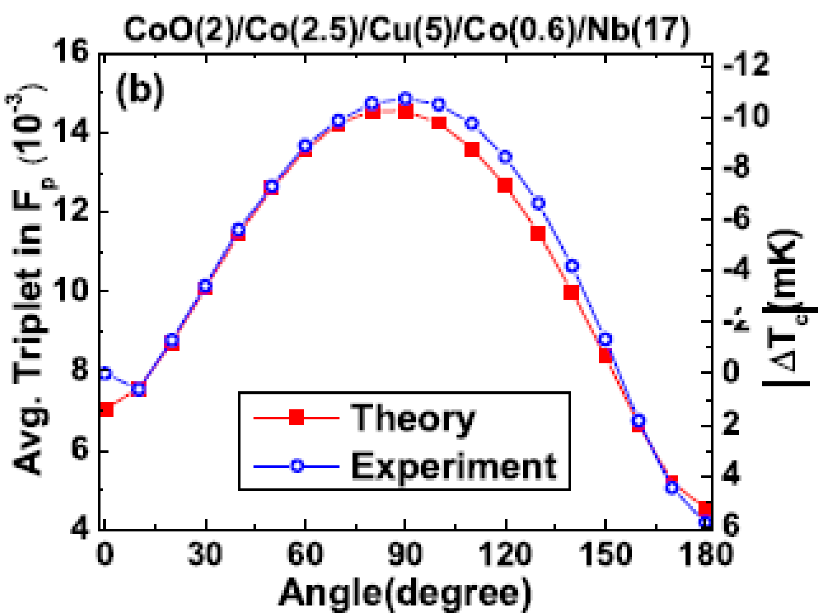

A.A. Jara et al., Phys. Rev. B 89, 184502 (2014)

$$F_t(y,t) \equiv \sqrt{|f_0(y,t)|^2 + |f_1(y,t)|^2},$$

Spin valve with ferromagnetic insulator

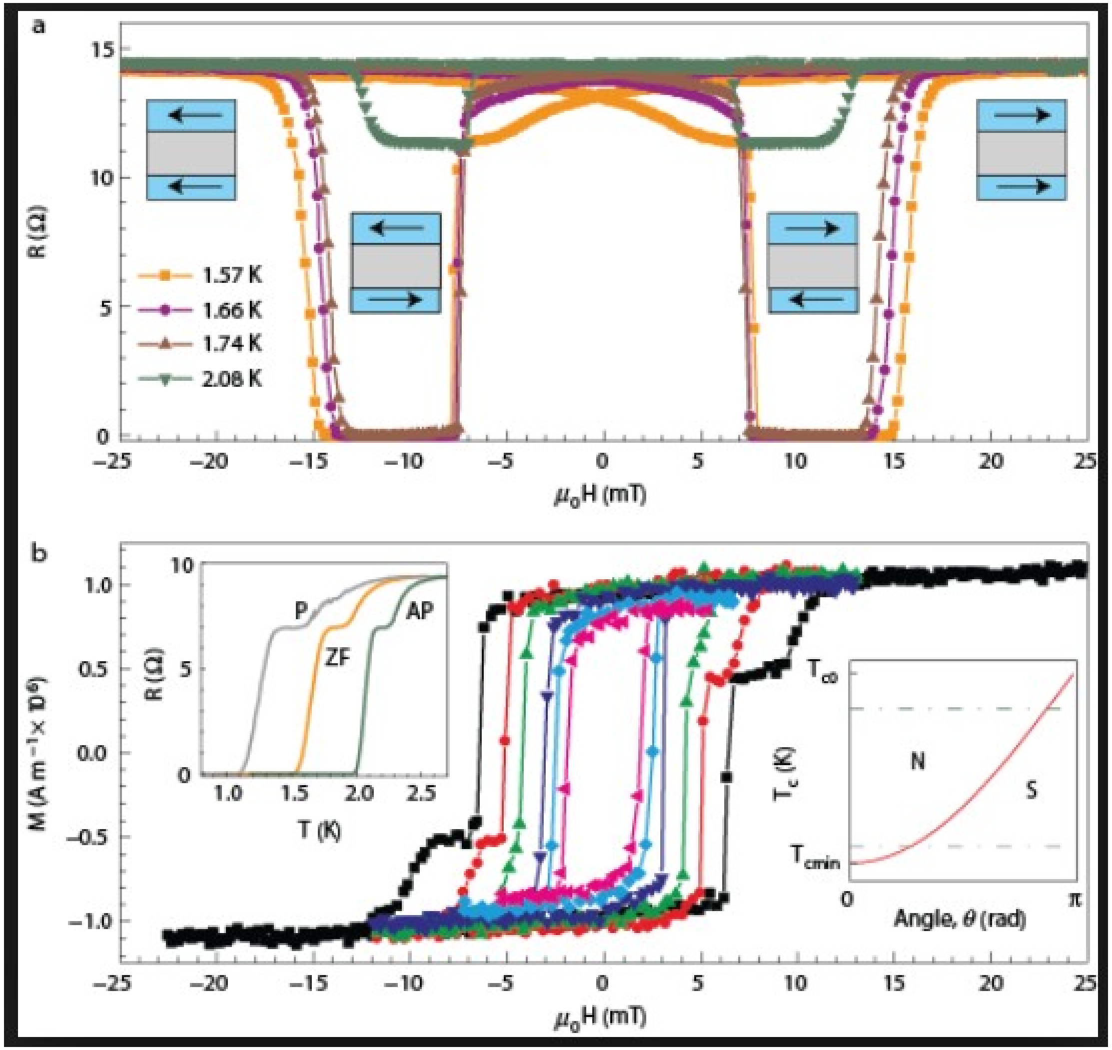

Stronger effect!

You can even control magnetization with superconductive order

Y. Zhu, A. Pal, M. G. Blamire, Z. H. Barber, Nature Materials, 16, 195–199 (2017)

Josephson spin valve devices

B. Baek et al., Nature Communications, 5, 3888 (2014)

Nb/Cu(3 nm)/$Ni_{0.7}Fe_{0.17}Nb_{0.13}$(2.1 nm)/Cu(5 nm)/Ni/Cu(3 nm)/Nb.

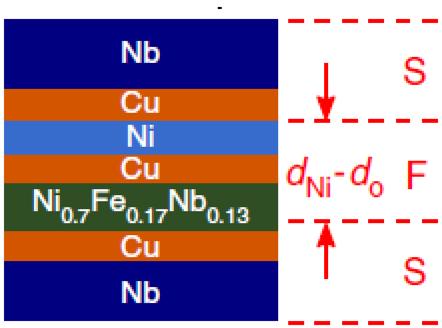

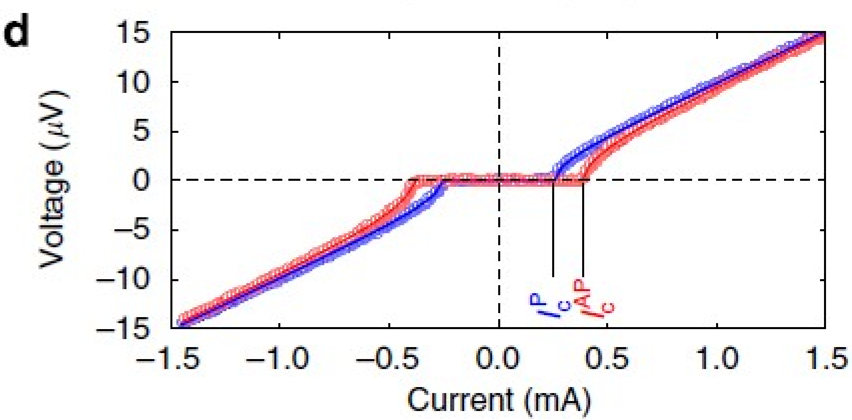

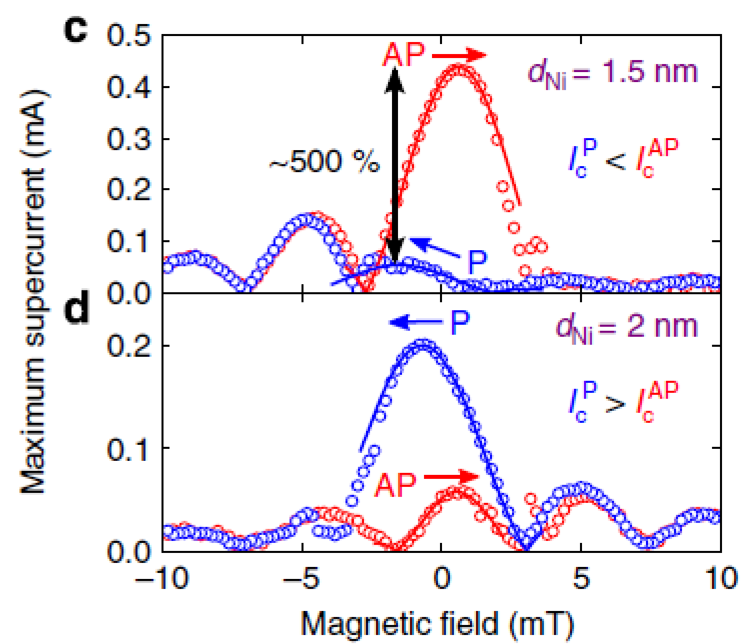

Structures with long range proximity effects

M. Houzet and A. I. Buzdin, Phys. Rev. B 76, 060504_R_ (2007)

B. M. Niedzielski et al., IEEE Tran. on Appl. Supercond. (2014)

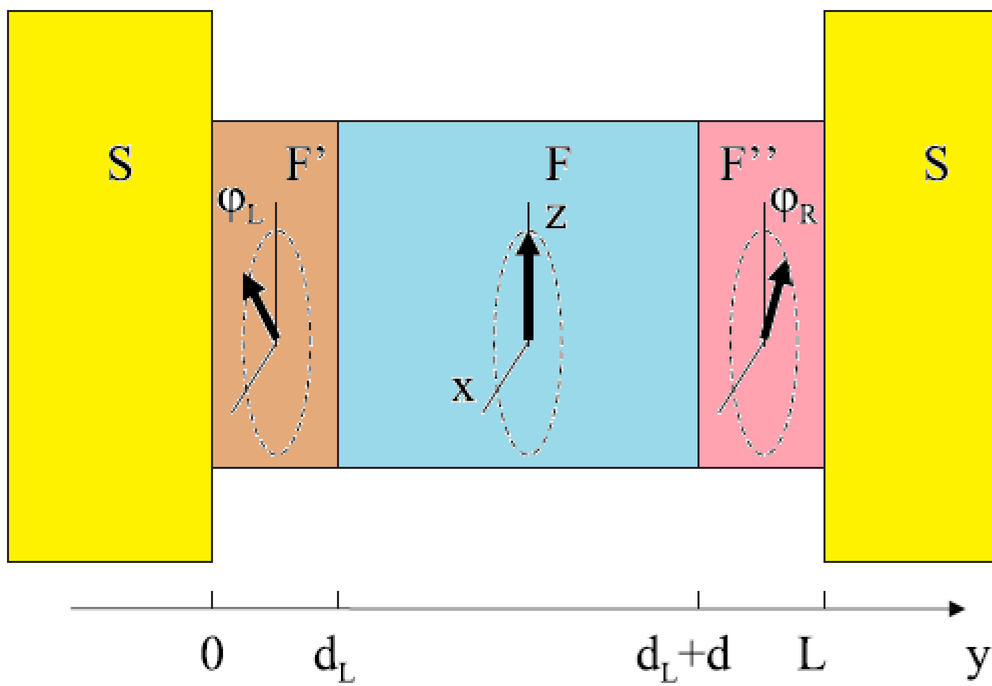

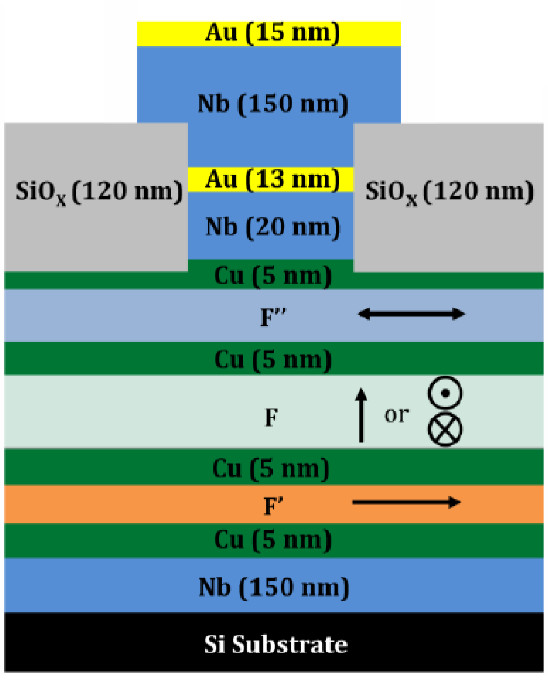

$$I_c = \frac{2\pi TG}{e} \sum_{\omega>0} \frac{\Delta^2}{\omega^2} \left(\mathrm{Re}\, \frac{q_+ d}{\mathrm{sh} q_+ d} - \frac{q_0 d}{\mathrm{sh} q_0 d} \frac{d_L^2 d_R^2}{\xi_f^4} \sin\phi_L \sin\phi_R \right)$$

Structures with long range proximity effects

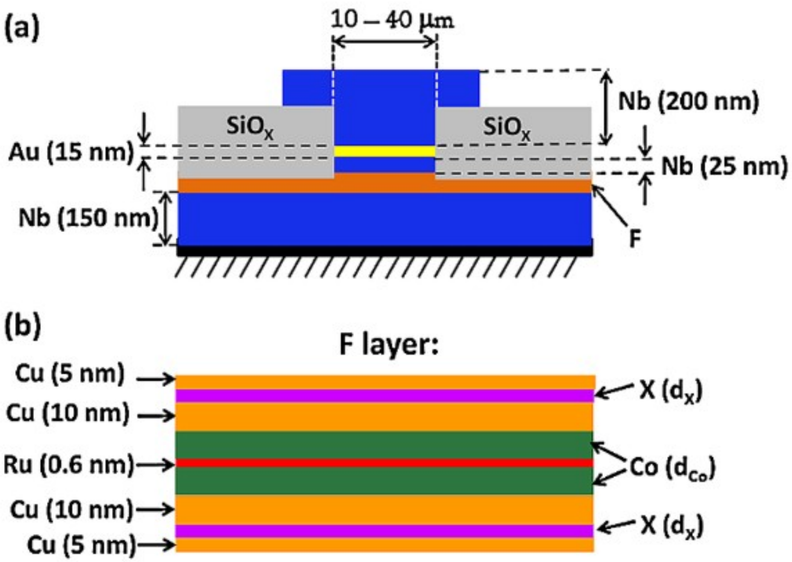

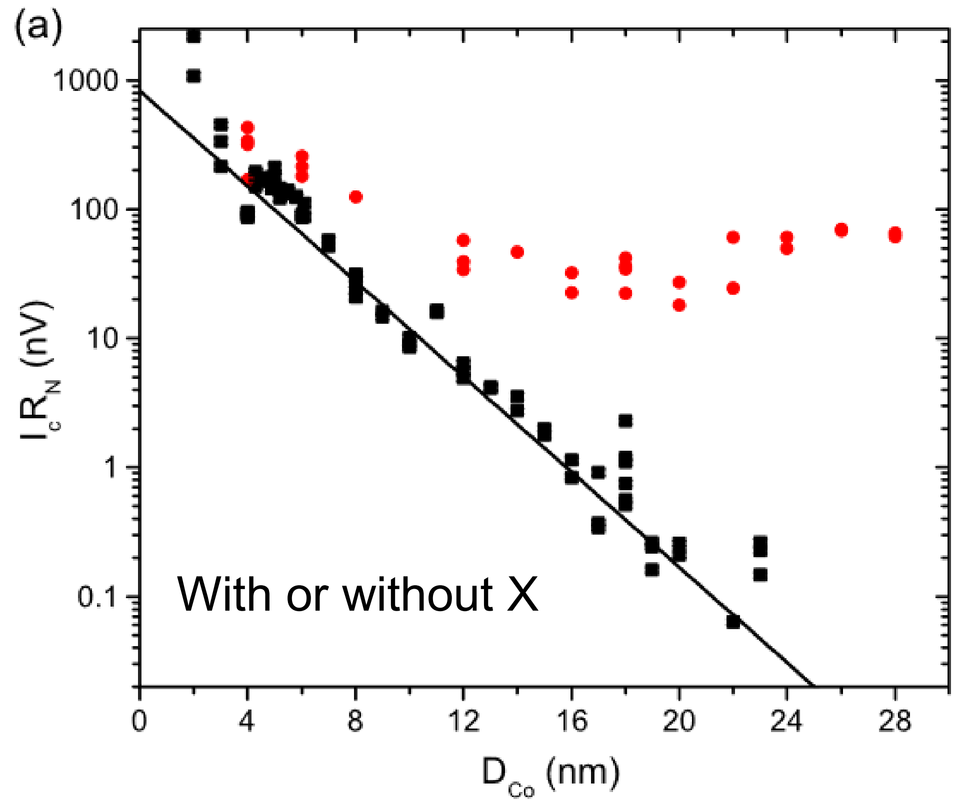

Khaire, T. S., Khasawneh, M. A., Pratt Jr, W. P., & Birge, N. O. (2010). Observation of spin-triplet superconductivity in Co-based Josephson junctions. *Physical review letters*, *104*(13), 137002.

Structures with long range proximity effects

B. M. Niedzielski et al., IEEE Tran. on Appl. Supercond. (2014)

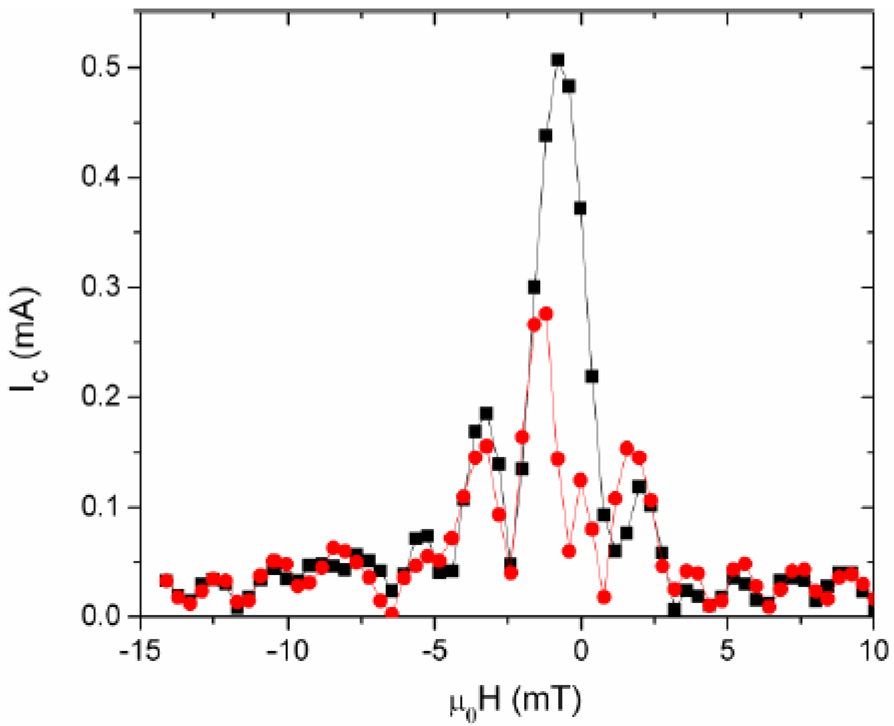

Fig 4. Critical current vs applied magnetic field for a Josephson junction of diameter 3 μm with F=Co(6)/Ru(0.6)/Co(6) and F″=Pd-Fe(15) alloy. The black squares and red circles represent data taken with the external field increasing in the positive and negative directions, respectively. At low field values, hysteresis is observed.

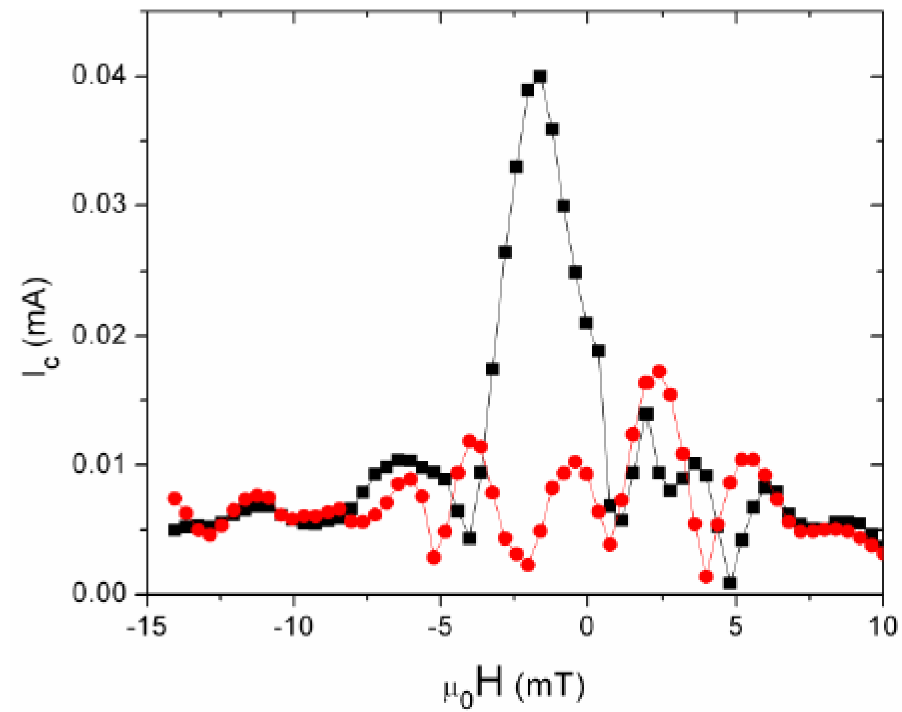

Fig 6. Critical current vs applied field for a Josephson junction of diameter 3 μm with F= Co(6)/Ru(0.6)/Co(6) and F″=Ni-Fe-Nb(1.5) alloy. The black squares and red circles indicate positive and negative field sweep directions respectively. Again, hysteresis is observed at low field values.

The largest value of I_cR_N observed in these samples is only 50 nV

Devices with single ferromagnetic layer

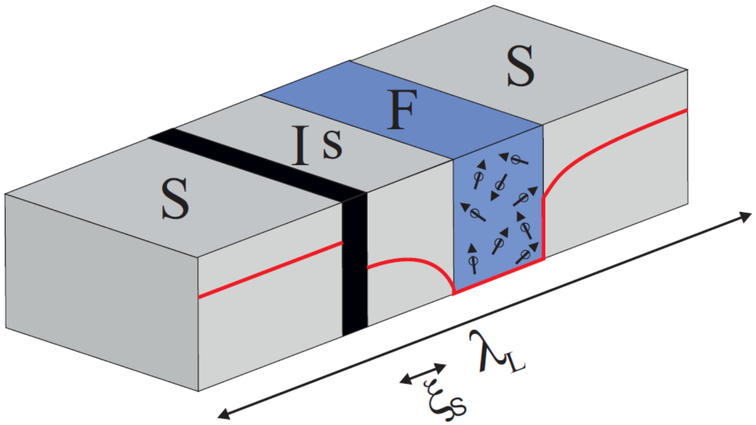

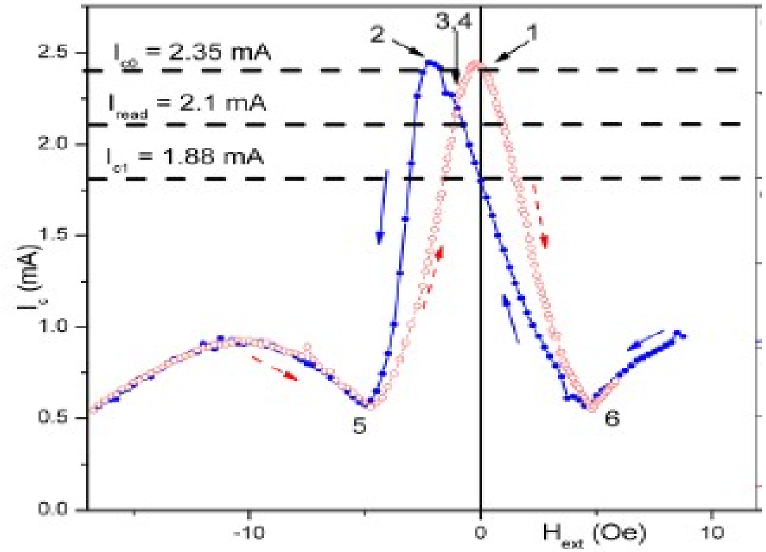

Control of the shift on Fraunhofer dependence

$$I_C(H_{ext}) = I_{C0}\left|\frac{\sin(\pi\Phi/\Phi_0)}{\pi\Phi/\Phi_0}\right|,$$

$$\Phi = W|L_{eff}H_{ext} + L_F H_0 N(n_\uparrow - n_\downarrow)|$$

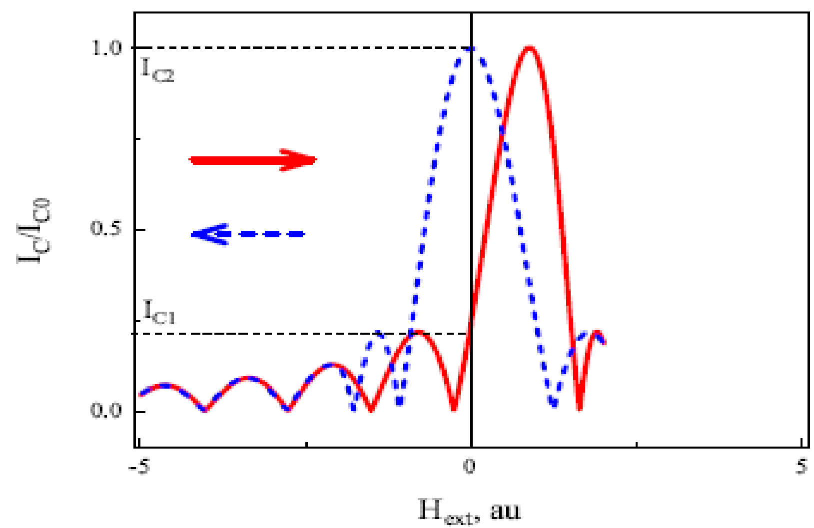

Bol'ginov V.V., Stolyarov V.S et al, JETP letters, 95, 7, 366, (2012)
I.V. Vernik et al, IEEE Trans on Appl. Supercon., 23, 1701208 (2013)
I. A. Golovchanskiy et al., Physical Review B 94 (21), 214514, (2016)
T. I. Larkin et al, Appl. Phys. Lett. 100, 222601 (2012)
S.V. Bakurskiy et al., Appl. Phys. Lett., 102, 192603, (2013)

Josephson magnetic rotary valve

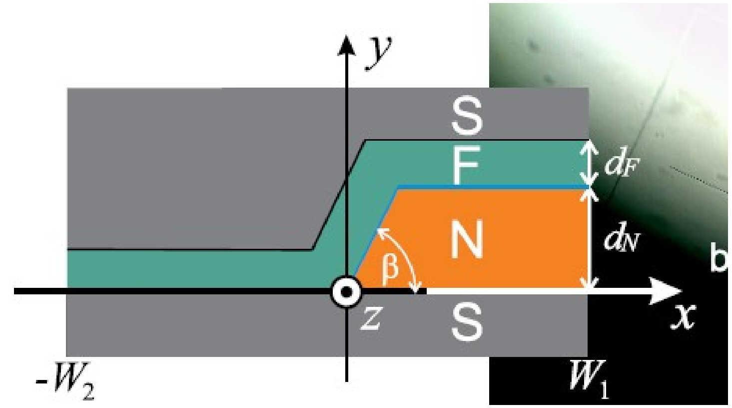

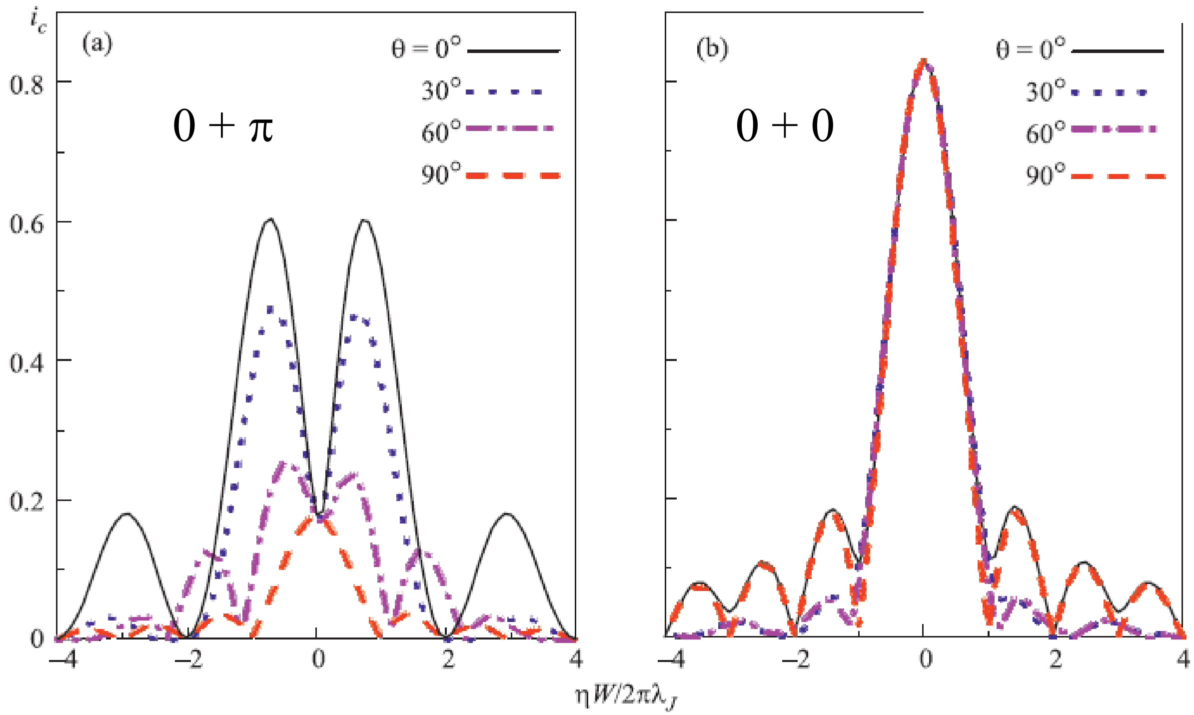

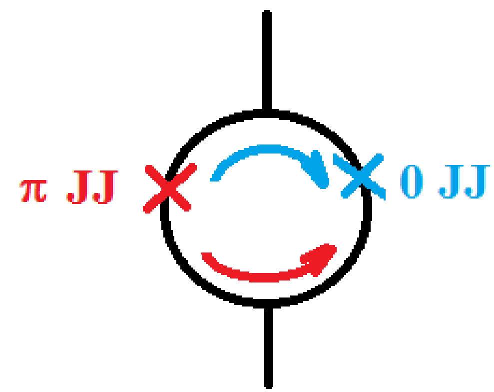

I. I. Soloviev,[1,2] N. V. Klenov,[3,2] S. V. Bakurskiy,[3,4,5] V. V. Bol'ginov,[6,7] V. V. Ryazanov,[6,7]
M. Yu. Kupriyanov,[1,4] and A. A. Golubov[4,5]

APPLIED PHYSICS LETTERS **105**, 242601 (2014)

Spin-orbit valve

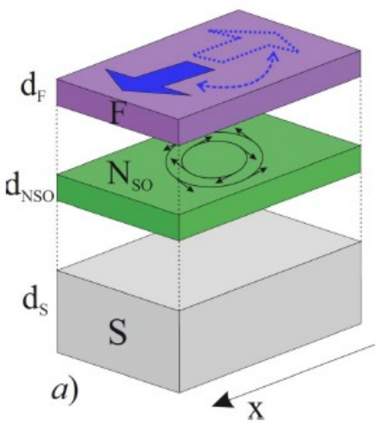

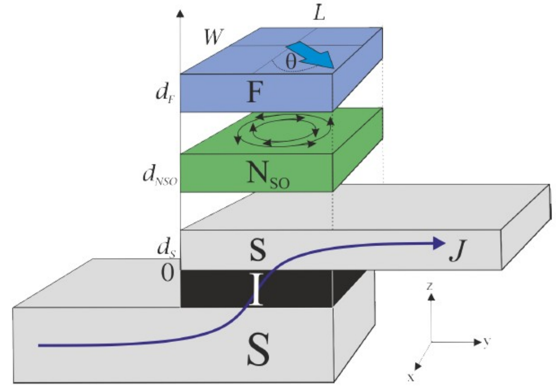

Complicated dispersion law

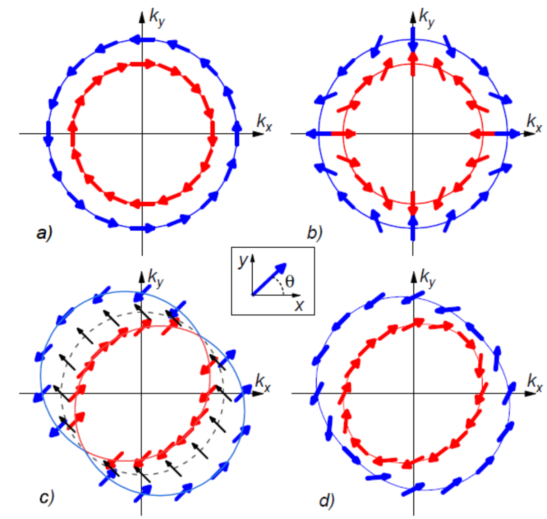

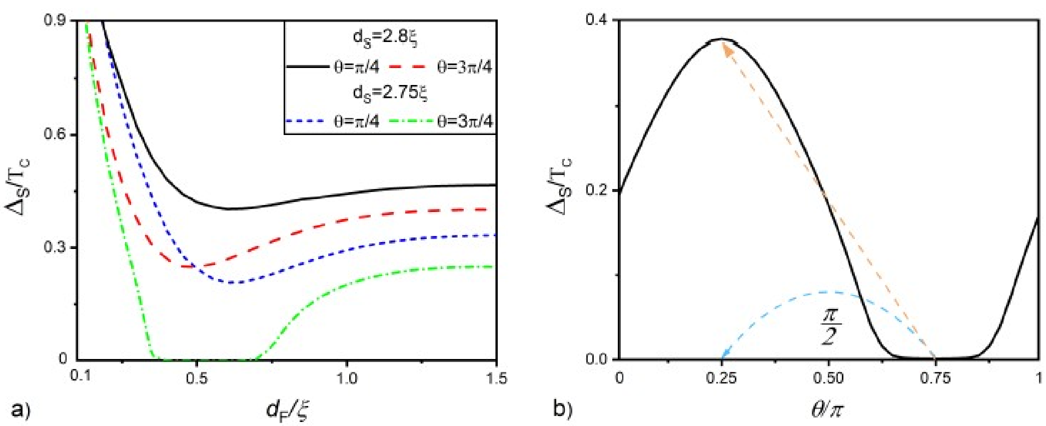

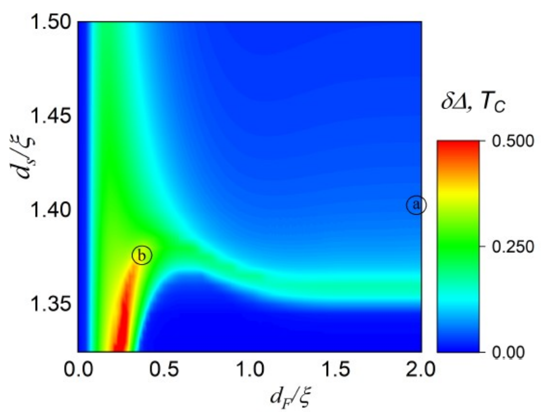

Neilo, A., Bakurskiy, S., Klenov, N., Soloviev, I., & Kupriyanov, M. (2022). Superconducting Valve Exploiting Interplay between Spin-Orbit and Exchange Interactions. *Nanomaterials*, *12*(24), 4426.

Neilo, A., Bakurskiy, S., Klenov, N., Soloviev, I., & Kupriyanov, M. (2023). Tunnel Josephson Junction with Spin–Orbit/Ferromagnetic Valve. *Nanomaterials*, *13*(13), 1970.

Tunable kinetic inductance

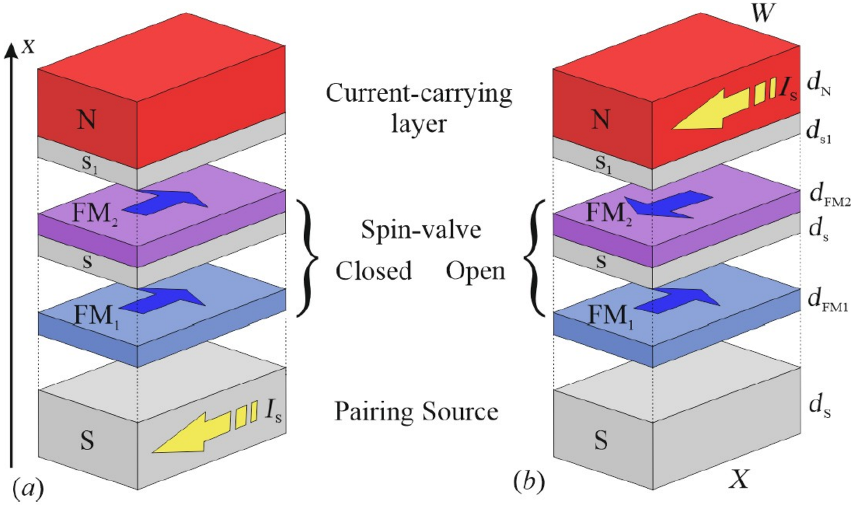

$$\lambda(x)^{-2} = \lambda_0^{-2} \frac{T}{T_C} \sum_{\omega>0} \mathrm{Re}\left(F(x)^2\right); \qquad \lambda_0^{-2} = \frac{2\pi\mu_0 k_B T_C}{\rho_S \hbar},$$

$$L_K = \frac{\mu_0 X}{W}\left[\int_0^d [\lambda(x)]^{-2} dx\right]^{-1},$$

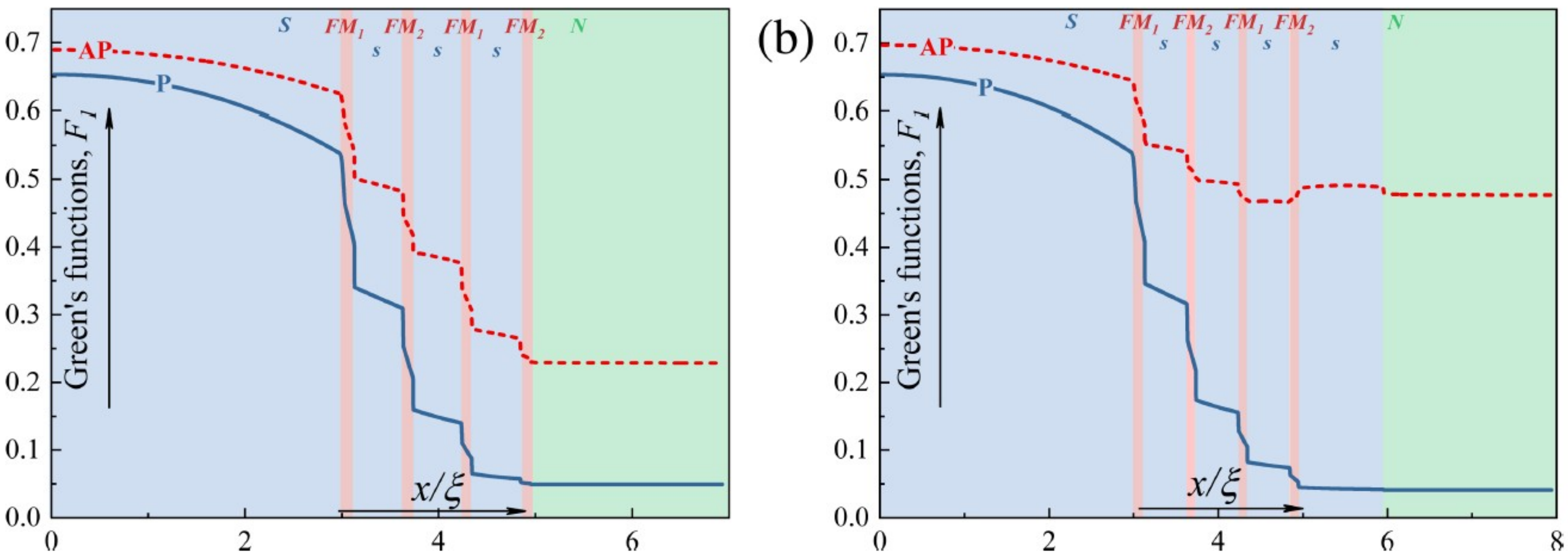

Andrey E. Schegolev, Nikolay V. Klenov, Sergey V. Bakurskiy, Igor I. Soloviev, Mikhail Yu Kupriyanov, Maxim V. Tereshonok, and Anatoli S. Sidorenko. Tunable superconducting neurons for networks based on radial basis functions. *Beilstein journal of nanotechnology*, 13:444–454, 2022. [DOI]

Contents

1. Motivation

2. Basic physics of S-F-N hybrids

3. Hybrid S-F-N structures

   - spin-valves
   - flux traps
   - bi-stable phase junctions
   - Josephson bridges

4. Implementation in applied schemes

   - Bio-inspired neuron
   - All-JJ Logic

RSFQ logic

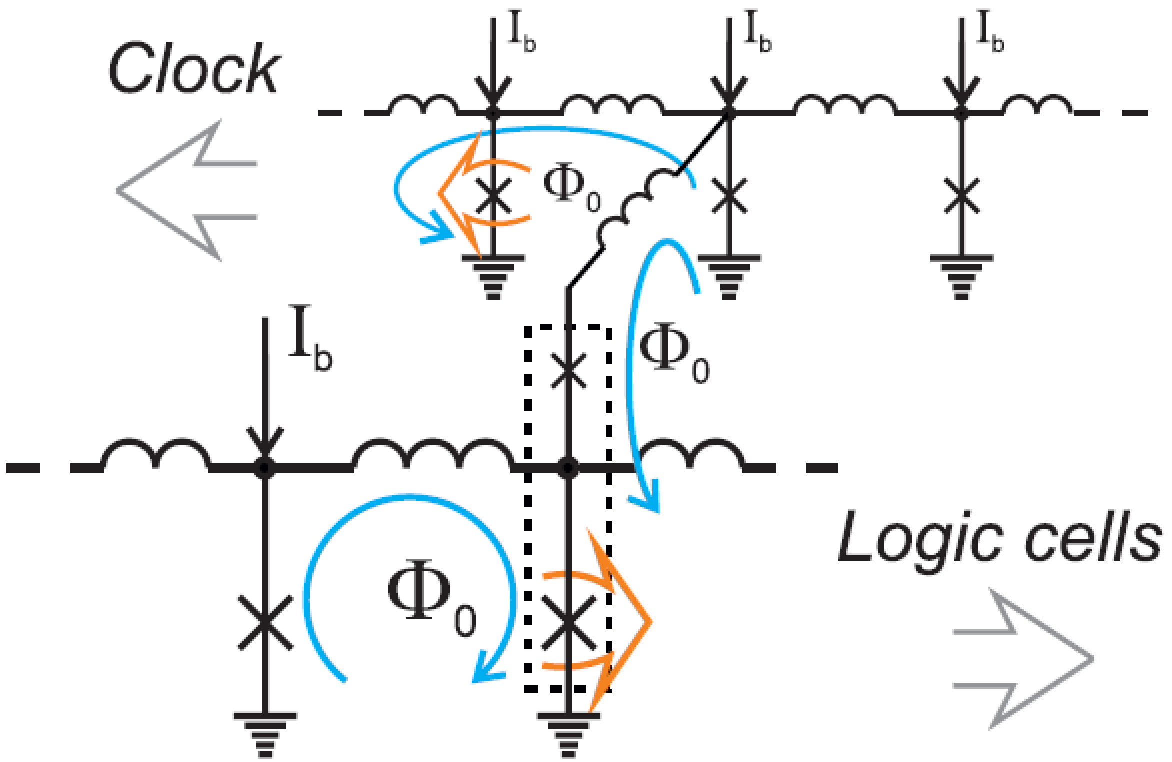

Semenov, V. K. Erasing logic-memory boundaries in superconductor electronics. In *Rebooting Computing (ICRC), IEEE International Conference on* (pp. 1-6). IEEE. (2016).

Soloviev I.I. et al, . After Moore's technologies: operation principles of a superconductor alternative, arXiv preprint arXiv:1706.09124 (2017)

Flux trap near Josephson junction

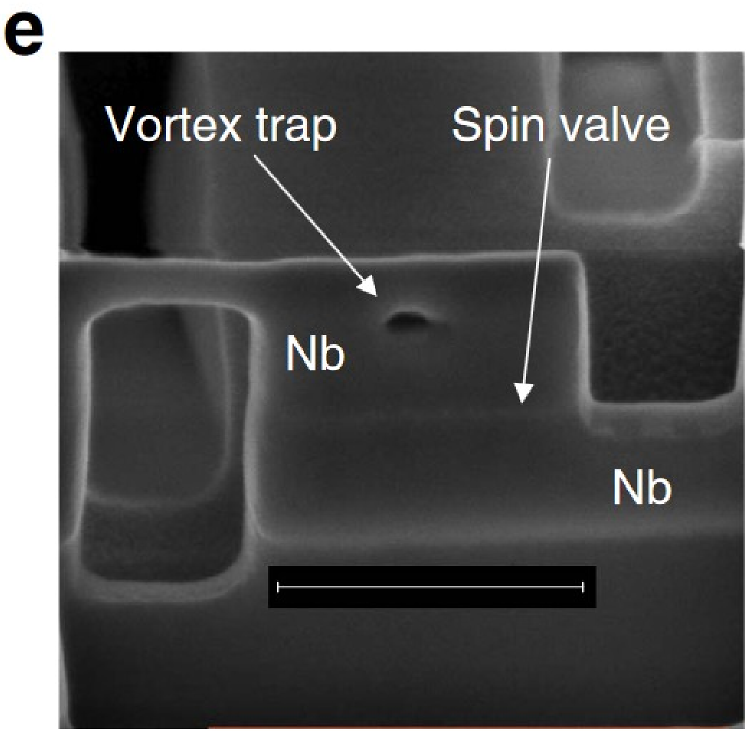

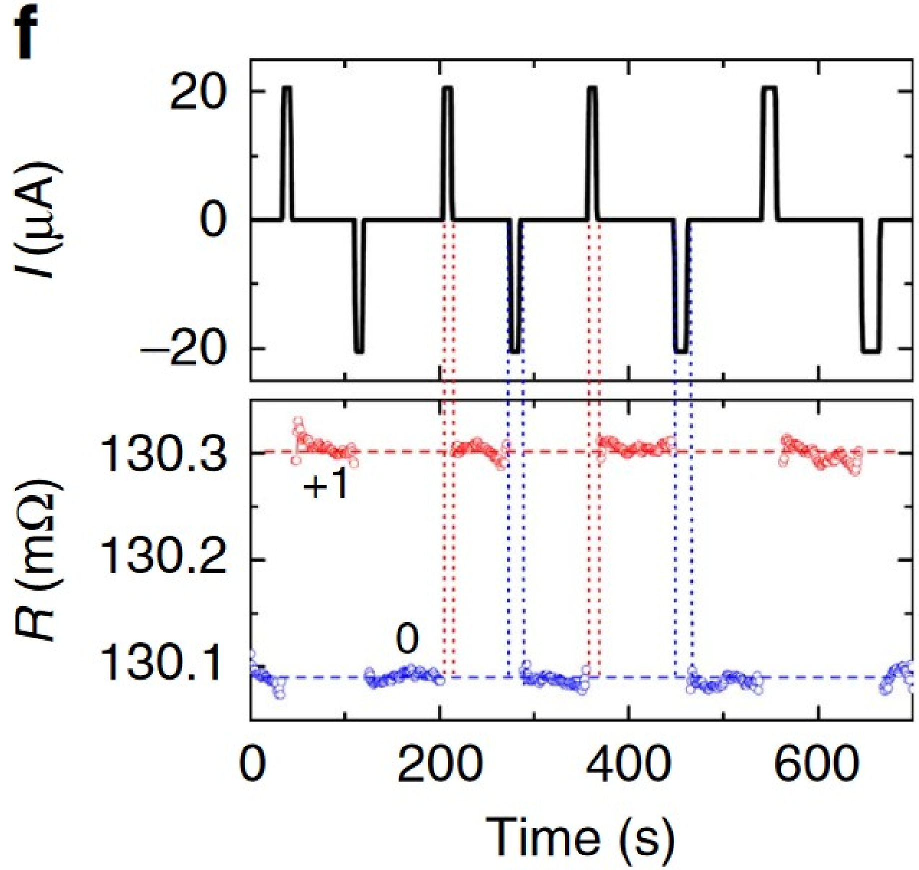

*T **Golod**, **A Iovan**, VM **Krasnov** - Nature communications, Nature communications, 6, 8628 (2015)*

Flux trap in nanowire

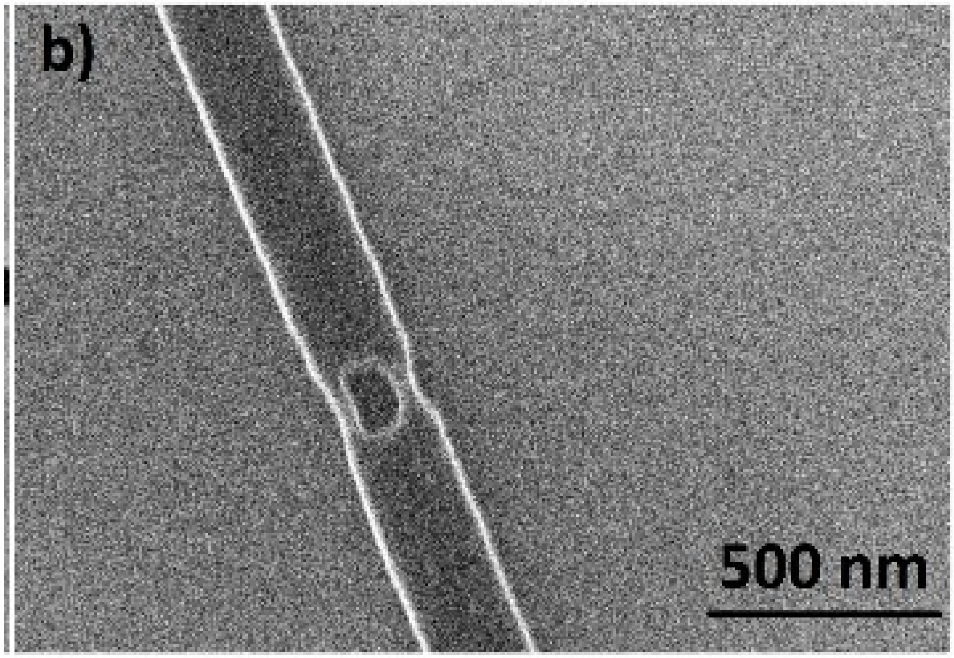

Murphy, A., Averin, D. V., & Bezryadin, A. Nanoscale superconducting memory based on the kinetic inductance of asymmetric nanowire loops. *New J. Phys*, *19*, 063015, (2017).

Flux based memory

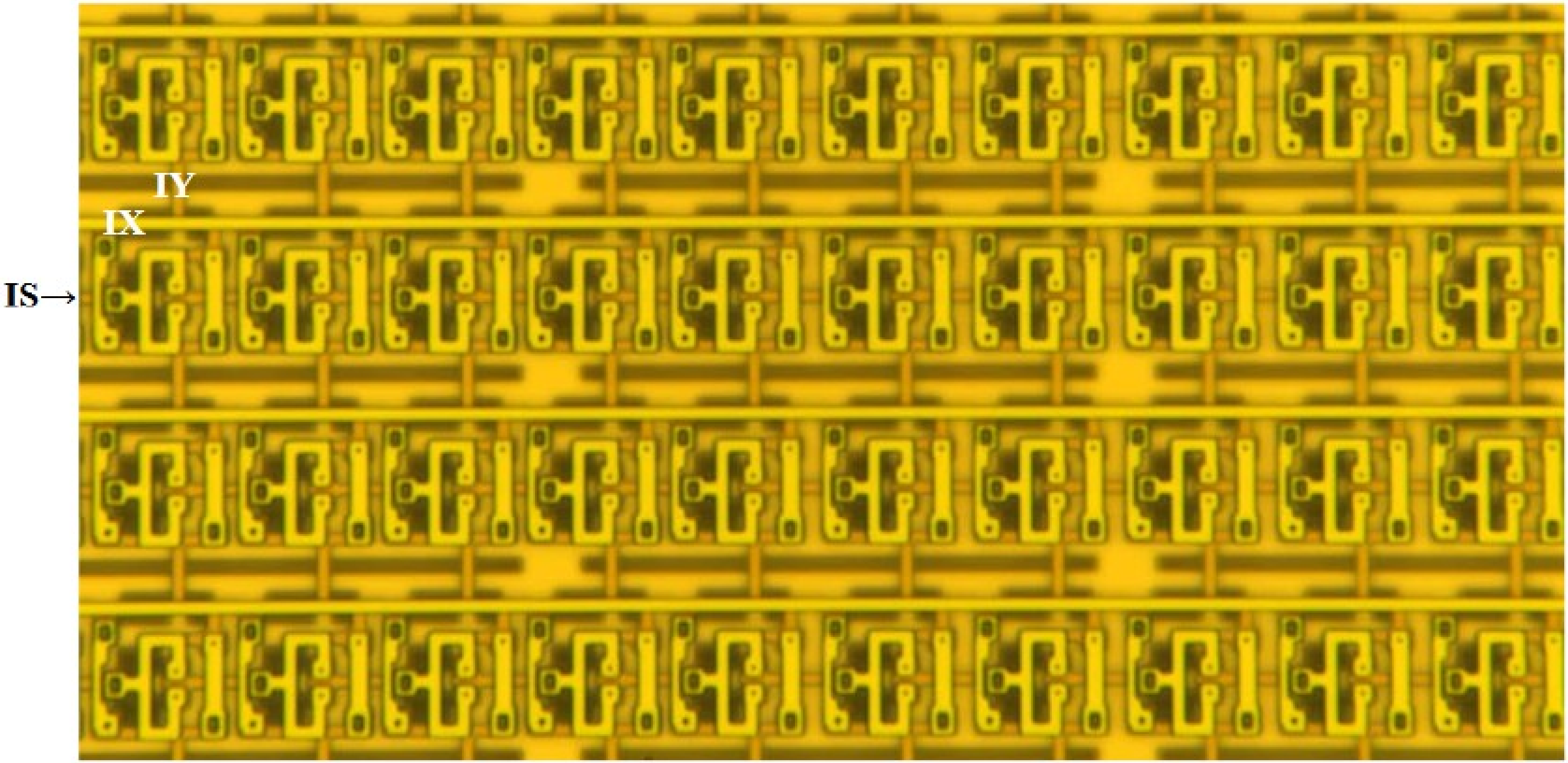

Fig. 5. A ten by four fragment of the 12 x 6 memory cell array fabricated using 600 μA/μm² technology. The word selection and bit selection lines IX and IY are marked in the picture along with the readout line IS. The chip was rotated about 90° for electrical testing, giving a difference in cell labeling in Fig. 6.

Density -1Mbit/cm^2

arXiv:1902.08302 (cross-list from physics.app-ph) [pdf]

Very Large Scale Integration of Josephson-Junction-Based Superconductor Random Access Memories

Vasili K. Semenov, Yuri A. Polyakov, Sergey K. Tolpygo **(2019)**

Contents

1. Motivation

2. Basic physics of S-F-N hybrids

3. Hybrid S-F-N structures

   - spin-valves
   - flux traps
   - bi-stable phase junctions
   - Josephson bridges

4. Implementation in applied schemes

   - Bio-inspired neuron
   - All-JJ Logic

Current Phase Relations

$I_S(\varphi) = A\,sin(\varphi) + B\,sin(2\varphi)+\ldots$

0-state | **π-state**

A>0 ***|B|<|A/2|*** (a) | ***A>0*** ***|B|<|A/2|*** (b)

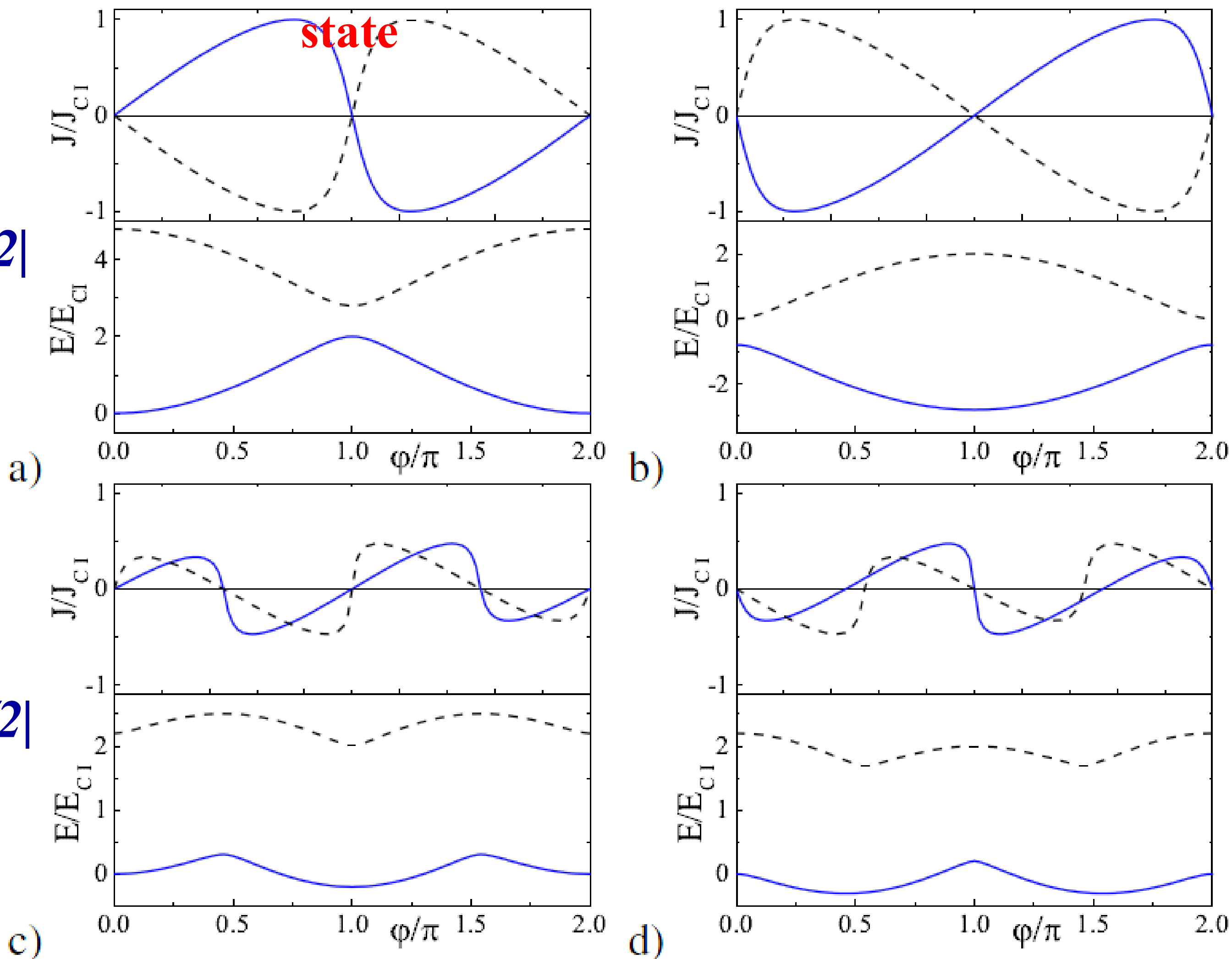

B>0 ***|B|<|A/2|*** (c) | ***B<0*** ***|B|<|A/2|*** (d)

0+π-state | **φ-state**

2^{nd} harmonic in the current-phase relation of SFS junction

Red line is sin(φ) and blue line is sin(2φ) amplitudes

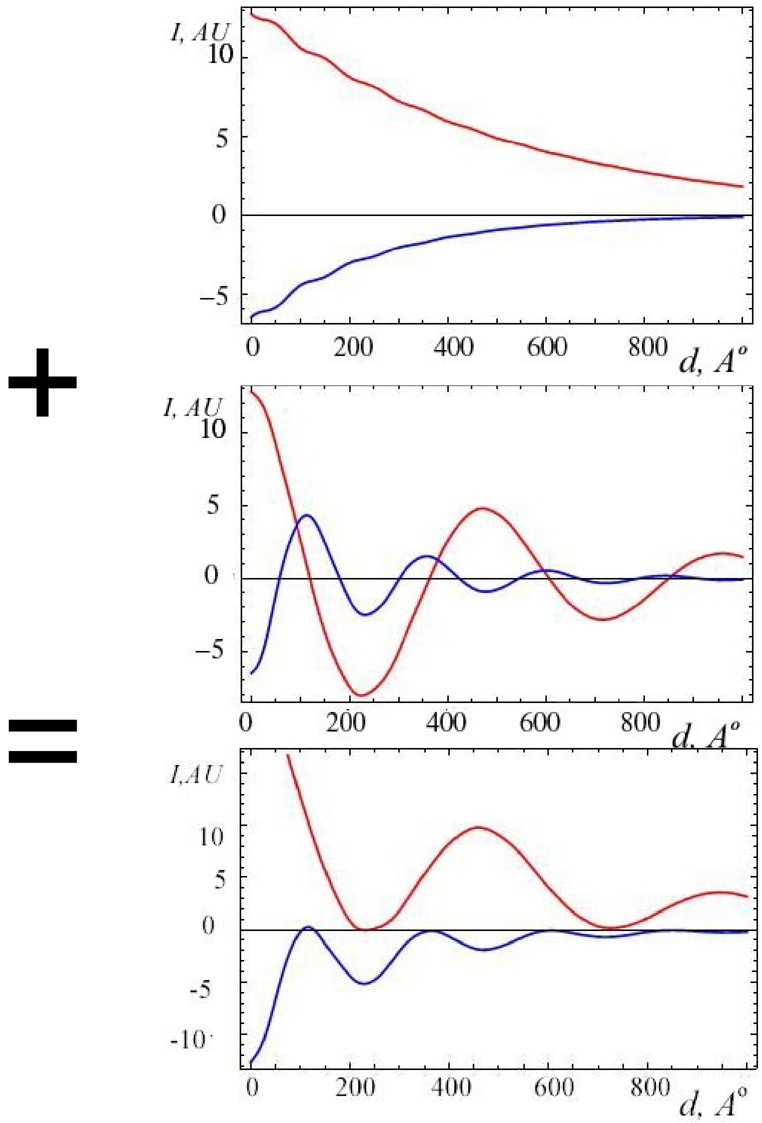

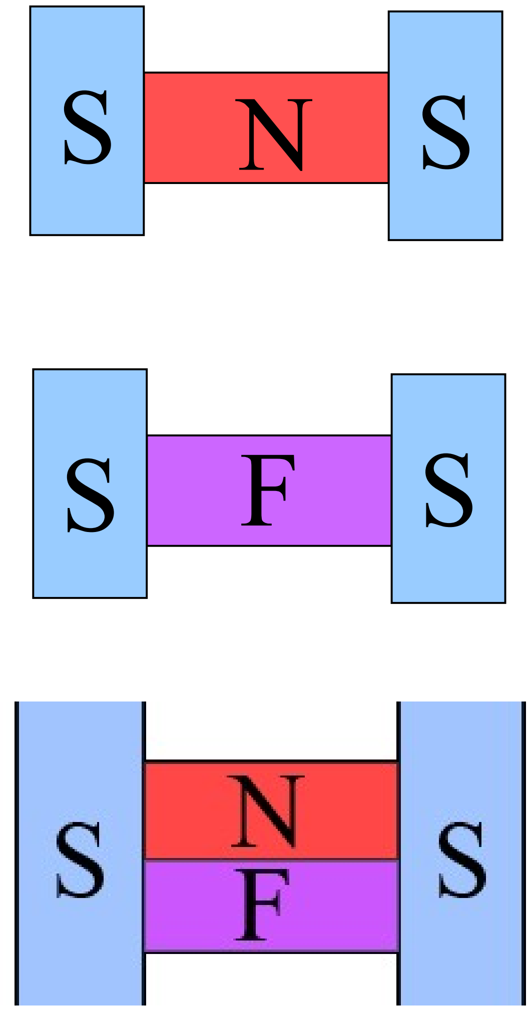

0-π transition

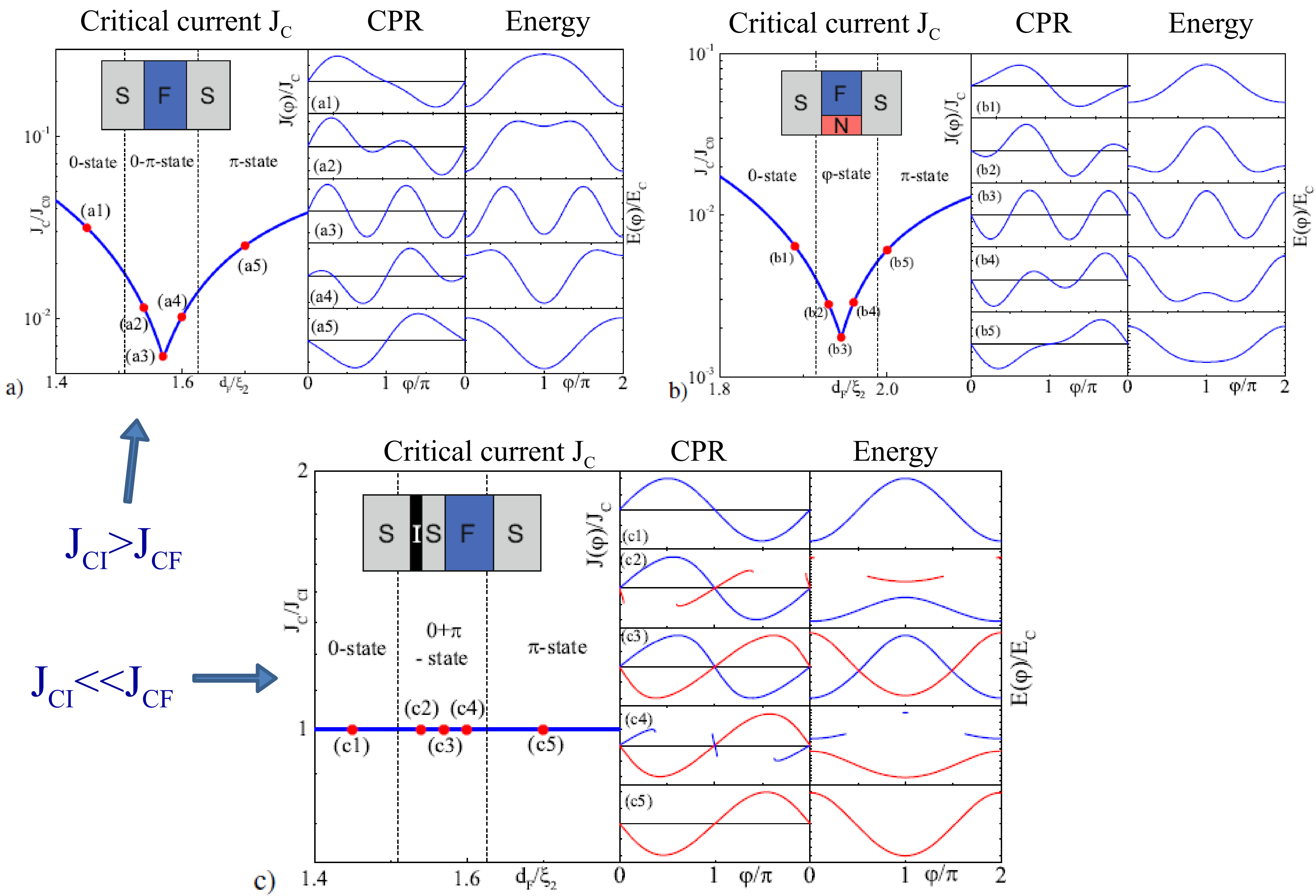

Memory cell based on φ-junction

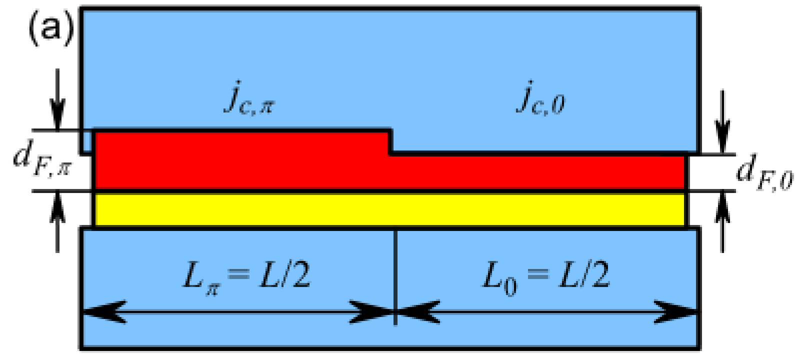

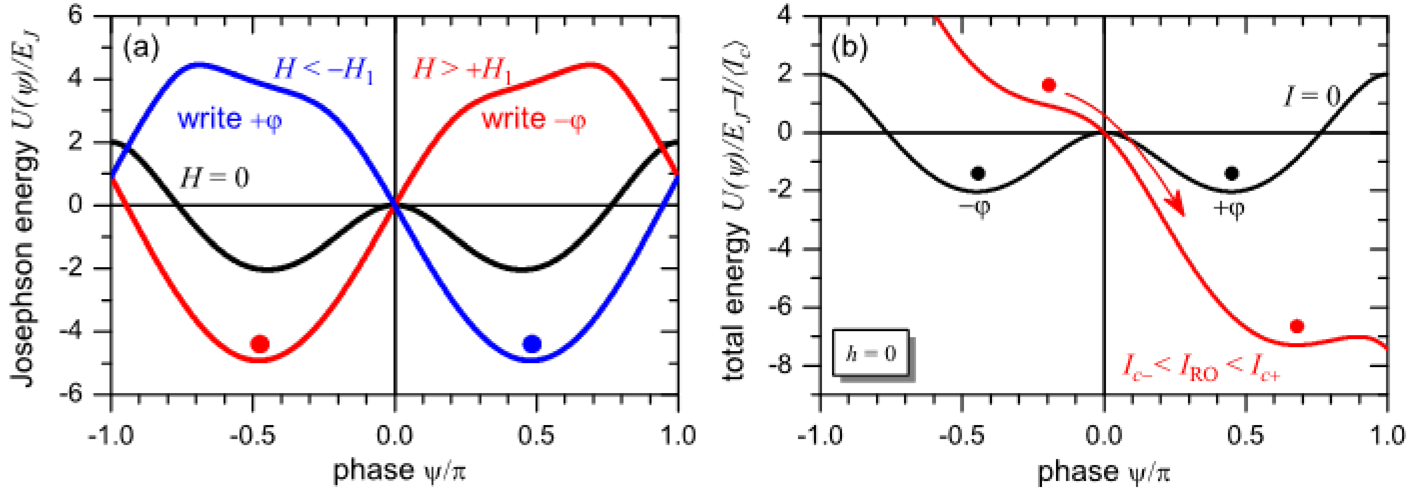

H Sickinger, A Lipman, M Weides, RG Mints, H Kohlstedt, D Koelle, R Kleiner, E Goldobin, Physical review letters 109 (10), 107002

E Goldobin, H Sickinger, M Weides, N Ruppelt, H Kohlstedt, R Kleiner, D Koelle Applied Physics Letters 102 (24), 242602-242602-4

Memory cell based on φ-junction

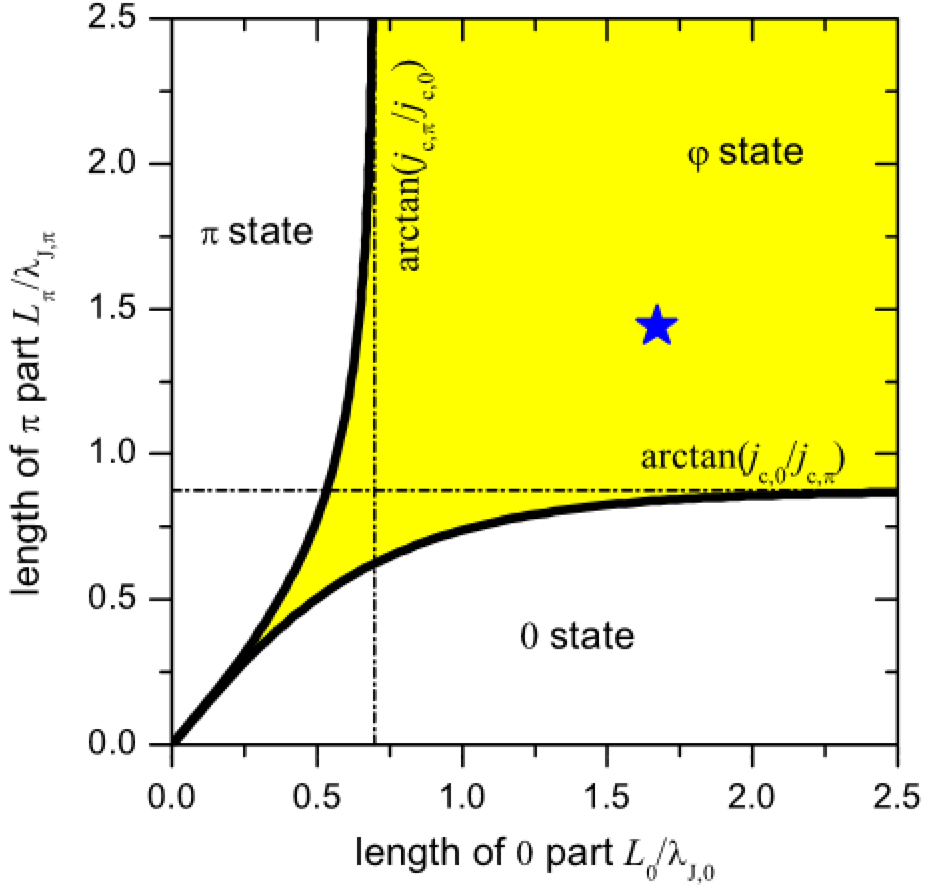

FIG. 3 (color online). Domain of existence of φ state. The ⋆ shows the position of the investigated JJ at $T = 2.35$ K.

φ-state in Nb-CuNi-Nb structures

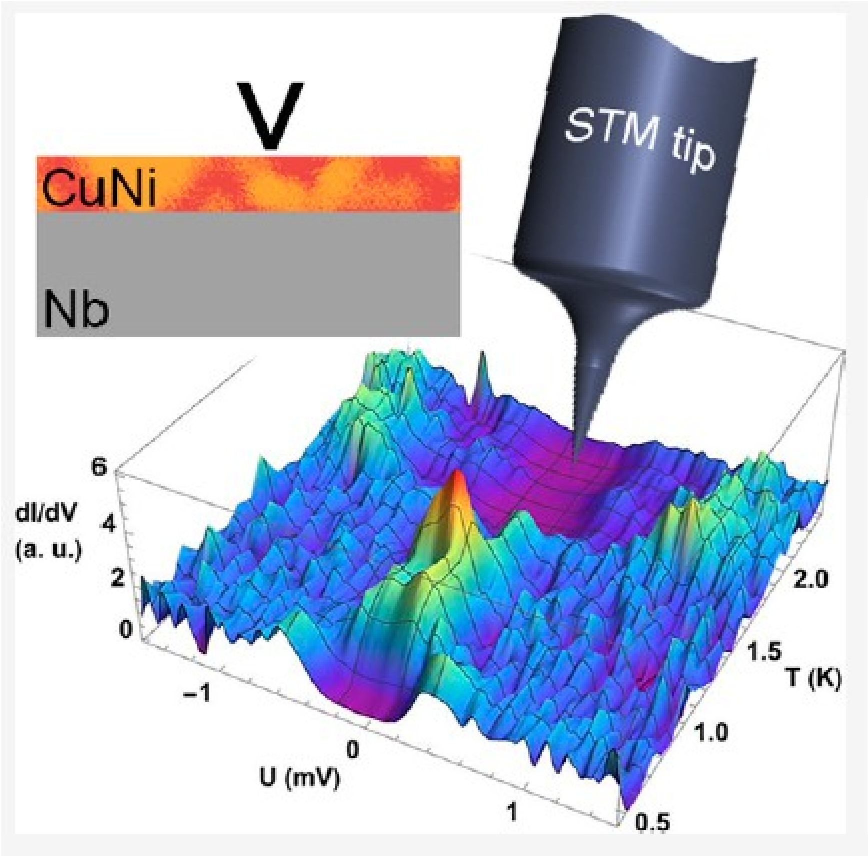

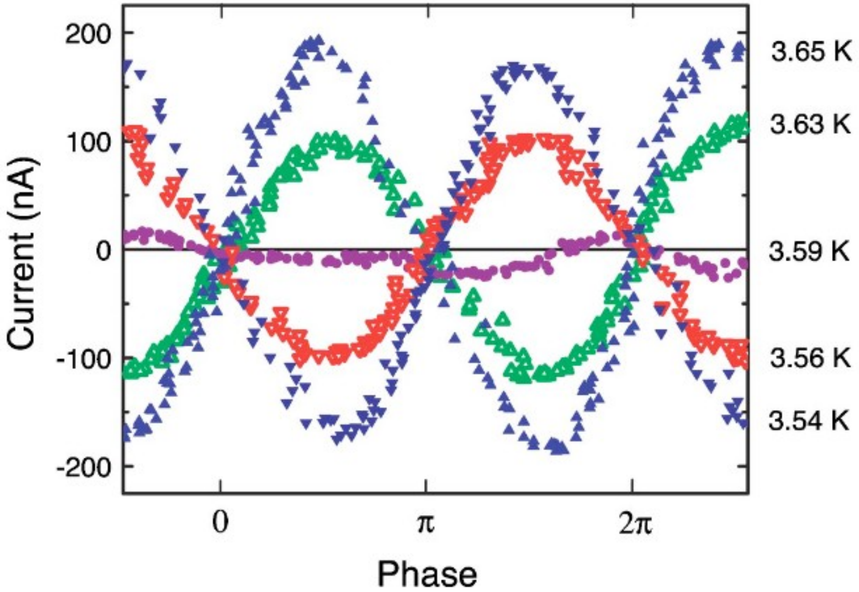

Stolyarov, V., Oboznov, V., Kasatonov, D., Neilo, A., Bakurskiy, S., Klenov, N., ... & Roditchev, D. (2022). Effective Exchange Energy in a Thin, Spatially Inhomogeneous CuNi Layer Proximized by Nb. *The Journal of Physical Chemistry Letters*, *13*(28), 6400-6406.

Frolov, S. M., Van Harlingen, D. J., Oboznov, V. A., Bolginov, V. V., & Ryazanov, V. V. (2004). Measurement of the current-phase relation of superconductor/ferromagnet/superconductor π Josephson junctions. *Physical Review B*, *70*(14), 144505.

Josephson SIsFS structure

0+π-state also has double-well potential,
It can be obtained in the structure with single F-layer

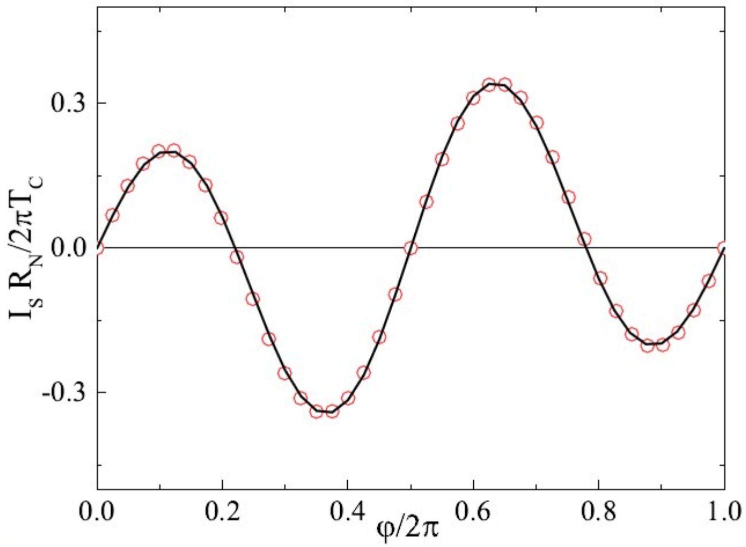

CPR of SFS junction
in the region of 0-π transition

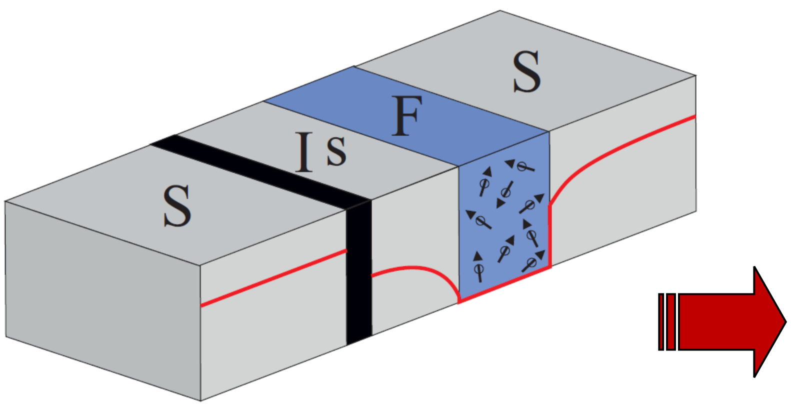

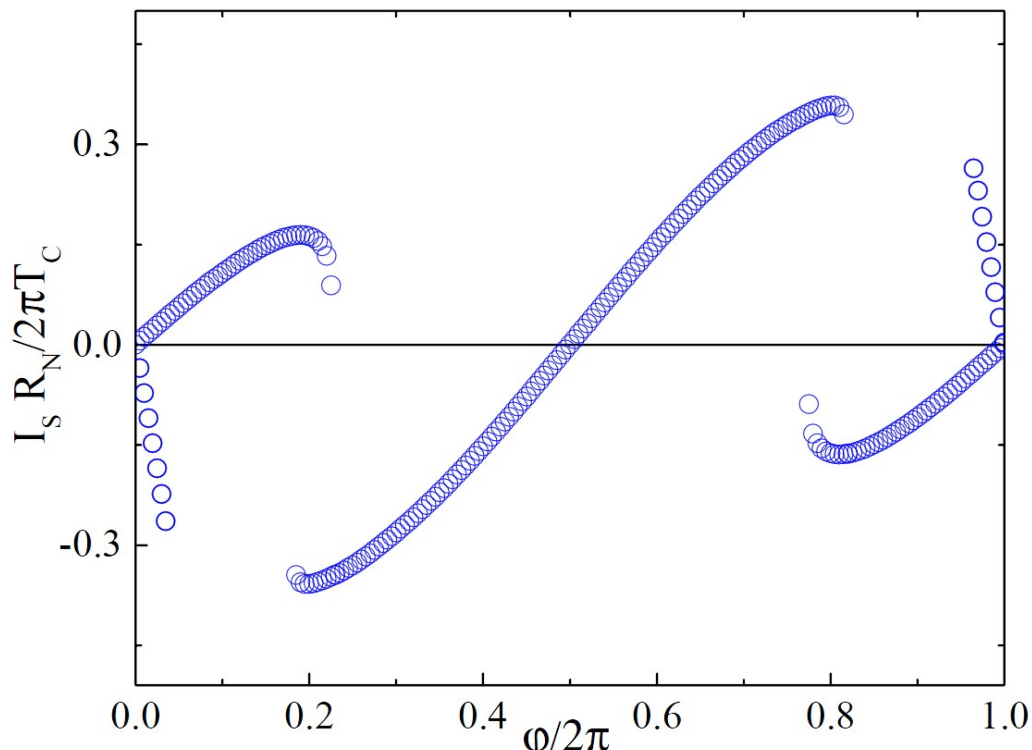

CPR transformation during decrease of d_s

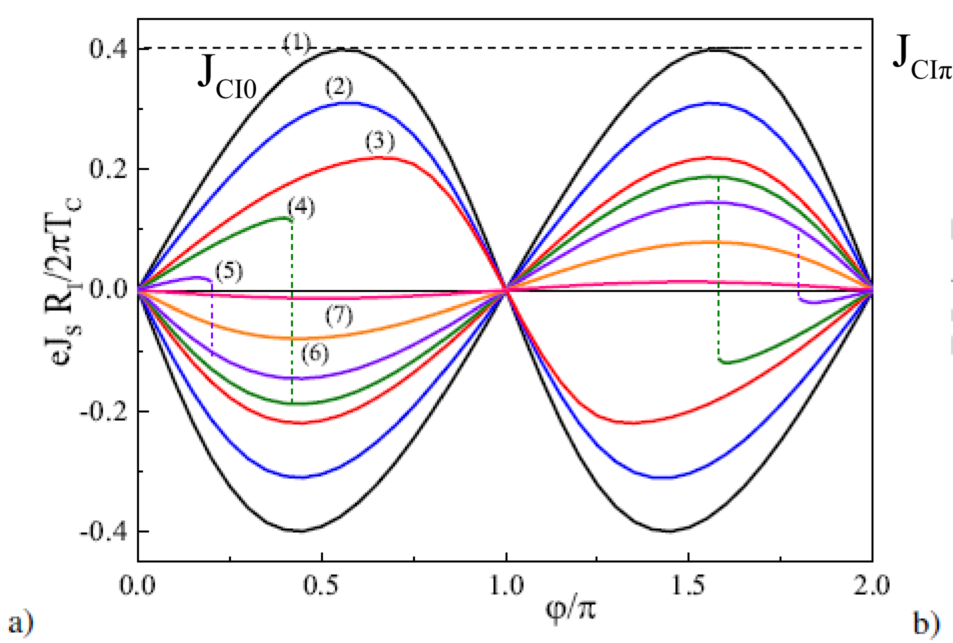

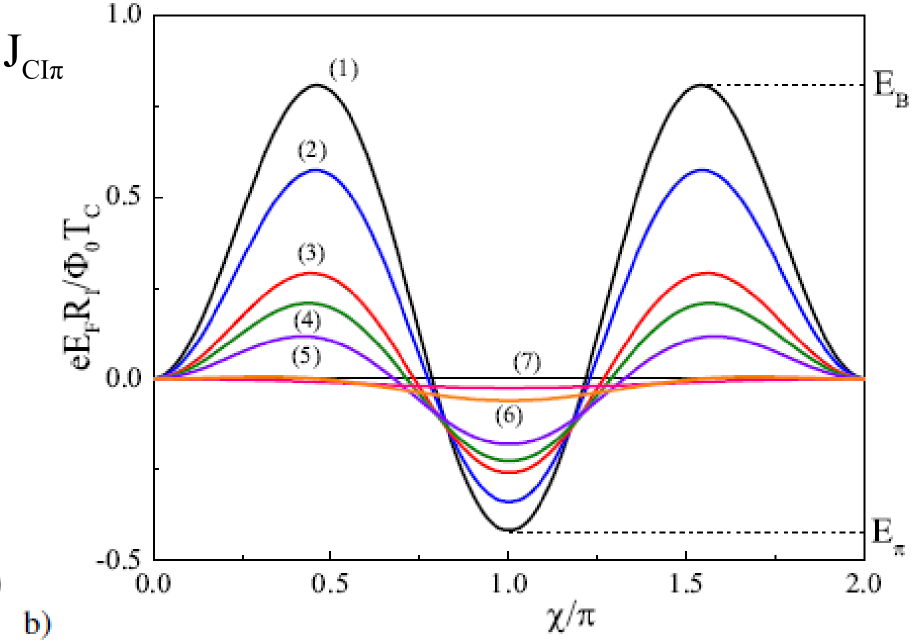

CPR of SIsFS junction for decrease of s-layer thickness

(1) d_s=5ξ, (2) d_s=3.5ξ,
(3) d_s=3ξ, (4) d_s=2.9ξ,
(5) d_s=2.8ξ, (6) d_s=2.7ξ,
(7) d_s=2.6ξ,

Energy phase relation of sFS junction for decrease of s-layer thickness

Local minimum of 0-state disappears near critical thickness d_s=2.7 ξ

Characteristic energies in SIsFS

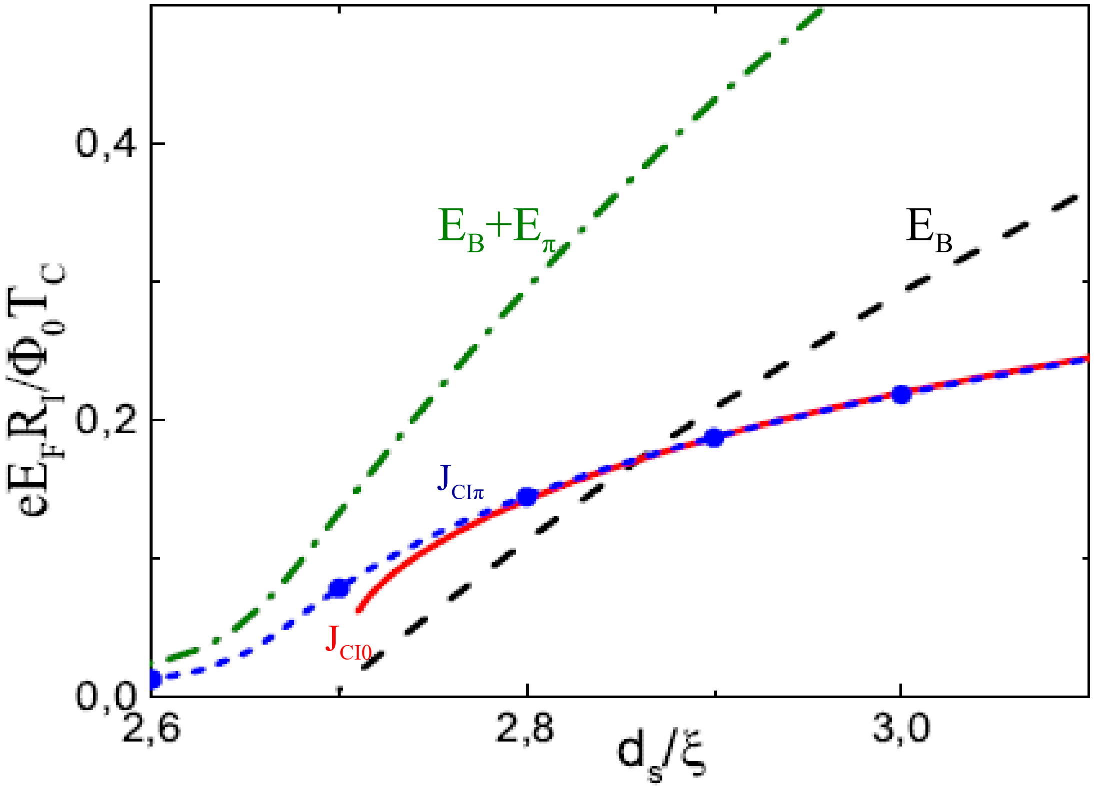

At small thickness of the s-layer the properties of s-layer in 0 and π are different

S. V. Bakurskiy, N. V. Klenov, I. I. Soloviev, N. G. Pugach, M. Y. Kupriyanov, and A. A. Golubov, Appl. Phys. Lett. **113**, 082602 (2018).

Characteristic energies in SIsFS

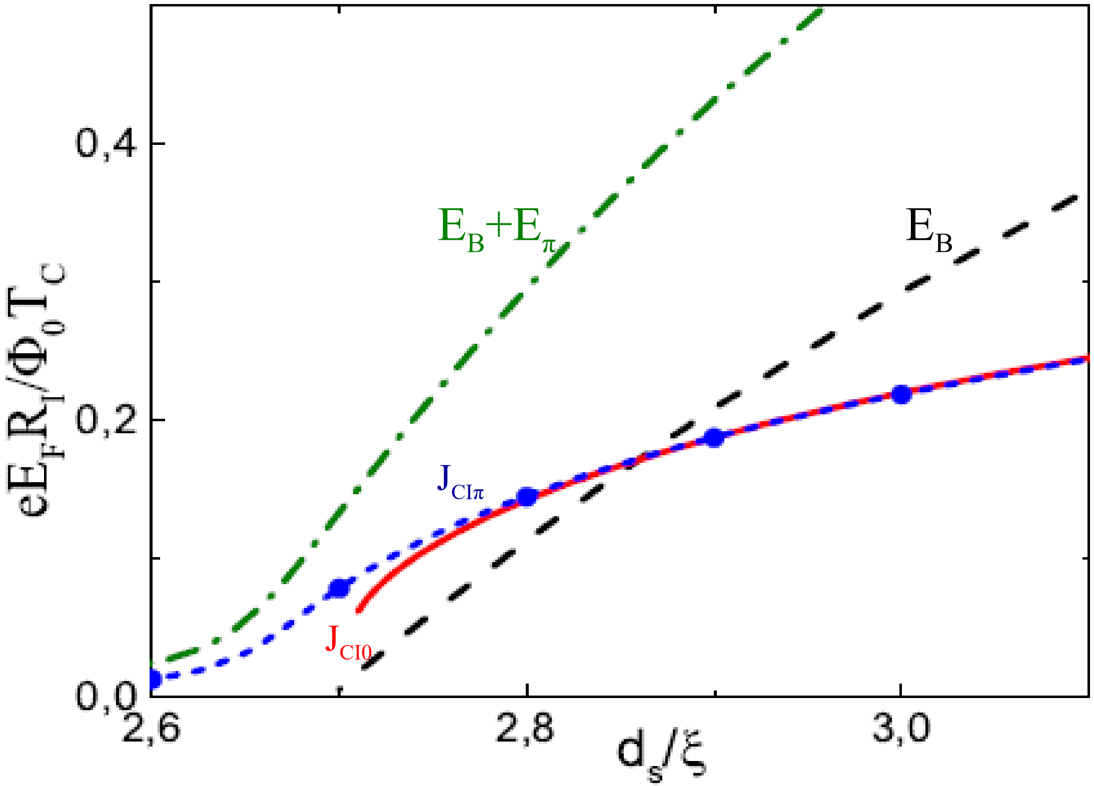

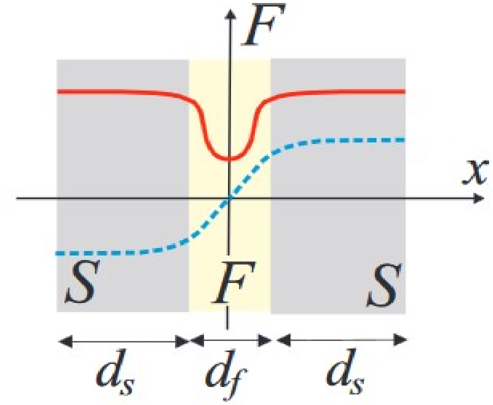

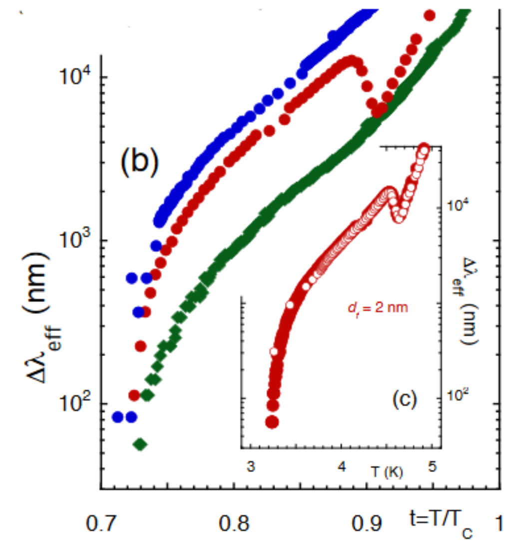

At small thickness of the s-layer the properties of s-layer in 0 and π are different

Measurement of this effect requires very untransparent I layer

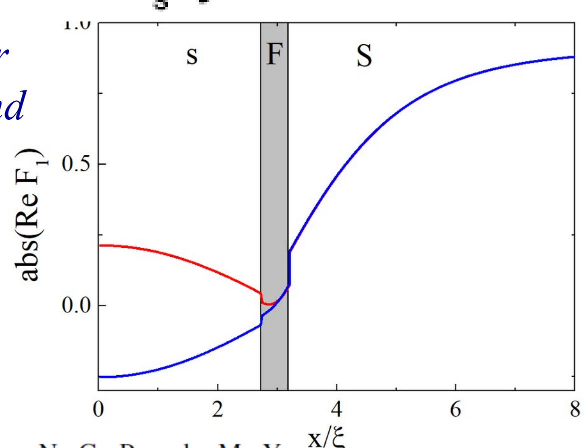

N. Pompeo, K. Torokhtii, C. Cirillo, A. V. Samokhvalov, E. A. Ilyina, C. Attanasio, A. I. Buzdin, and E. Silva Phys. Rev. B **90**, 064510 (2014).

S. N. Vdovichev, Yu. N. Nozdrin, E. E. Pestov, P. A. Yunin, A. V. Samokhvalov, JETP Lett. **104**, 329 (2016).

S. V. Bakurskiy, N. V. Klenov, I. I. Soloviev, N. G. Pugach, M. Y. Kupriyanov, and A. A. Golubov, Appl. Phys. Lett. **113**, 082602 (2018).

CPR of SIsFS with thin s-layer

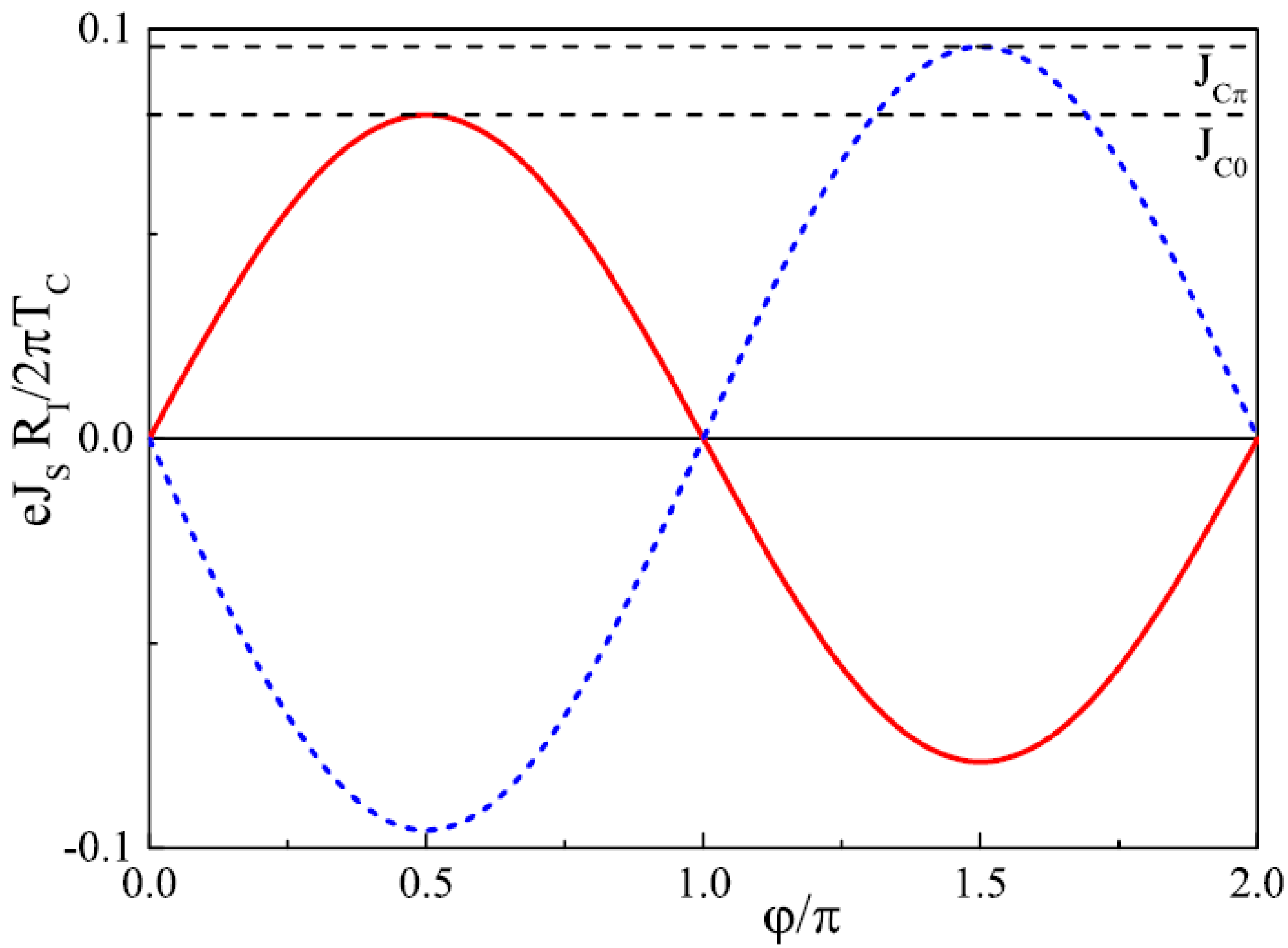

S. V. Bakurskiy, N. V. Klenov, I. I. Soloviev, N. G. Pugach, M. Y. Kupriyanov, and A. A. Golubov, Appl. Phys. Lett. **113**, 082602 (2018).

Truly Josephson Memory?

Electrical control

Read performance of SIS junction

Non-destructive read operation

Remagnitization is not need to write

Scalability

Narrow area of parameters

Small critical current

Nonequilibrium effects?

Superconducting Phase Domain Memory Element

If the size of electrode d_S is finite, the other solution exists.

Considering energy of the system we should take into account 3 terms

- Josephson Energy of SFs junction ΔE_{SFs}
- Josephson Energy of SNs junction ΔE_{SNs}
- Pairing Energy of certain volume ΔE_{DW}

$$\Delta E_{DW} = \Delta F_{GL} l_{DW} d_s W + \frac{\hbar j_{Cs} d_s W}{e} \sim d_s$$
$$\Delta E_{SFs} = \frac{\hbar j_{CF} l_F W}{e} \sim l_F$$
$$\Delta E_{SNs} = \frac{\hbar j_{CN} l_N W}{e} \sim l_N$$

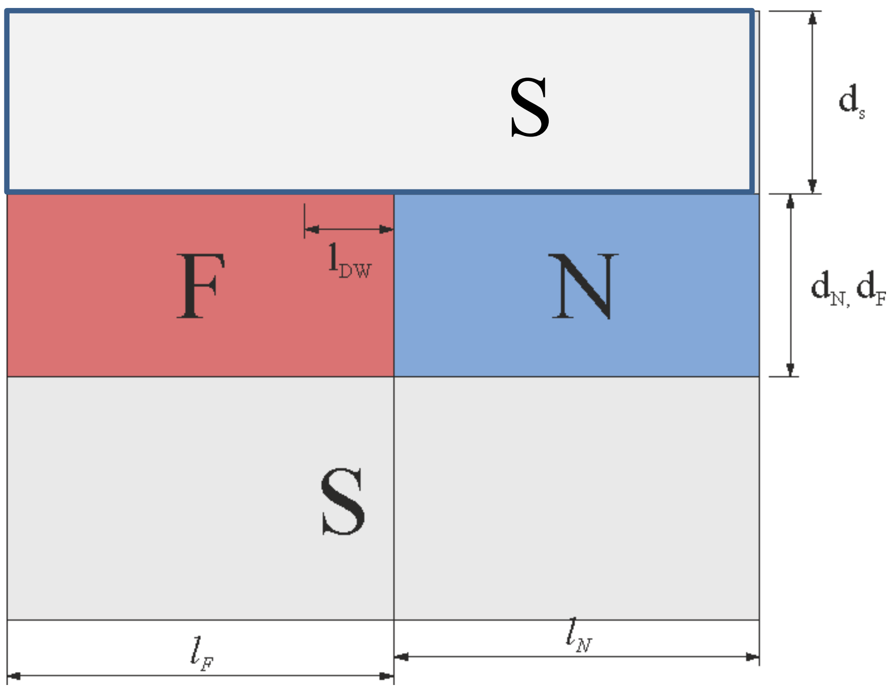

S.V. Bakurskiy, N.V. Klenov, I.I. Soloviev, M.Yu Kupriyanov, A.A. Golubov, Appl.Phys. Lett., 108(4):042602–1–5, (2016)

Superconducting Phase Domain Memory Element

If the size of electrode d_S is finite, the other solution exists.

Considering energy of the system we should take into account 3 terms

- Josephson Energy of SFs junction ΔE_{SFs}
- Josephson Energy of SNs junction ΔE_{SNs}
- Pairing Energy of certain volume ΔE_{DW}

$$\Delta E_{DW} = \Delta F_{GL} l_{DW} d_s W + \frac{\hbar j_{Cs} d_s W}{e} \sim d_s$$
$$\Delta E_{SFs} = \frac{\hbar j_{CF} l_F W}{e} \sim l_F$$
$$\Delta E_{SNs} = \frac{\hbar j_{CN} l_N W}{e} \sim l_N$$

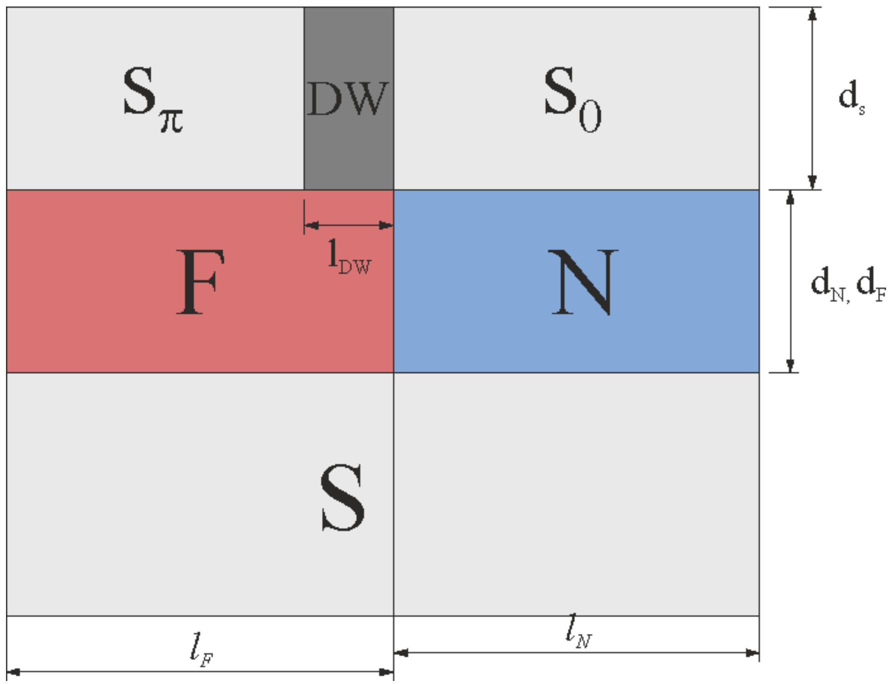

S.V. Bakurskiy, N.V. Klenov, I.I. Soloviev, M.Yu Kupriyanov, A.A. Golubov, Appl.Phys. Lett., 108(4):042602–1–5, (2016)

S-F/N-s system with thin s electrode

Numerical Solution for Pair Potential Δ

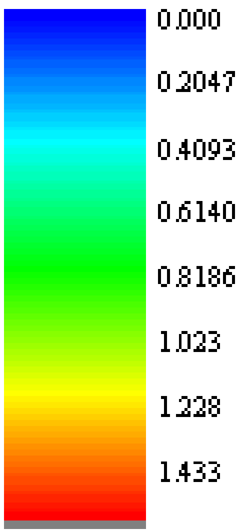

$d_F = 1\,\xi_S$

$W = 16\,\xi_S$

$H = 10\pi T_C$

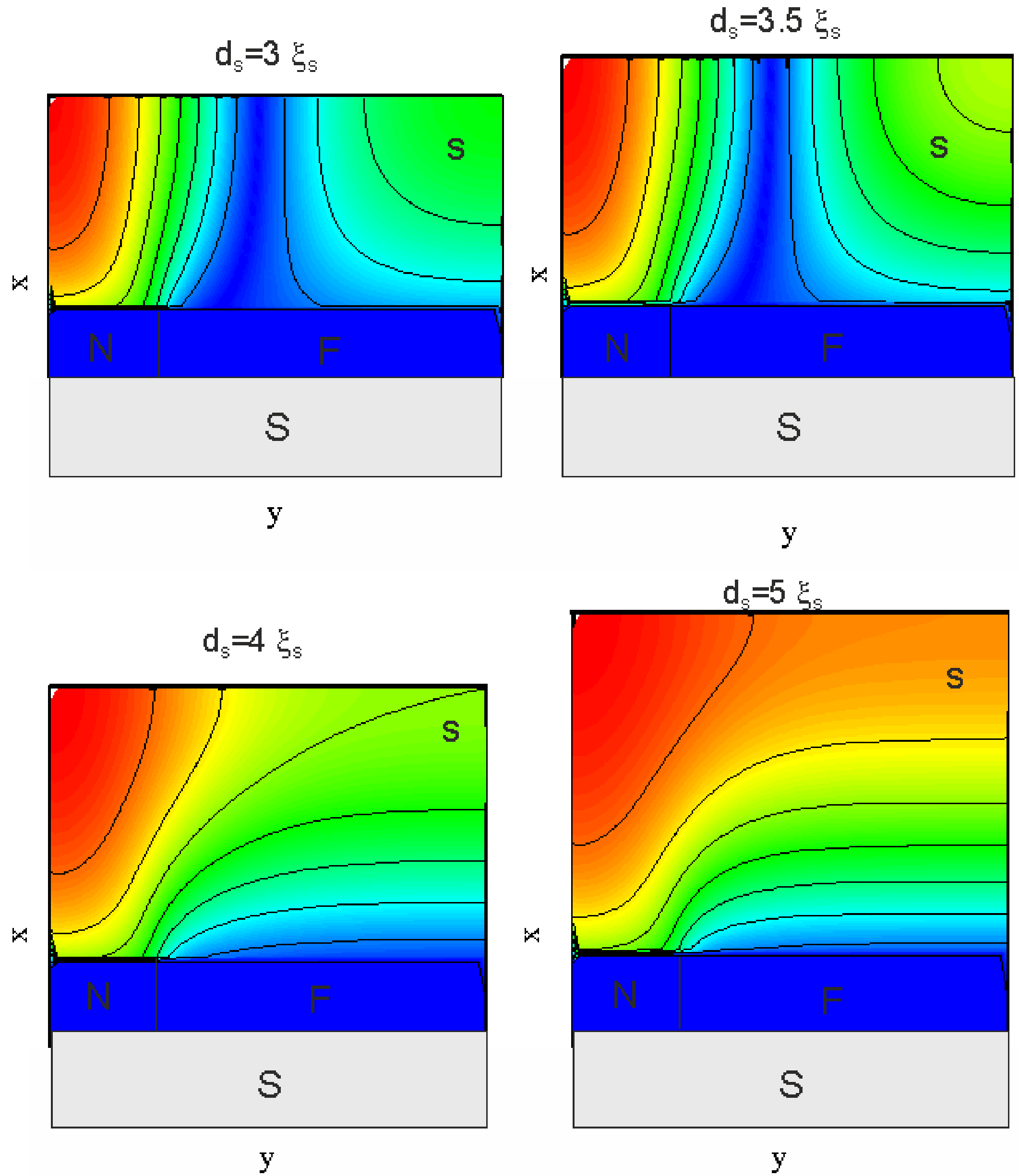

Is it possible to use it for memory element?

$$E = \frac{\hbar J_{Cs}(l_{DW})}{2e}(1-\cos\varphi) + \frac{\hbar J_{CSFs}}{2e}(1-\cos(\pi-\varphi)) + \Delta E_{DW}(l_{DW})$$

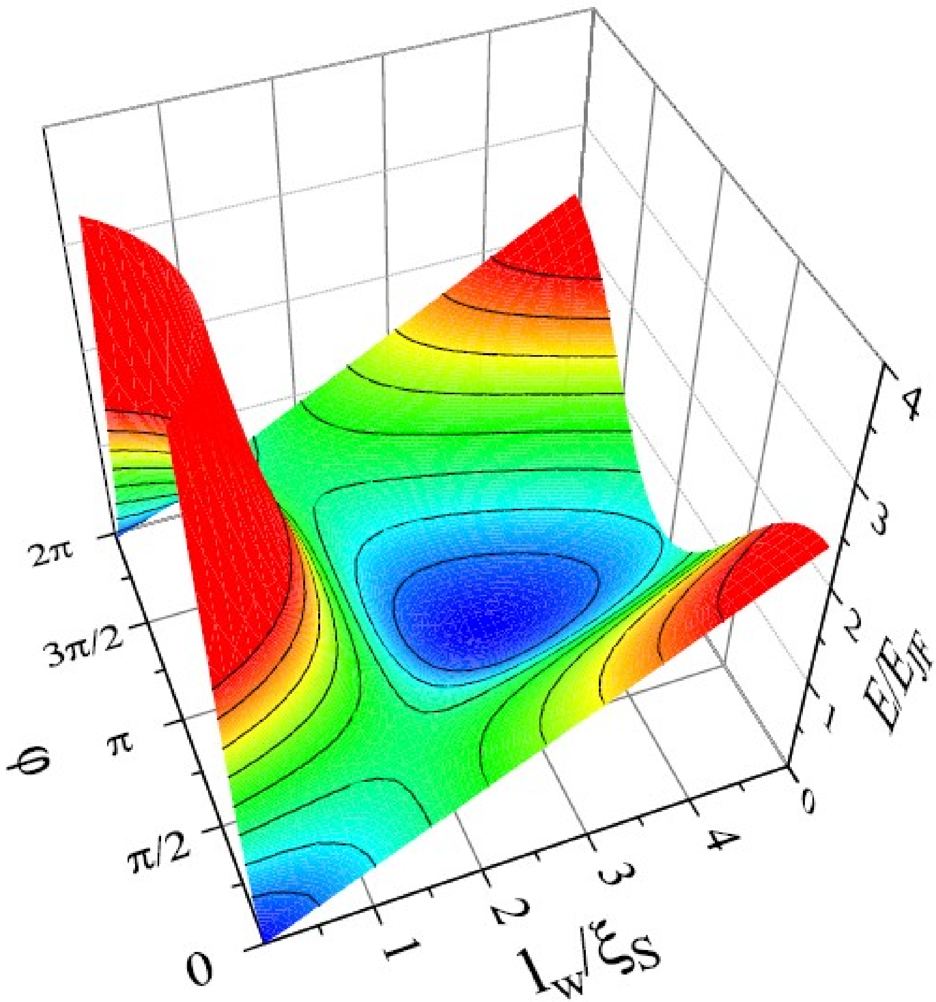

Yes!

Choose critical parameters
$E_{SFS} = E_{Dwall}$

This system has double well potential with 2 possible states: domain and single

Superconducting Phase Domain Memory Element

Domain states can be controlled by current pulses

WRITE SPD-state operation

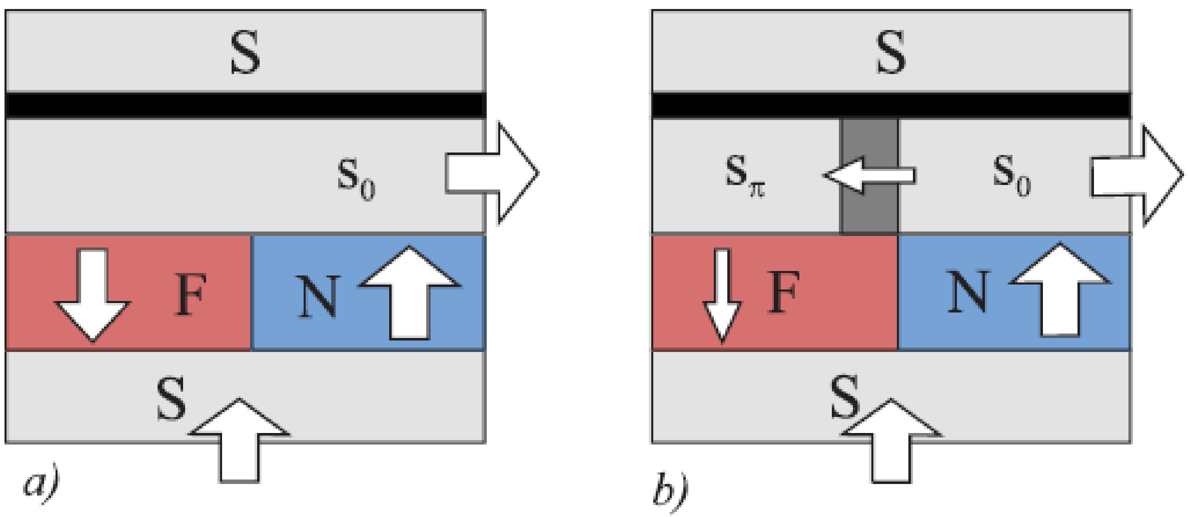

Critical current of SPD-wall < Critical current of SFS junction

 Reverse current of SPD state is smaller than in single state

 SPD-state has larger critical current

 Switch to SPD state

Superconducting Phase Domain Memory Element

Domain states can be controlled by current pulses

WRITE Single-state operation

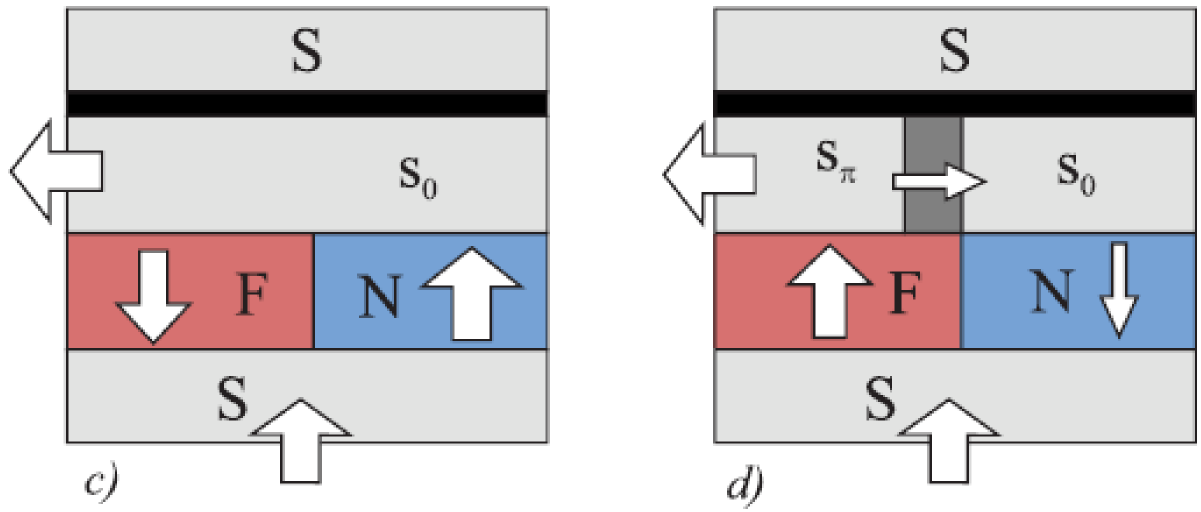

Critical current of SPD-wall < Critical current of SFS junction

Reverse current limited by SPD-wall

Total current: J_{SFS}-J_{SPD} is much smaller J_{SNS}

Switch to Single state

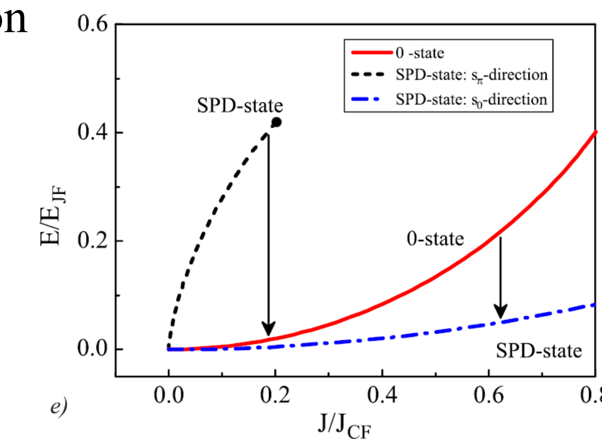

Superconducting Phase Domain Memory Element

READ operation

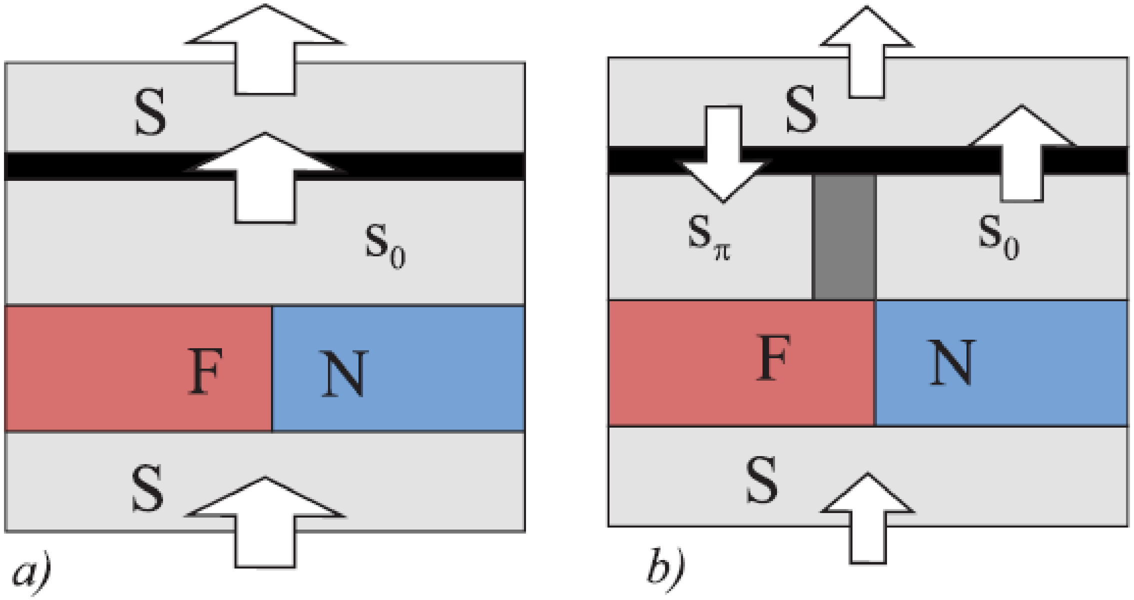

Additional electrode is protected by tunnel barrier and doesn't impact on the properties of the system

Critical current of domain state (b) is much less, than critical current of single state (a)!

S.V. Bakurskiy, N.V. Klenov, I.I. Soloviev, M.Yu Kupriyanov, A.A. Golubov, Appl.Phys. Lett., 108(4):042602–1–5, (2016)

Contents

1. Motivation

2. Basic physics of S-F-N hybrids

3. Hybrid S-F-N structures

- spin-valves
- flux traps
- bi-stable phase junctions
- Josephson bridges

4. Implementation in applied schemes

- Bio-inspired neuron
- All-JJ Logic

SN-N-NS Bridges

Motivation: scalability
and reproducibility!

In short limit $L_B << \xi_N$
properties are determined by
under-electrode area

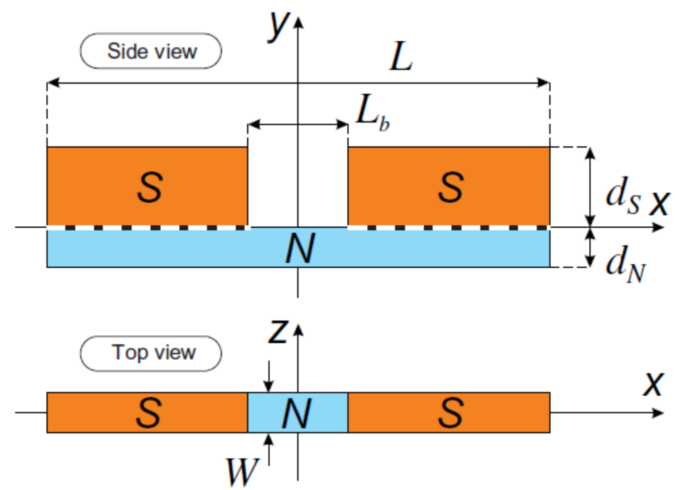

Perspective candidate for 100 nm-scale electronics

PHYSICAL REVIEW APPLIED **16,** 044060 (2021)

Miniaturization of Josephson Junctions for Digital Superconducting Circuits

I.I. Soloviev,[1,2,3,*] S.V. Bakurskiy,[1,3,4] V.I. Ruzhickiy,[1,2,3] N.V. Klenov,[1,2,3] M.Yu. Kupriyanov,[1]
A.A. Golubov,[4,5,†] O.V. Skryabina,[1,4,6] and V.S. Stolyarov[3,4]

Short bridges $L_B << \xi_N$

Transparent interface

$$\sqrt{\gamma_{BM}} \ll L_b/\xi_N \ll 1$$

$$\frac{eR_N J_S}{2\pi k_B T_c} = t \sum_{\omega \geq 0} \frac{2\Delta \cos\frac{\varphi}{2}}{\Omega_1} \arctan \frac{\Delta \sin\frac{\varphi}{2}}{\Omega_1},$$

$$\Omega_1 = \sqrt{\Omega^2 + \Delta^2 \cos^2 \frac{\varphi}{2}},$$

$$\Omega = \omega\left(1 + \gamma_{BM}\sqrt{\omega^2 + \Delta^2}\right)$$

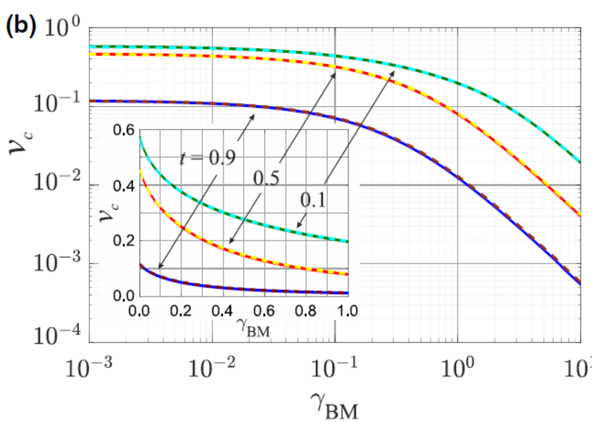

Untransparent interface

$$\frac{L_b}{\xi_N} \ll \frac{\gamma_{BM}}{(1+\gamma_{BM})},$$

$$\frac{eR_N J_S}{2\pi k_B T_c} = t \sum_{\omega \geq 0} \frac{\sqrt{2}\Delta^2 \sin\varphi}{\Omega_1 \sqrt{\left(\sqrt{\Omega^2 + \Delta^2} + \Omega_1\right)} \sqrt{\omega^2 + \Delta^2}},$$

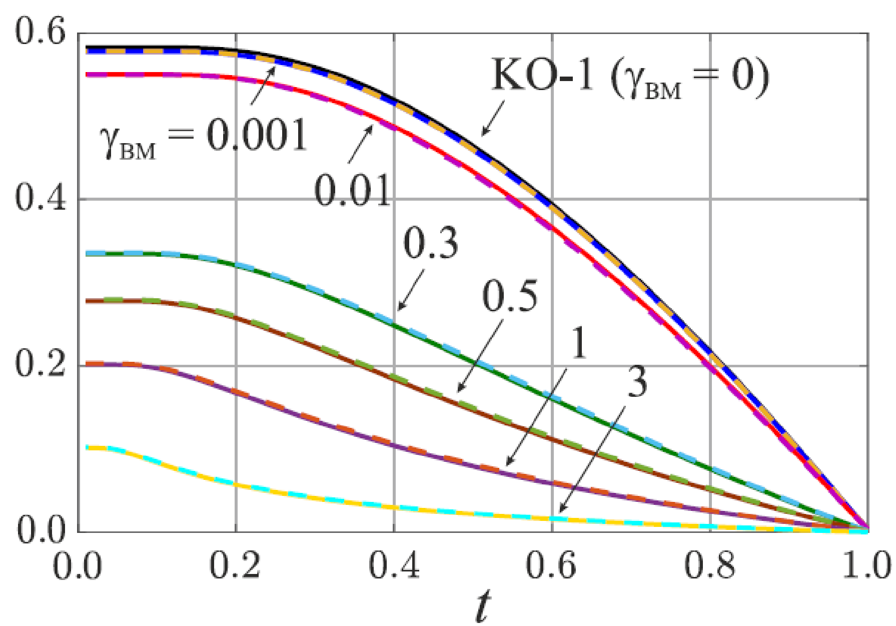

Soloviev, I. I., Bakurskiy, S. V., Ruzhickiy, V. I., Klenov, N. V., Kupriyanov, M. Y., Golubov, A. A., ... & Stolyarov, V. S. (2021). Miniaturization of Josephson Junctions for Digital Superconducting Circuits. *Physical review applied*, *16*(4), 044060.

Long SNS junction, L>>ξ

Thouless energy: $\epsilon_c = \hbar D / L^2$.

$D = v_F l_e / 3$

$$eR_N I_c = \frac{32}{3+2\sqrt{2}} \epsilon_c \left[\frac{L}{L_T}\right]^3 e^{-L/L_T}.$$

At zero temperature

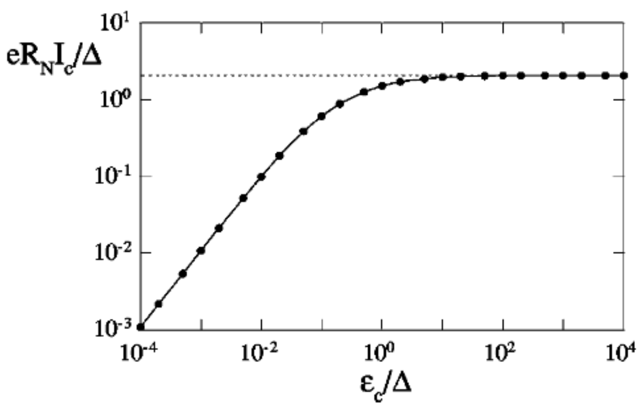

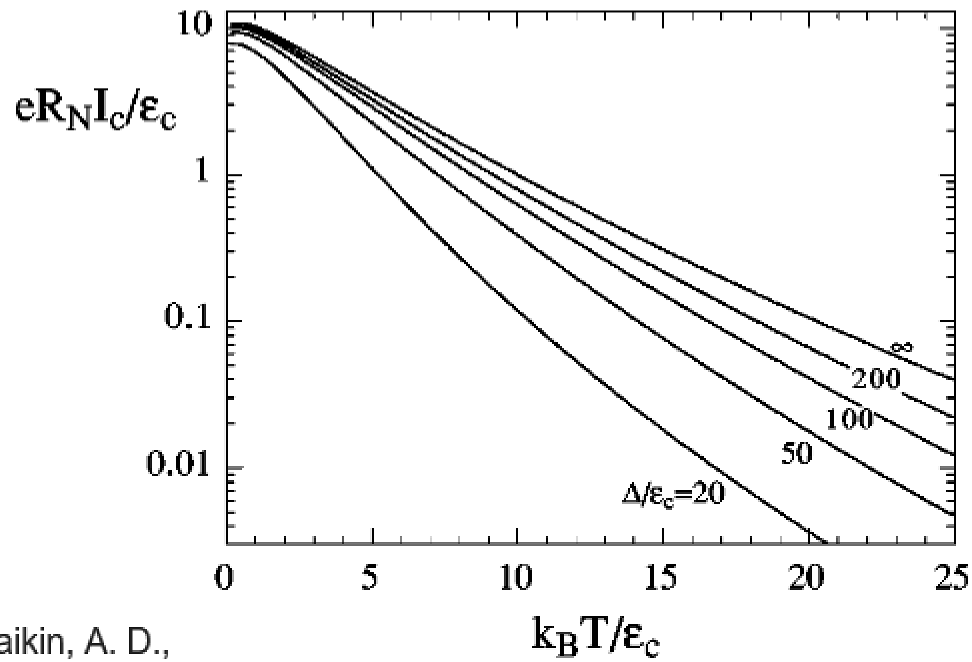

Dubos, P., Courtois, H., Pannetier, B., Wilhelm, F. K., Zaikin, A. D., & Schön, G. (2001). Josephson critical current in a long mesoscopic SNS junction. *Physical Review B*, *63*(6), 064502.

External flux dependence

$$\frac{\hbar D}{\pi}\nabla\cdot(\hat{G}^R\check{\nabla}\hat{G}^R)+\epsilon[\hat{\tau}_3,\hat{G}^R]=\frac{ieD}{\pi}\mathbf{A}\cdot[\hat{\tau}_3,\hat{G}^R\check{\nabla}\hat{G}^R].$$

$$\hat{G}^R=\begin{pmatrix} g^R & f^R \\ \tilde{f}^R & \tilde{g}^R \end{pmatrix}$$

$$\left(\nabla-\frac{2ie}{\hbar}\mathbf{A}\right)^2\gamma^R+\frac{\tilde{f}^R}{i\pi}\left[\left(\nabla-\frac{2ie}{\hbar}\mathbf{A}\right)\gamma^R\right]^2=-2i\frac{\epsilon}{\hbar D}\gamma^R,$$

$$\left(\nabla+\frac{2ie}{\hbar}\mathbf{A}\right)^2\tilde{\gamma}^R+\frac{f^R}{i\pi}\left[\left(\nabla+\frac{2ie}{\hbar}\mathbf{A}\right)\tilde{\gamma}^R\right]^2=-2i\frac{\epsilon}{\hbar D}\tilde{\gamma}^R.$$

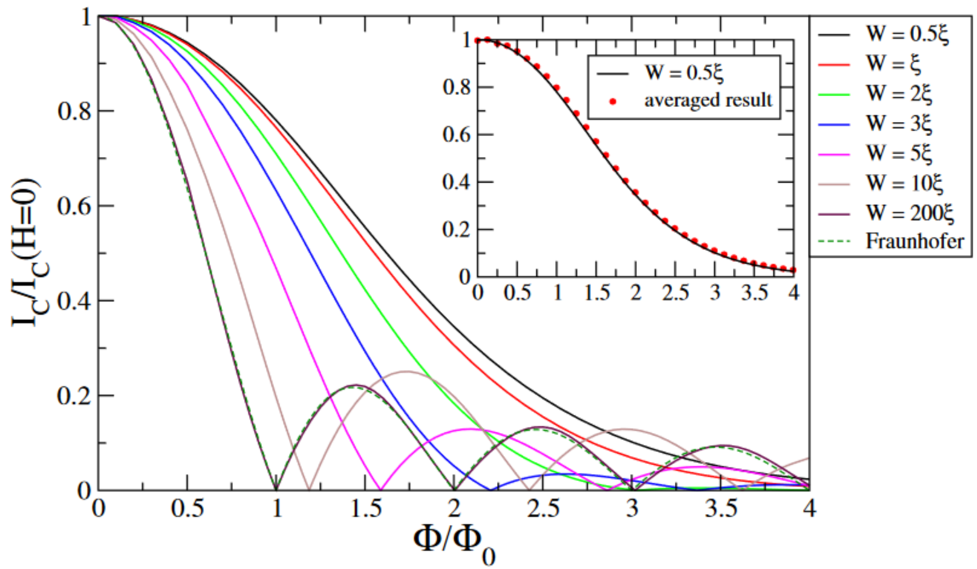

Change of operator ∇

Cuevas, J. C., & Bergeret, F. S. (2007). Magnetic interference patterns and vortices in diffusive SNS junctions. *Physical review letters*, *99*(21), 217002.

Nanowire limit

$$w \ll \xi_H=(\Phi_0/H)^{1/2}.$$

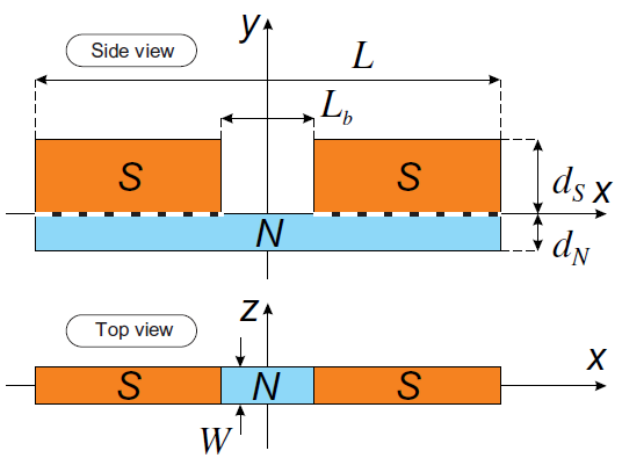

$$\omega_H=\frac{T}{T_C}(2n+1)+\frac{1}{3}\left(\frac{e\xi wH}{\hbar}\right)^2$$

Bergeret, F. S., & Cuevas, J. C. (2008). The vortex state and Josephson critical current of a diffusive SNS junction. *Journal of Low Temperature Physics*, *153*(5), 304-324.

Transport in electrodes

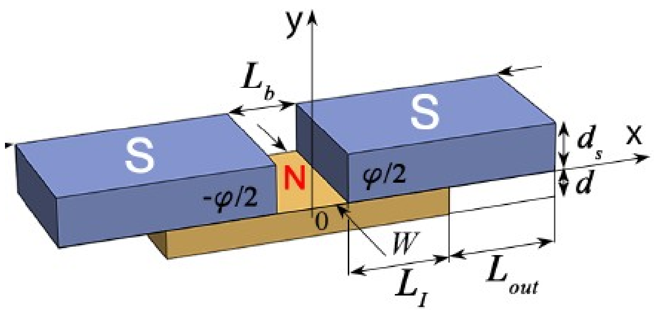

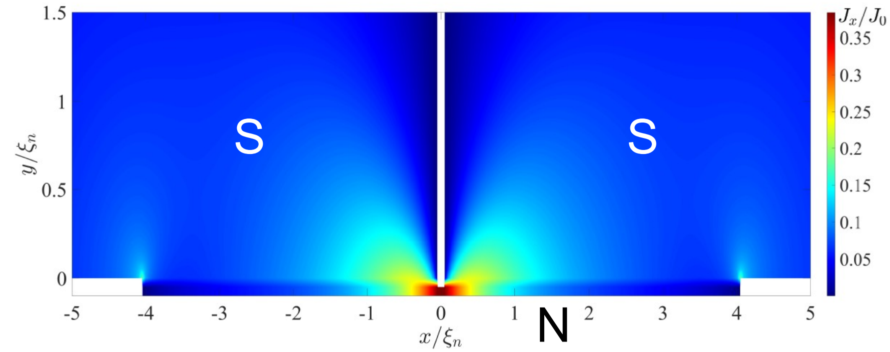

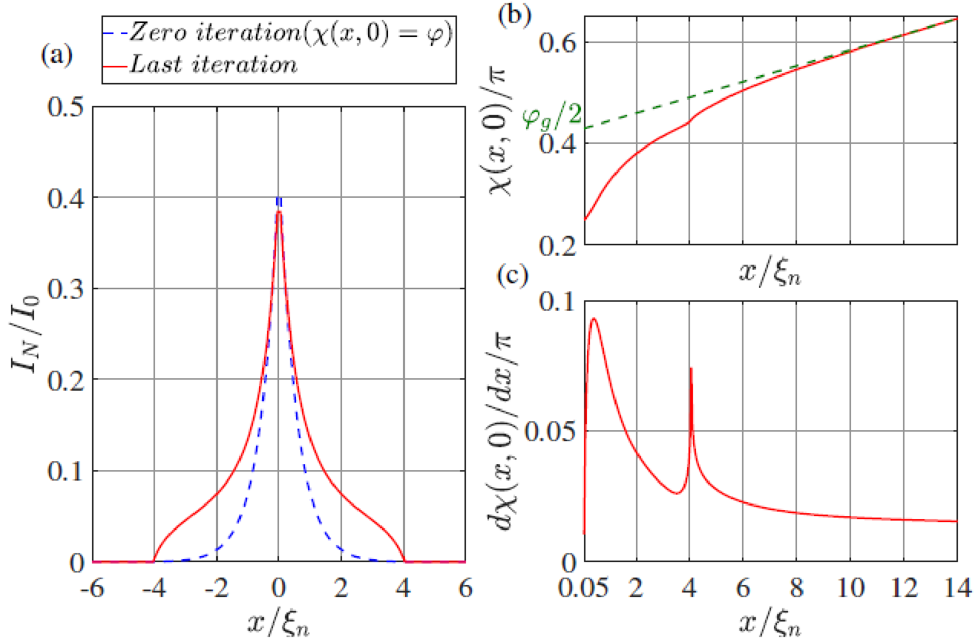

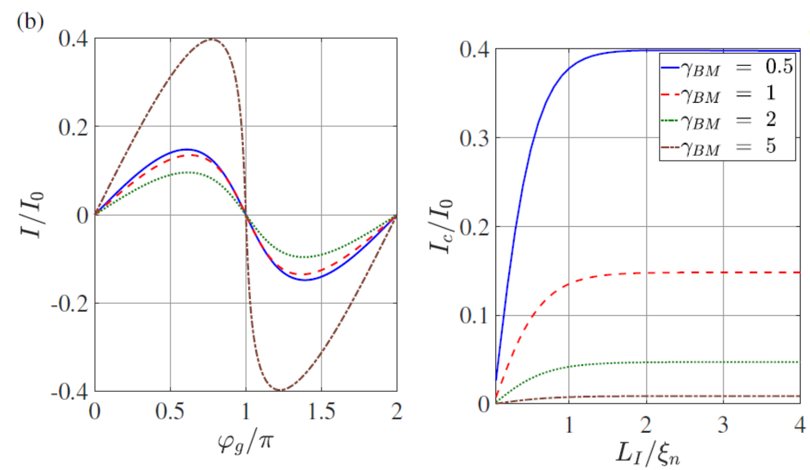

Ruzhickiy, V., Bakurskiy, S., Kupriyanov, M., Klenov, N., Soloviev, I., Stolyarov, V., & Golubov, A. (2023). Contribution of Processes in SN Electrodes to the Transport Properties of SN-N-NS Josephson Junctions. *Nanomaterials*, *13*(12), 1873.

Example: Nb-Cu nanowire bridge

Long SN-N-NS bridge

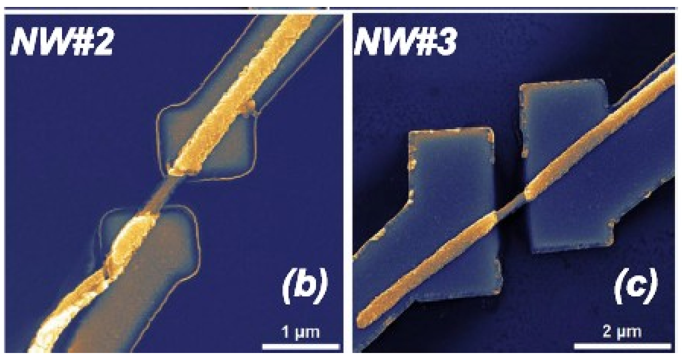

Sample	Geometry	L_{wl} (nm)	d (nm)	R (Ω)
NW#1	4-p, 20 mK	1765 ± 116	108 ± 10	2.20
NW#2	2-p, 1.2 K	609 ± 112	114 ± 6	0.46
NW#3	2-p, 1.2 K	671 ± 105	168 ± 9	0.37

D (m^2/s)	ξ_N (nm)	I_c (μA)	T_c/T_c^* (K)	γ_B
0.03	66	0.7	…	…
0.04	80	30	8.3/5.0	4.4
0.03	65	17	8.3/5.2	4.2

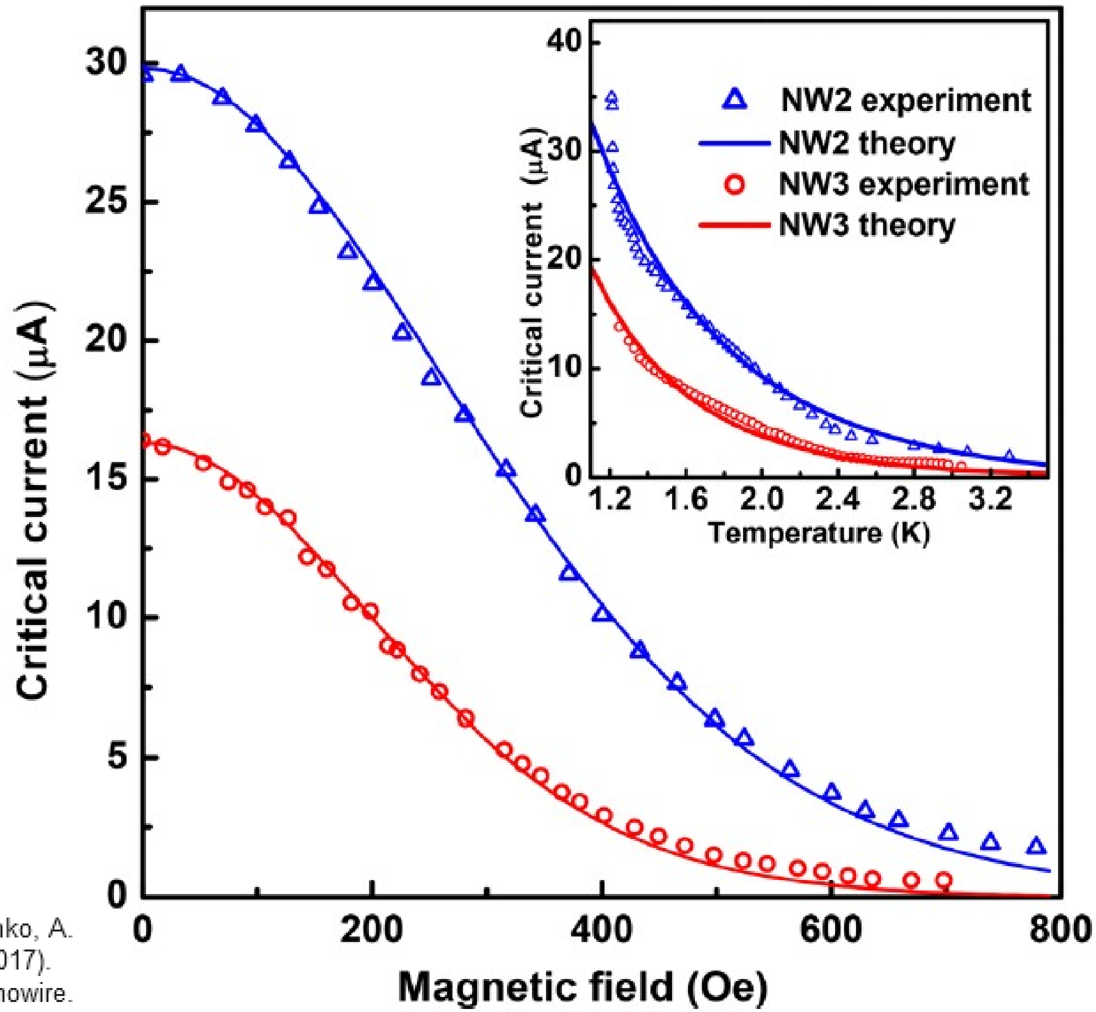

Skryabina, O. V., Egorov, S. V., Goncharova, A. S., Klimenko, A. A., Kozlov, S. N., Ryazanov, V. V., ... & Stolyarov, V. S. (2017). Josephson coupling across a long single-crystalline Cu nanowire. *Applied physics letters*, *110*(22), 222605.

Example: Nb-Au nanowire bridge

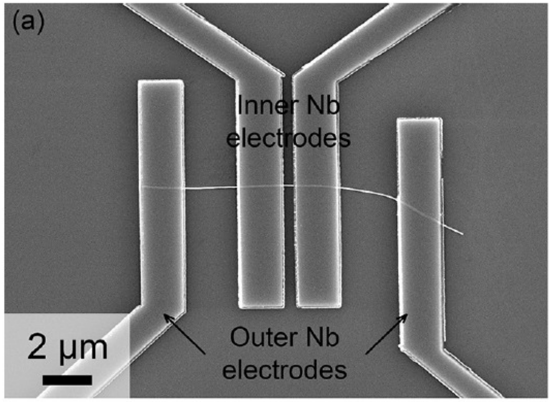

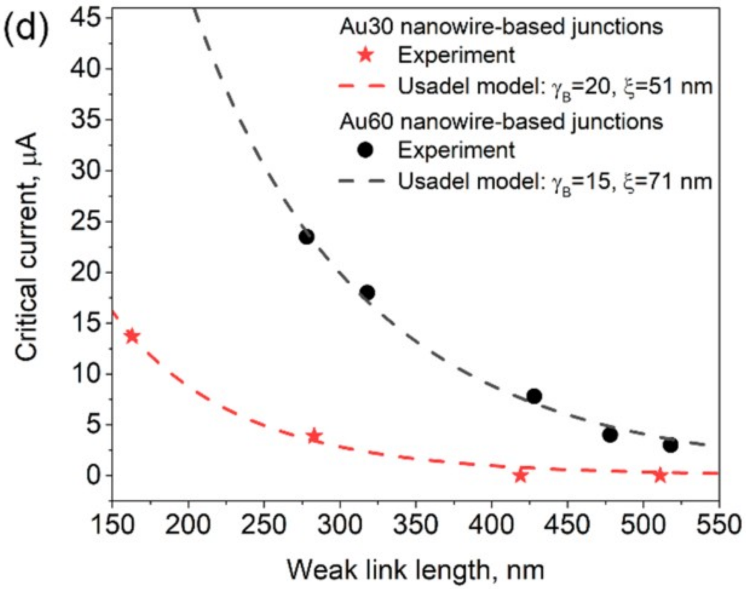

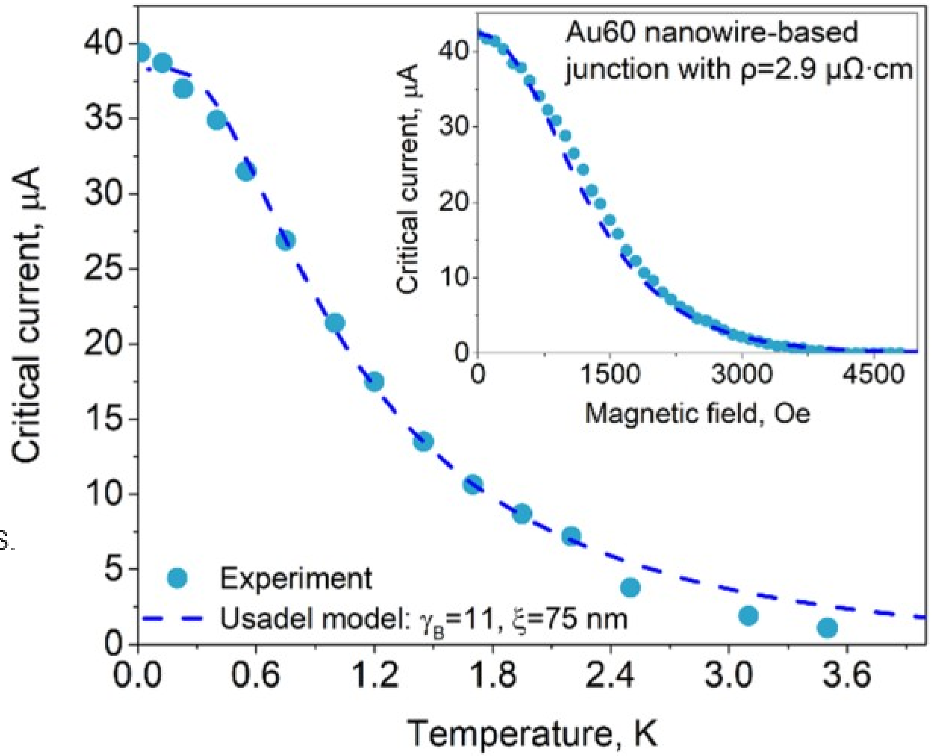

Sotnichuk, S. V., Skryabina, O. V., Shishkin, A. G., Bakurskiy, S. V., Kupriyanov, M. Y., Stolyarov, V. S., & Napolskii, K. S. (2022). Long Single Au Nanowires in Nb/Au/Nb Josephson Junctions: Implications for Superconducting Microelectronics. *ACS Applied Nano Materials*, *5*(11), 17059-17066.

Bridge in resistive state

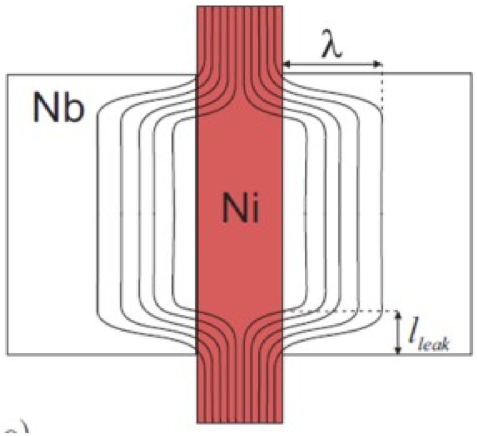

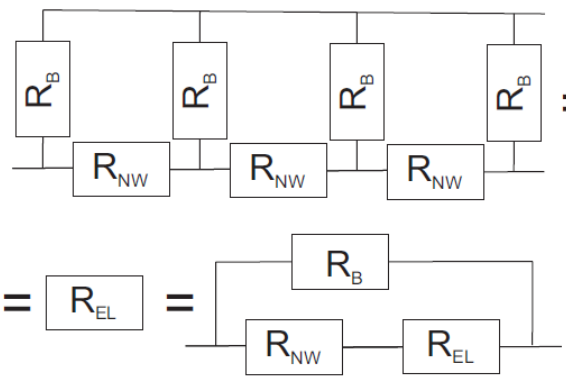

$$\frac{1}{R_{EL}} = \frac{1}{R_B} + \frac{1}{R_{NW} + R_{EL}}.$$

$$R_{EL} = \frac{2\sqrt{\rho_{Ni}\rho_B}}{\pi d^{3/2}}$$

$$R(T) = R_{Ni} + A(1 - T/T_C)^{-1/4}.$$

Resistance calculation

$$R = R_{Ni} + 2R_{EL},$$

$$R_{Ni} = 4 l_{NW} \rho_{Ni} / \pi d^2$$

$$R_{NW} = \frac{4\rho_{Ni}\Delta l}{\pi d^2}.$$

Conversion resistance

$$R_B = \frac{\rho_B}{\Delta l\ \pi d}, \qquad \rho_B \sim \xi(T) \sim \xi_{Nb}(1 - T/T_C)^{-1/2}.$$

Skryabina, O. V., Kozlov, S. N., Egorov, S. V., Klimenko, A. A., Ryazanov, V. V., Bakurskiy, S. V., ... & Stolyarov, V. S. (2019). Anomalous magneto-resistance of Ni-nanowire/Nb hybrid system. *Scientific reports*, 9(1), 14470.

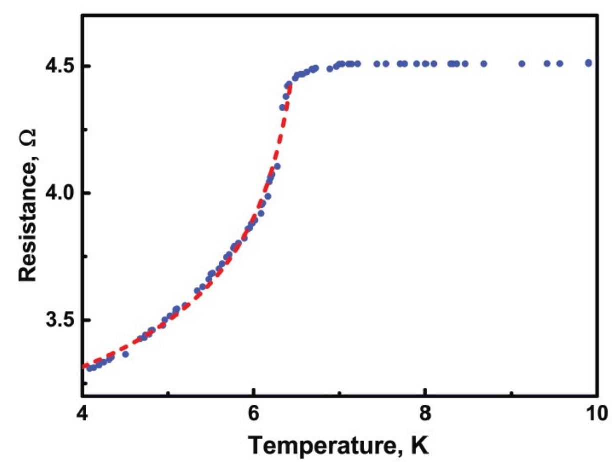

FIG. 4. $R(T)$ for 4-probe measurement scheme (points - experiment, dashed line - model)

$$\rho_{Ni} \approx 4.26\ \mu\Omega\ \text{cm}$$

Bridge in resistive state

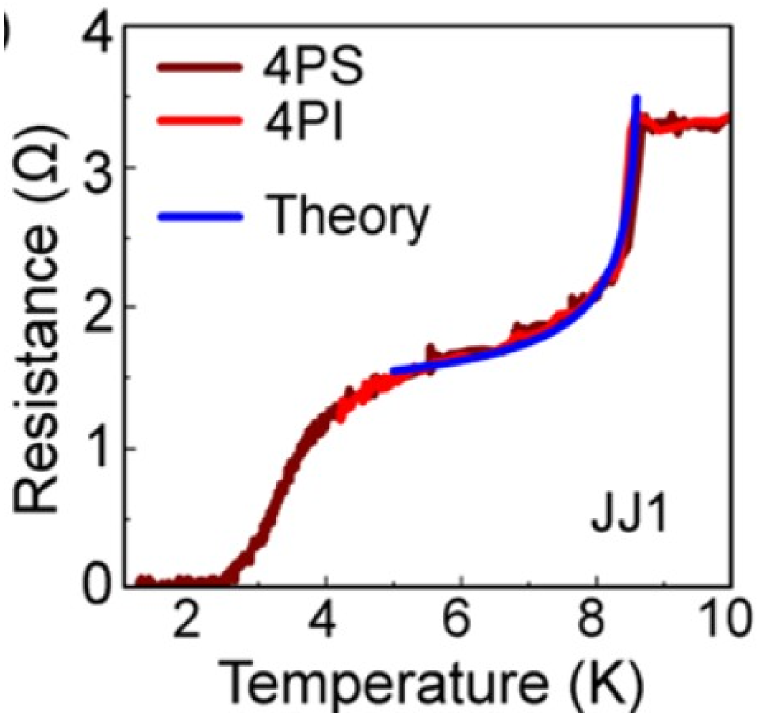

Measuring current
I = 1 μA

At high temperature it larger than critical current

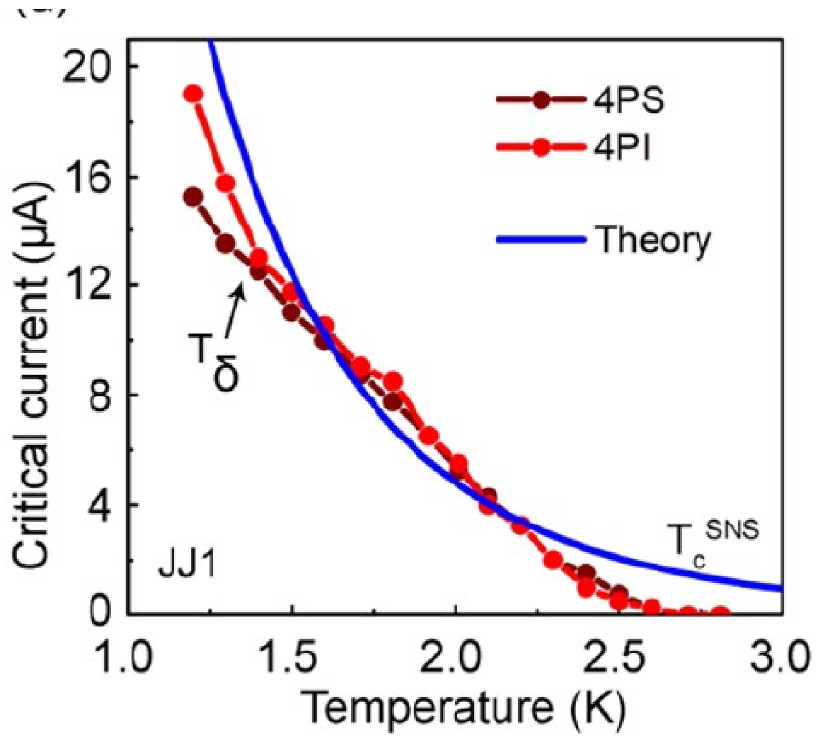

$$\rho_{Au} = 0.43\ \mu\Omega\,\mathrm{cm}.$$

Skryabina, O. V., Bakurskiy, S. V., Shishkin, A. G., Klimenko, A. A., Napolskii, K. S., Klenov, N. V., ... & Stolyarov, V. S. (2021). Environment-induced overheating phenomena in Au-nanowire based Josephson junctions. *Scientific reports*, *11*(1), 1-6.

Bridge overheating

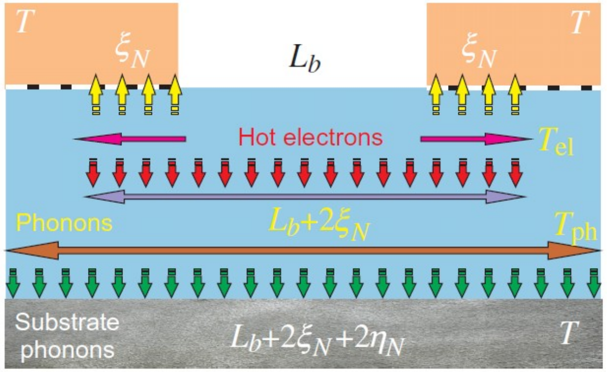

Power gain

$$E = \int_0^{t_{sw}} I_N V d\tau, \qquad E \approx I_c \Phi_0, P = E/T_{clk}.$$

Power loss in phonons

$$P_{\text{e-ph}} = \frac{K_*}{T_*}\left(\frac{15\zeta(5)}{3\pi}\frac{c_t^4}{c_l^4}\frac{T_{\text{loc}}^4}{T_*^4} + \frac{16\pi^2}{45}\frac{T_{\text{loc}}^3}{T_*^3}\right)\delta T_{\text{e-ph}},$$

$$K_* = \frac{N_0 \tau_{sc} k_B T_*}{d_{fn}\ell^5}\left(\frac{p_F^2}{m_e}\right)^2, T_* = \frac{\hbar c_t}{k_B \ell}$$

Power loss in electrodes

$$P_{SN} = \frac{2\Delta}{e^2 R_B} A \sqrt{\frac{2\pi\Delta}{k_B T_{\text{loc}}}} \exp\left(-\frac{\Delta}{k_B T_{\text{loc}}}\right) k_B \delta T,$$

Main channel at 4.2 K

Main channel at 10-100 mK

Soloviev, I. I., Bakurskiy, S. V., Ruzhickiy, V. I., Klenov, N. V., Kupriyanov, M. Y., Golubov, A. A., ... & Stolyarov, V. S. (2021). Miniaturization of Josephson Junctions for Digital Superconducting Circuits. *Physical review applied*, *16*(4), 044060.

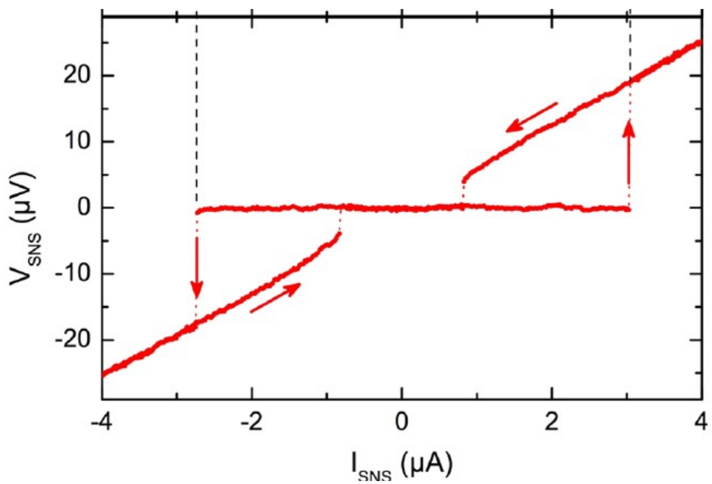

Courtois, H., Meschke, M., Peltonen, J. T., & Pekola, J. P. (2008). Origin of hysteresis in a proximity Josephson junction. *Physical review letters*, *101*(6), 067002.

Measured I_C depends on method

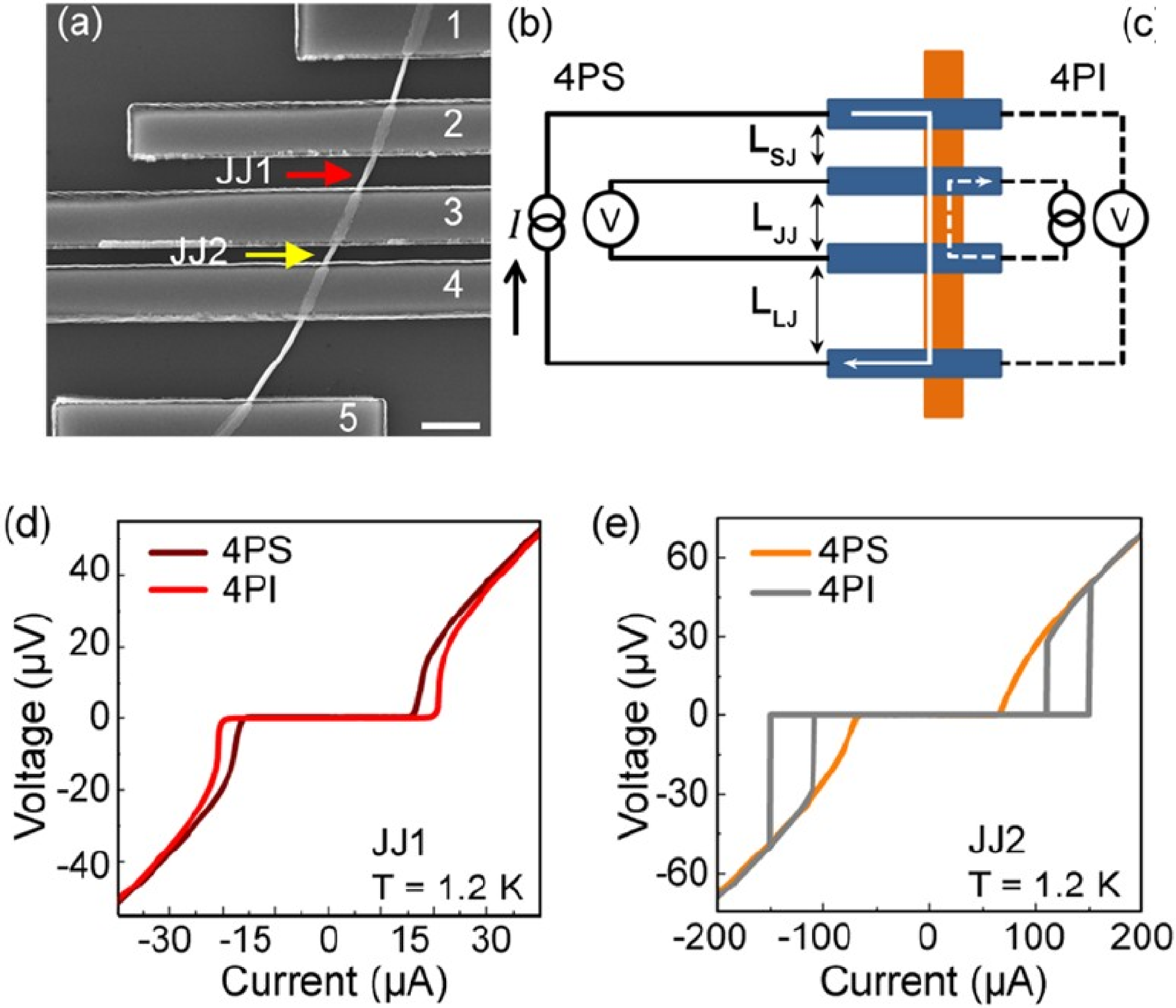

Skryabina, O. V., Bakurskiy, S. V., Shishkin, A. G., Klimenko, A. A., Napolskii, K. S., Klenov, N. V., ... & Stolyarov, V. S. (2021). Environment-induced overheating phenomena in Au-nanowire based Josephson junctions. *Scientific reports*, *11*(1), 15274.

Overheat induced by neighboor

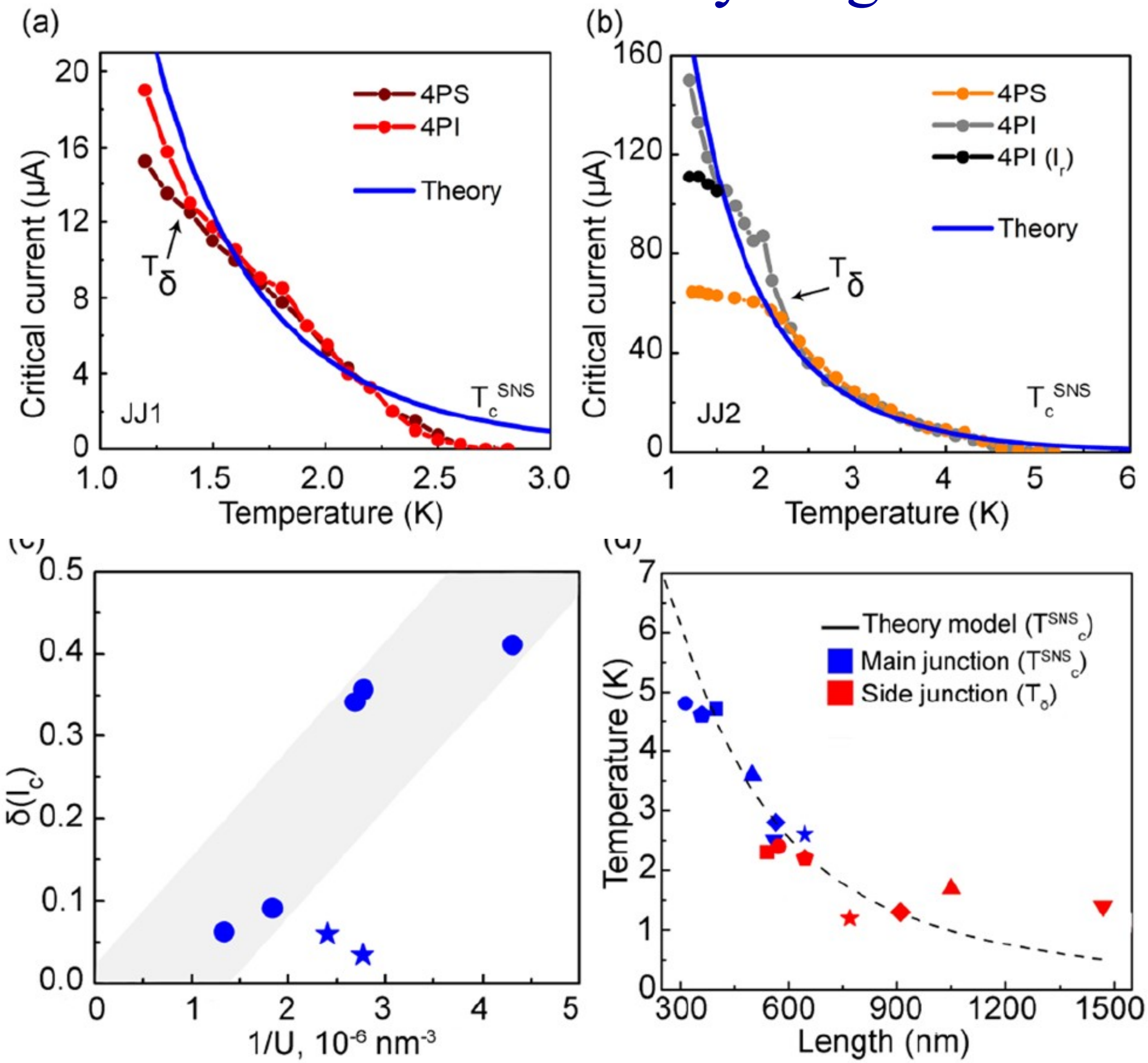

Skryabina, O. V., Bakurskiy, S. V., Shishkin, A. G., Klimenko, A. A., Napolskii, K. S., Klenov, N. V., ... & Stolyarov, V. S. (2021). Environment-induced overheating phenomena in Au-nanowire based Josephson junctions. *Scientific reports*, *11*(1), 15274.

Contents

1. Motivation
2. Basic physics of S-F-N hybrids
3. Hybrid S-F-N structures
   - spin-valves
   - flux traps
   - bi-stable phase junctions
   - Josephson bridges
4. Implementation in applied schemes
   - Bio-inspired neuron
   - All-JJ Logic

Bio-inspired Au-Nanowire-Based Neurons

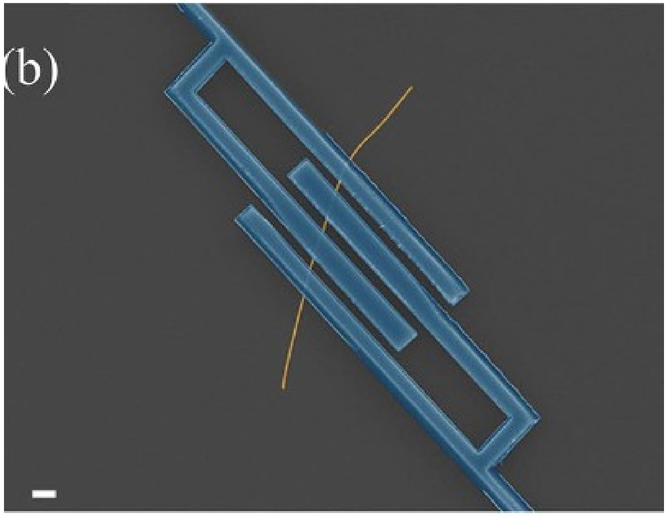

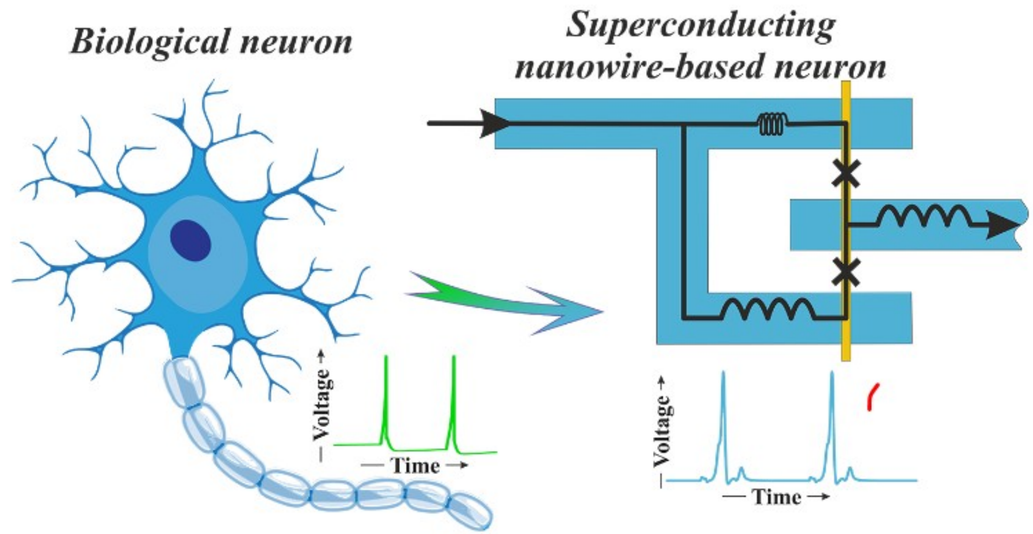

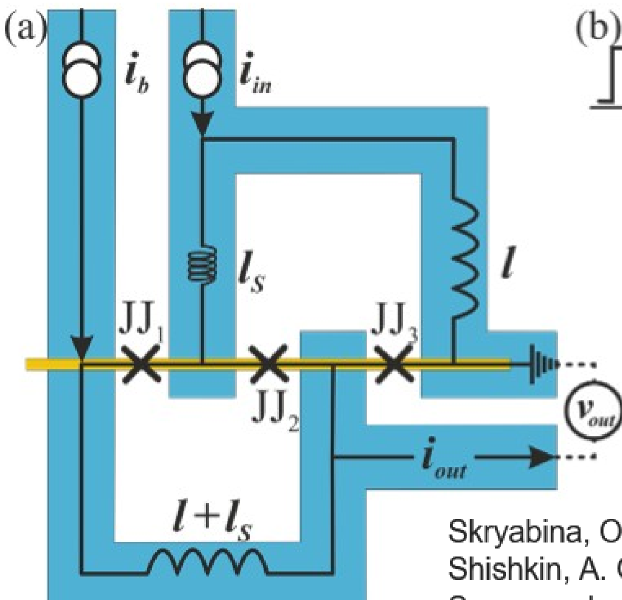

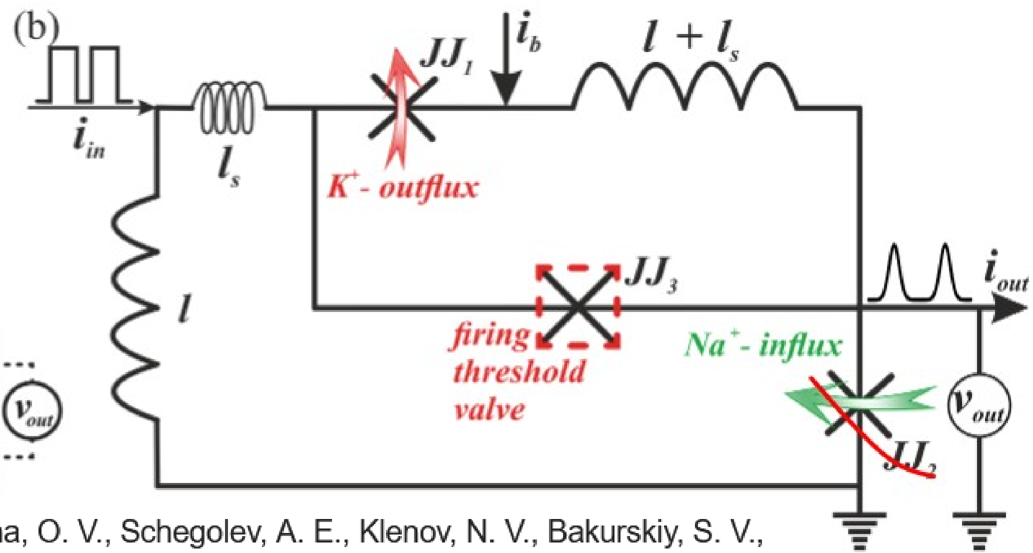

Skryabina, O. V., Schegolev, A. E., Klenov, N. V., Bakurskiy, S. V., Shishkin, A. G., Sotnichuk, S. V., ... & Stolyarov, V. S. (2022). Superconducting Bio-Inspired Au-Nanowire-Based Neurons. *Nanomaterials*, *12*(10), 1671.

Bio-inspired Au-Nanowire-Based Neurons

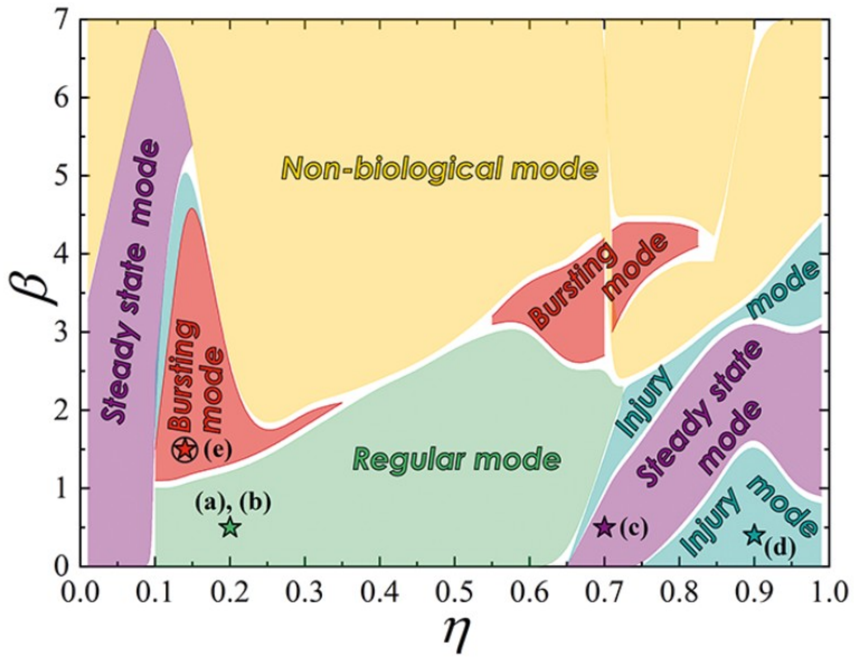

η is the ratio of I_{C3} to I_{C0} $\beta = \omega_c RC$

Skryabina, O. V., Schegolev, A. E., Klenov, N. V., Bakurskiy, S. V., Shishkin, A. G., Sotnichuk, S. V., ... & Stolyarov, V. S. (2022). Superconducting Bio-Inspired Au-Nanowire-Based Neurons. *Nanomaterials*, *12*(10), 1671.

It is possible to switch modes by bias current!

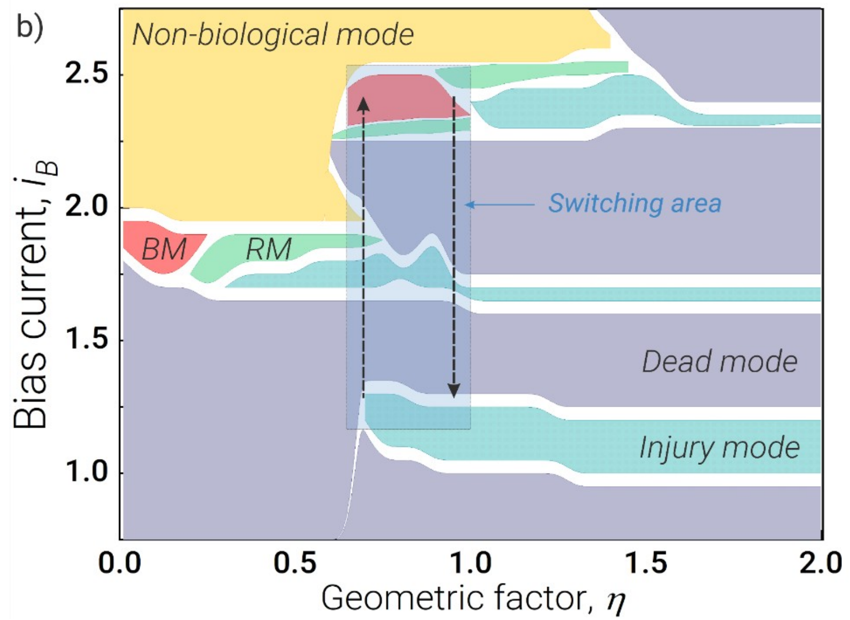

Schegolev, A. E., Klenov, N. V., Gubochkin, G. I., Kupriyanov, M. Y., & Soloviev, I. I. (2023). Bio-Inspired Design of Superconducting Spiking Neuron and Synapse. *Nanomaterials*, *13*(14), 2101.

Contents

1. Motivation

2. Basic physics of S-F-N hybrids

3. Hybrid S-F-N structures
   - spin-valves
   - flux traps
   - bi-stable phase junctions
   - Josephson bridges

4. Implementation in applied schemes
   - Bio-inspired neuron
   - All-JJ Logic

All-JJ electronics
Superconducting circuits without inductances

Magnetic JJ (π-, φ- or 2φ-JJ)

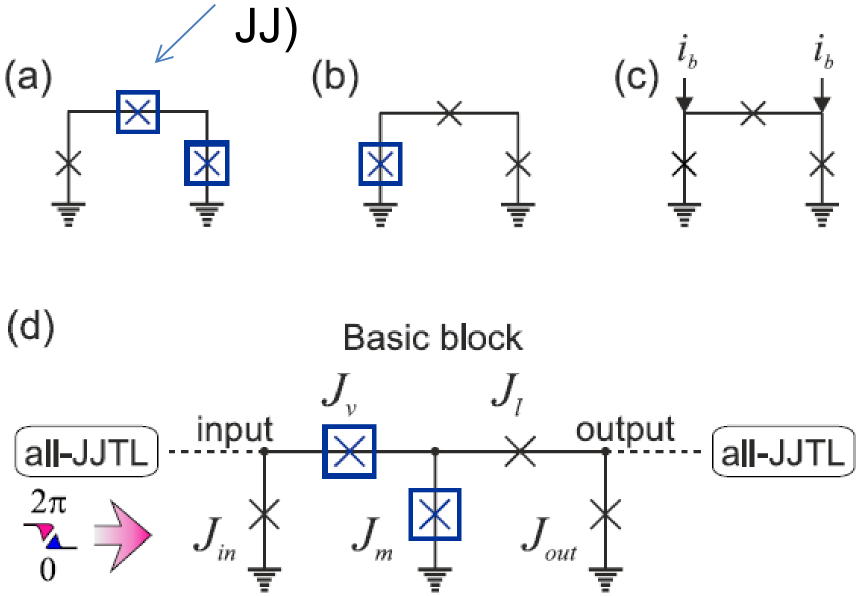

Energy-phase relation of 0-JJ and 2φ-JJ

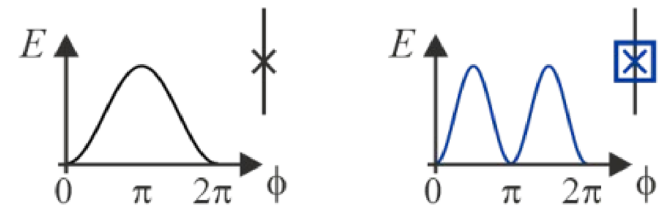

✓ In the "inductanceless" circuit the superconducting phase kink is no more correspond to the magnetic flux

Phase drop in the input circuit in response to incoming 2π phase kink

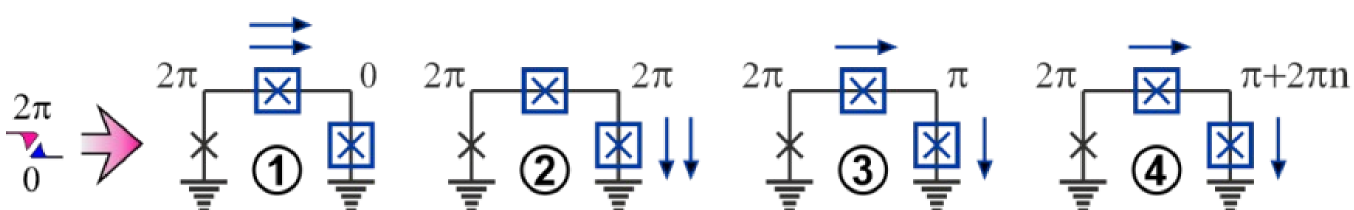

Soloviev, I. I., Ruzhickiy, V. I., Bakurskiy, S. V., Klenov, N. V., Kupriyanov, M. Y., Golubov, A. A., ... & Stolyarov, V. S. (2021). Superconducting circuits without inductors based on bistable Josephson junctions. *Physical review applied*, *16*(1), 014052.

Schematics of the All-JJ triggers

Basic block with readout circuit

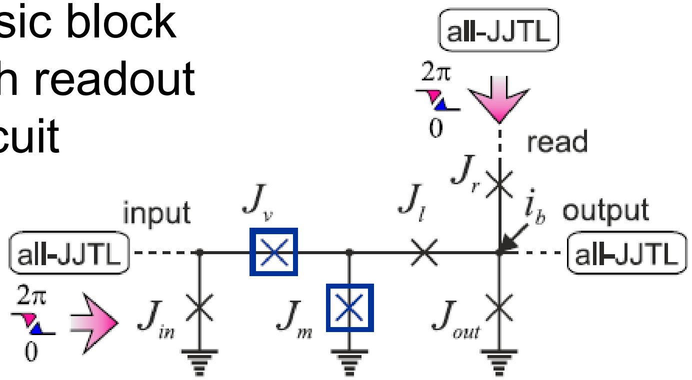

Basic block with inverted readout circuit

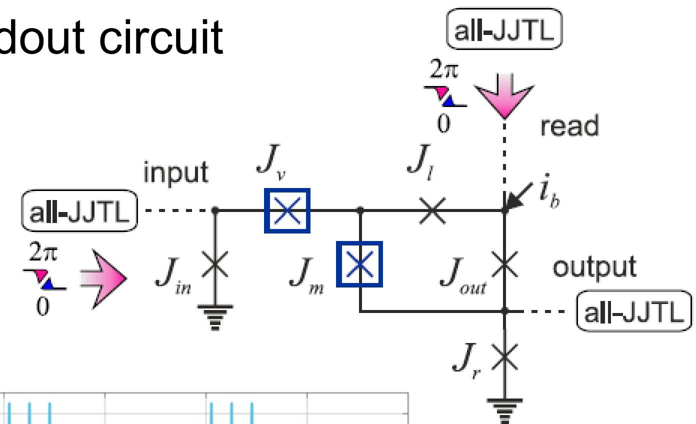

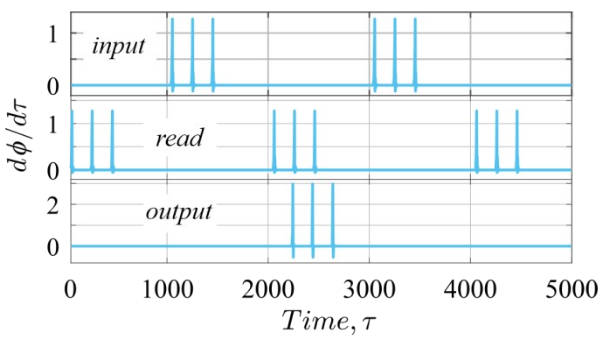

DRO similar to DFF

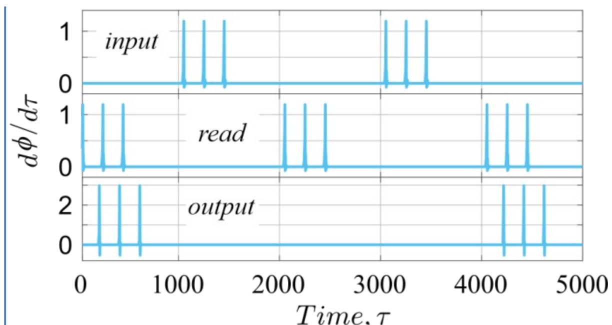

DRO with inverted output

NDRO

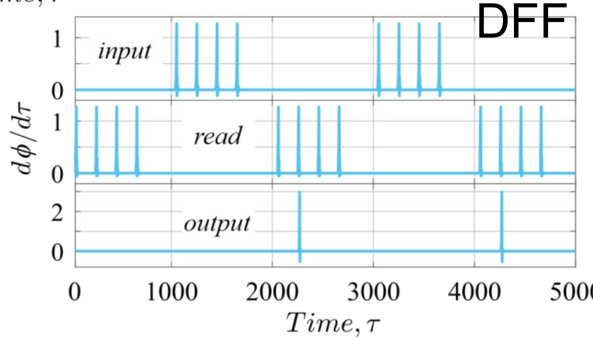

NDRO with inverted output

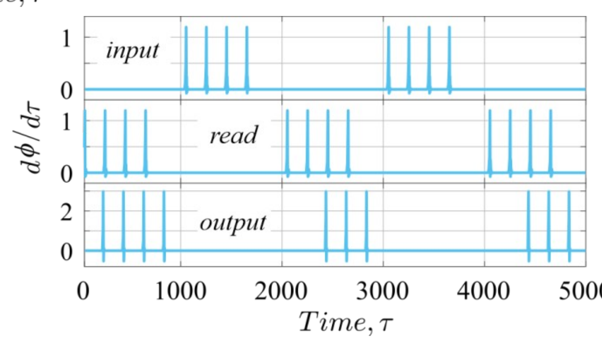

All-JJ 8-bit parallel adder

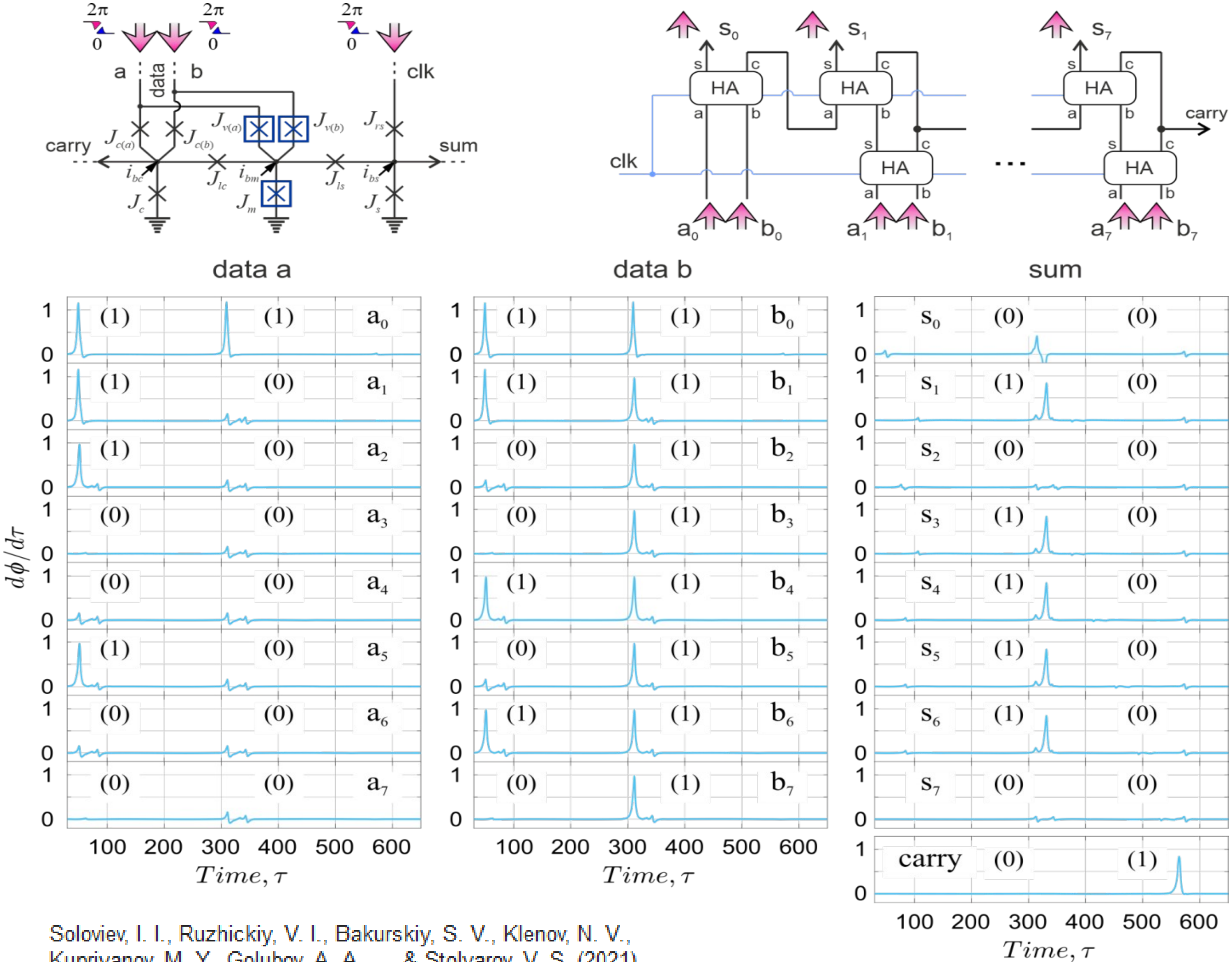

Soloviev, I. I., Ruzhickiy, V. I., Bakurskiy, S. V., Klenov, N. V., Kupriyanov, M. Y., Golubov, A. A., ... & Stolyarov, V. S. (2021). Superconducting circuits without inductors based on bistable Josephson junctions. *Physical review applied*, *16*(1), 014052.

π-JJ based all-JJ circuits

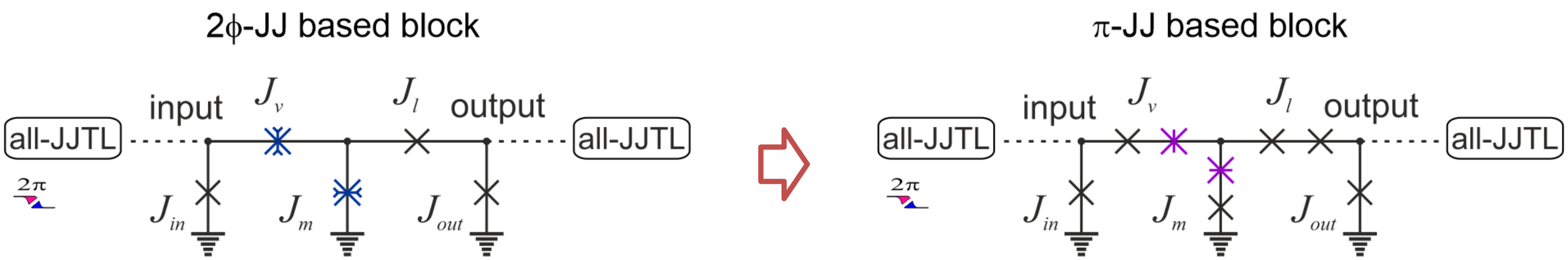

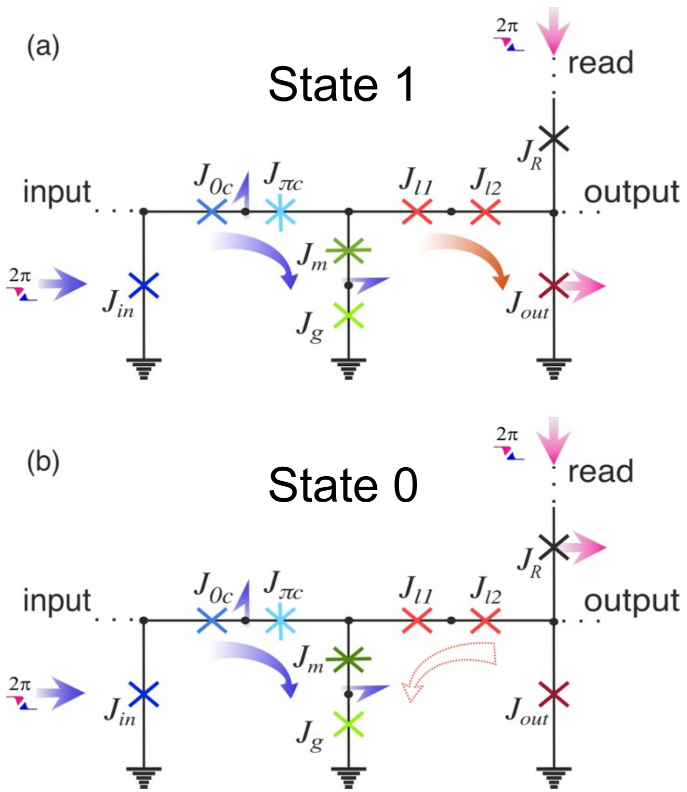

Destructive readout

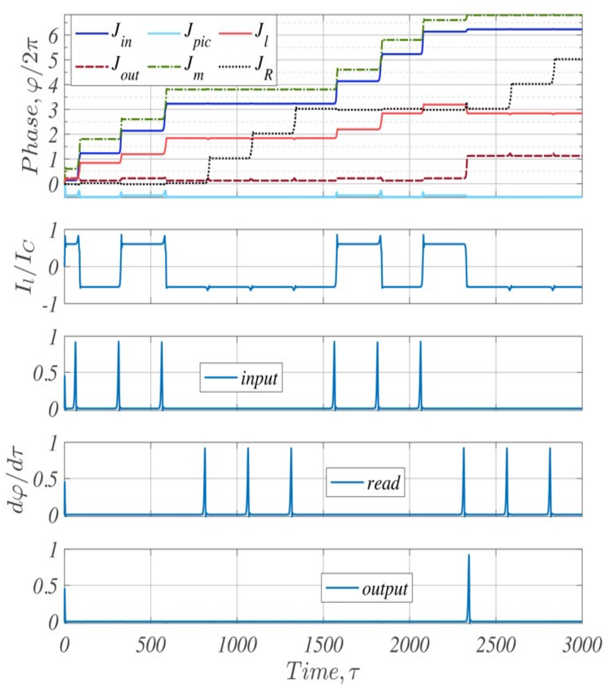

Maksimovskaya, A. A., Ruzhickiy, V. I., Klenov, N. V., Bakurskiy, S. V., Kupriyanov, M. Y., & Soloviev, I. I. (2022). Phase Logic Based on π Josephson Junctions. *JETP Letters*, *115*(12), 735-741.

Thank you for your attention!